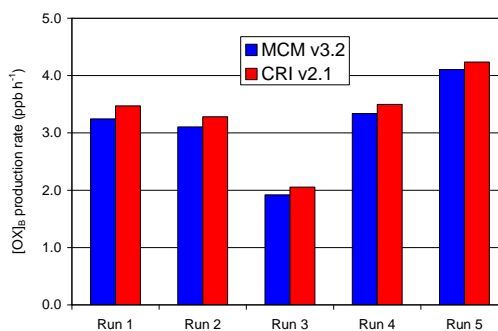# Modelling of Tropospheric Ozone

Annual Report 2011

Ozone AOT40
2020

■	BELOW 2000
■	2000 − 4000
■	4000 − 6000
■	6000 − 9000
■	9000 − 12000
■	12000 − 1500
■	15000 − 1800
■	ABOVE 18000
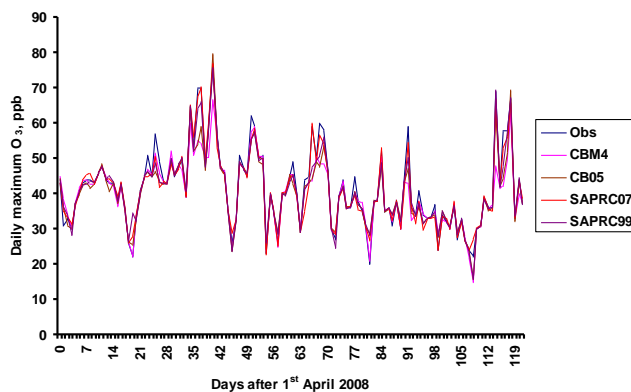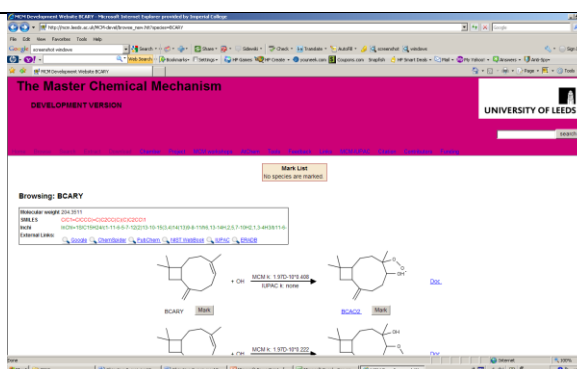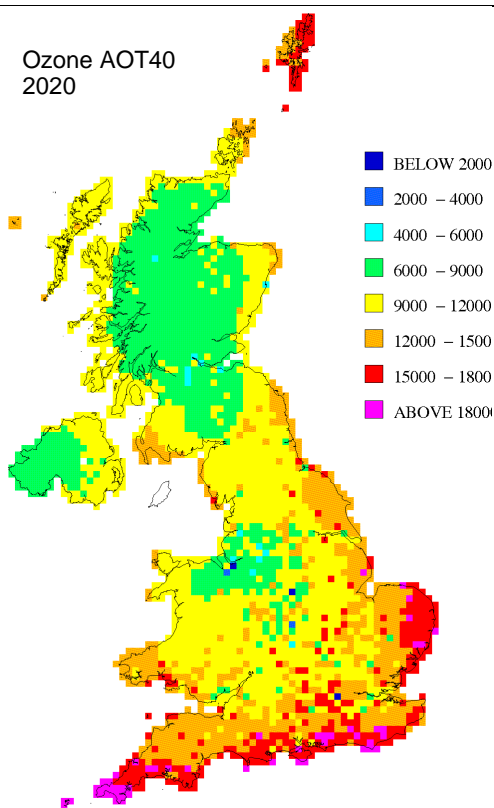
Oxidant production rate in London – July 1999

Report for Defra

Customer:

The Department for Environment, Food and Rural Affairs, Welsh Assembly Government, the Scottish Executive and the Department of the Environment for Northern Ireland

Customer reference:

AQ0704

Confidentiality, copyright & reproduction:

This report is the Copyright of Defra and has been prepared by AEA Technology plc under contract to Defra (AQ0704) dated 8/2/2010. The contents of this report may not be reproduced in whole or in part, nor passed to any organisation or person without the specific prior written permission of Defra. AEA Technology plc accepts no liability whatsoever to any third party for any loss or damage arising from any interpretation or use of the information contained in this report, or reliance on any views expressed therein

Contact:

Tim Murrells
AEA Technology plc
Gemini Building, Harwell International Business Centre, Didcot, OX11 0QR
t: 0870 190 6539
f: 0870 190 6318
e: tim.p.murrells@aeat.co.uk
AEA is a business name of AEA Technology plc
AEA is certificated to ISO9001 and ISO14001

Author:

Tim Murrells
Sally Cooke
John Abbott
Andrea Fraser
Prof Dick Derwent (rdscientific)
Mike Jenkin (Atmospheric Chemistry Services)

Approved By:

Geoff Dollard

Date:

15 March 2012

Signed:

AEA reference:

ED47546- Issue Number 1

Executive summary

The concentrations of ground-level ozone, a pollutant that affects human health, ecosystems and materials, widely exceed environmental quality standards across the UK and Europe. Ozone is not emitted directly into the atmosphere, but is a secondary photochemical pollutant formed in the lower atmosphere from the sunlight-initiated oxidation of volatile organic compounds (VOCs) in the presence of nitrogen oxides (NO_x). Elevated concentrations of ozone over the UK are especially generated when slow-moving or stagnant high pressure (anticyclonic) weather systems occurring in the spring or summer bring in photochemically reacting air masses from mainland Europe.

The non-linear nature of ground-level ozone production requires the use of sophisticated chemical transport models to understand the factors affecting its production and subsequent control on a wide spatial scale.

This report describes the work undertaken in 2011 during the final year of the second phase of the project "*Modelling of Tropospheric Ozone*" funded by the Department for Environment, Food and Rural Affairs (Defra) and the Devolved Administrations (the Scottish Executive, the Welsh Assembly Government and the Department of the Environment for Northern Ireland).

The overall purpose of the project is to maintain, develop, and apply tools for modelling tropospheric ozone formation and distribution over a range of spatial scales (global, regional and national). The modelling is used to support and guide Defra's policy on emission reductions and objectives for pollutants that influence ozone and to verify compliance with UK policy and with European directives on ground-level ozone concentrations. The project scope has been extended to include secondary organic aerosols (SOA), another secondary air pollutant formed in the atmosphere from emitted VOCs requiring similar modelling approaches to predict their concentrations.

The overall programme consisted of 12 main objectives, 9 of which had been completed during previous years of the project. The report describes the work programme and presents a summary and conclusions of the work on the remaining 3 objectives completed during 2011. These are fully amalgamated in the report's Conclusions section 10. A brief synopsis of the summary and conclusions is as follows.

Improvement to Photochemical Reaction Schemes

- **A new chemical reaction scheme has been developed and successfully tested describing the oxidation of chlorinated solvents in the atmosphere**
- **This allows models to be used in future solvent assessment activities relating to atmospheric ozone formation covering a wider range of solvent types.**

Modelling the UK Ozone Climate in 2009 and 2010

- **The Ozone Source Receptor Model (OSRM) was used to model the UK's ground-level ozone climate in 2009 and 2010 at 10x10km resolution. Both these years were fairly "low ozone" years and compared with results from monitoring data, the model tended to overestimate concentrations in both years.**

Modelling Secondary Organic Aerosol Formation with the OSRM

- **A new chemical mechanism describing formation of secondary organic aerosol (SOA, a component of particulate matter in the atmosphere) has been successfully incorporated into the OSRM.**

- **The results from the OSRM show that when averaged over a year, total organic aerosol mass concentrations are similar at different sites and show little inter-year variability, with annual mean concentrations falling within a range of 1-3 µgm^{-3} OA.**

- **However this masks a large range in spatial and temporal variation with maximum concentrations at different sites, months and years varying over a range of 10-80 µgm^{-3} OA**

- **Maps have been developed at 10x10km resolution showing the spatial distribution of different components of SOA. Biogenic SOA components show a different distribution to the anthropogenic components**

Modelling Support for Ozone Policy

- **The OSRM has been used to model the future UK ground-level ozone climate at 10x10 km resolution for a number of different UK and European emission scenarios assuming meteorological conditions representative of 2006 and 2007**

- **Some of these referred to changes in UK emissions according to the latest DECC energy scenarios up to 2030. All scenarios led to increases in the EU Air Quality Directive ozone concentration metrics for 2020-2030 relative to values calculated for 2006.**

- **Further simulations were carried out for different UK and European emission scenarios with different levels of ambition for 2020. The analysis indicated that it will be important for comparable reductions in emissions to be achieved across Europe as well as in the UK to prevent ozone concentrations in the UK rising.**

- **It also shows the benefits to be achieved by reducing VOC emissions across Europe.**

- **The Photochemical Trajectory Model (PTM) was used to carry out a Monte Carlo parametric uncertainty analysis of the likely impact of 7 different European emission reduction scenarios with different levels of ambition on peak concentrations of ozone at the Harwell site in southern England**

- **The analysis showed that there is a high probability that the European emission scenarios for 2020 will reduce daily maximum ozone levels under the meteorological conditions modelled and that the most ambitious emission reductions would lead to reductions in peak ozone that were small, but statistically significant compared with the 2020 base scenario**

- **However, even with the most ambitious emission reductions, there would be only a 4% chance that the highest daily maximum ozone would be reduced to below the 50 ppb level at this site**

- **Taking into account only reductions in UK emissions according to the latest DECC energy scenarios up to 2030, there would be less than 1% chance that peak ozone would be reduced to below 50 ppb in any of the model years.**

- **The impact of the choice of chemical mechanism used in models for ozone air quality policy was studied in detail. The response of ozone concentrations to changes in NO$_x$ and VOC emissions predicted by versions of the PTM using 6 different chemical schemes of varying degrees of complexity was assessed and found to be quite varied.**

- **The impact of climate change on ozone has been assessed, focusing on the**

response of predicted ozone concentrations to increasing isoprene emissions from natural sources occurring as a result of rising surface temperatures.

- **The work has indicated how the representation of atmospheric chemistry processes in global and regional air quality models is important in determining how changes in biogenic emissions caused by climate change will affect predicted changes in ground-level ozone formation.**

Assessments of Background and Urban-Scale Oxidant

- **The geographical variation of annual mean oxidant (O_3 + NO_2) over the UK has been characterised and the higher resolution mapping methodology developed to produce a 1km x 1km map for 2010. This will inform NO_2 and ozone modelling activities using the Pollution Climate Model (PCM) in the Defra UKAAQA programme**

- **The potential impact of urban-scale photochemistry on oxidant production over the London conurbation has been assessed using a boundary layer box model to simulate chemical processing.**

- **Oxidant production rates inferred from observational data under photochemical episode conditions can broadly be explained by current understanding of the chemical processing of the urban atmosphere, but the results are sensitive to VOCs and NO_x emissions in the model, the applied VOC speciation and the prevailing temperature and relative humidity.**

- **The work has allowed a limited evaluation of the emissions inputs to the model in relation to observational data. This provided some support for the reported data, but the input of reactive VOCs of both anthropogenic and biogenic origin appeared to be under-represented by the emissions data used in the assessment.**

Table of contents

1 Introduction

The concentrations of ground-level ozone, a pollutant that affects human health, ecosystems and materials, widely exceed environmental quality standards across the UK and Europe. Ozone is not emitted directly into the atmosphere, but is a secondary photochemical pollutant formed in the lower atmosphere from the sunlight-initiated oxidation of volatile organic compounds (VOCs) in the presence of nitrogen oxides (NO_x). Elevated concentrations of ozone over the UK are especially generated when slow-moving or stagnant high pressure (anticyclonic) weather systems occurring in the spring or summer bring in photochemically reacting air masses from mainland Europe.

Under conditions characteristic of photochemical pollution episodes, the formation and transport of ozone and other secondary air pollutants can occur over hundreds of kilometres, with concentrations at a given location influenced by the history of the airmass over a period of up to several days. In addition to this, the increasing levels of ozone in the free troposphere on a global scale also influences regional scale photochemical processes by providing an increasing background ozone level upon which the regional and national scale formation is superimposed. This effect has to be considered when assessing whether proposed air quality standards for ozone are likely to be achieved.

The non-linear nature of ground-level ozone production requires the use of sophisticated chemical transport models to understand the factors affecting its production and subsequent control on a wide spatial scale. The Department for Environment, Food and Rural Affairs (Defra) and the Devolved Administrations (DAs, the Welsh Assembly Government, the Scottish Executive and the Department of the Environment for Northern Ireland) have funded the development of ozone modelling tools over the years and the application of the scientific understanding that underpins the models. Defra and the DAs have a need to further develop, maintain and refine the models as further evidence emerges on factors influencing ozone levels on different spatial sales and timescales. They also have a need to apply the models in order to establish the effectiveness of policies changing precursor emissions in the UK and the rest of Europe and how these will affect ozone concentrations in the future in the context of current and future air quality target values and objectives for ozone.

The "*Modelling of Tropospheric Ozone*" contract started in January 2007 and completed in December 2011. The overall aims of the project were to maintain, develop, and apply tools for modelling tropospheric ozone and other secondary air pollutant formation and distribution over a range of spatial scales (global, regional and national). The first phase of the project completed in August 2009 met a number of key objectives and was summarised in the report by Murrells et al (2009a). The objectives involved:

- the maintenance and application of the Ozone Source Receptor Model (OSRM) and Photochemical Trajectory Model (PTM) to support Defra's ozone policy.
- a programme of improvements to the Master Chemical Mechanism (MCM), a near-explicit and comprehensive photochemical reaction scheme describing the atmospheric processes forming ozone in the troposphere from emitted VOCs and NO_x, following a comprehensive review of the MCM
- detailed assessments of ambient data to understand the local-scale coupling between NO_x and ozone in urban environments in order to improve the prediction of ozone and NO_2 in other national and local scale models used for Defra policy
- an initial screening and assessment of more complex Eulerian chemical transport models and the development of a protocol to enable a consistent, robust and transparent approach in comparing the performances of different air quality models used for Defra policy.

- The development of a methodology for assessing the wider costs, benefits and trade-offs of solvent reduction and substitution policies

As well as ozone, the model development work addressed the formation of secondary organic aerosols (SOA) for the first time, since these are also formed in the atmosphere from emitted VOCs and require similar modelling approaches to predict their concentrations and contributions to fine airborne particulate matter, PM_{10} and $PM_{2.5}$.

The second phase of the project started in September 2009 to build on the achievements of the first phase through a programme of work consisting of four main objectives to meet the overall aims of the project. Continuing from the objectives of Phase 1, the Phase 2 objectives were:

Objective 9:   Improvement to Photochemical Reaction Schemes for Treatment of Biogenic Emissions and Emissions of Chlorinated VOCs from Solvents

Objective 10: Application of Ozone and Secondary PM Chemical Transport Models for Defra Policy

Objective 11: Assessments of Background and Urban-Scale Oxidant

Objective 12: Update of Ozone Flux Model in the OSRM

These objectives are described in more detail in Section 2. The work carried out on these objectives during the period from September 2009 to December 2010 was described in the project Annual Report 2010 (Murrells et al, 2011). This report describes the work carried out from January 2011 to the completion of the project in December 2011.

2 Overview of Project Aims and Structure

The work of Phase 2 is divided into four main Objectives that involve the further research and development relating to the underlying chemistry behind formation of tropospheric ozone and secondary organic aerosol and factors controlling them, understanding trends in observations of ground-level ozone and other secondary air pollutants, the application of current modelling tools to support Defra ozone air quality policy and further development of components of models to address the uptake of ozone by vegetation.

Objective 9:   Improvement to Photochemical Reaction Schemes for Treatment of Biogenic Emissions and Emissions of Chlorinated VOCs from Solvents

This objective involved the further improvements to photochemical reactions schemes used in models. The aim was to:

- Develop new and revised schemes for the Master Chemical Mechanism covering emissions of VOCs from natural sources (biogenic emissions) and from use of chlorinated solvents;

- Develop new reduced chemical schemes for chlorinated solvent emissions

- Revise reduced codes for Secondary Organic Aerosol formation suitable for implementation in the OSRM

- Evaluate revised MCM schemes using the Photochemical Trajectory Model (PTM)

- Maintain the MCM website

Objective 10: Application of Ozone and Secondary PM Chemical Transport Models for Defra Policy

This objective involved the application of current models in support of Defra policy on ozone and secondary PM, including:

- the modelling of UK ozone in 2008, 2009 and 2010 using the OSRM

- the use of the OSRM or PTM for modelling specific emission scenarios on an ad-hoc basis to support Defra's development and implementation of policies on ozone and secondary particulate matter (PM)

- specific modelling with the PTM to assess policy development on secondary air pollutants, by examining the spatial distribution of secondary organic aerosols across the UK and the sensitivity to meteorology, emissions and input parameters relating to climate change.

Objective 11: Assessments of Background and Urban-Scale Oxidant

This objective involved assessment of background and urban-scale oxidant through analysis of ambient data for ozone, nitrogen dioxide (NO_2) and nitrogen oxides (NO_x) to further improve local effects in air quality models used for Defra policy.

Objective 12: Update of Ozone Flux Model in OSRM Using New Formulations from SEI's DO$_3$SE Ozone Deposition Model

This objective involved the implementation and evaluation with the OSRM of a new ozone flux model developed by the Stockholm Environment Institute, University of York.

There are strong linkages between the different objectives as shown in Figure 2.1.

Figure 2.1: Linkages among core programme
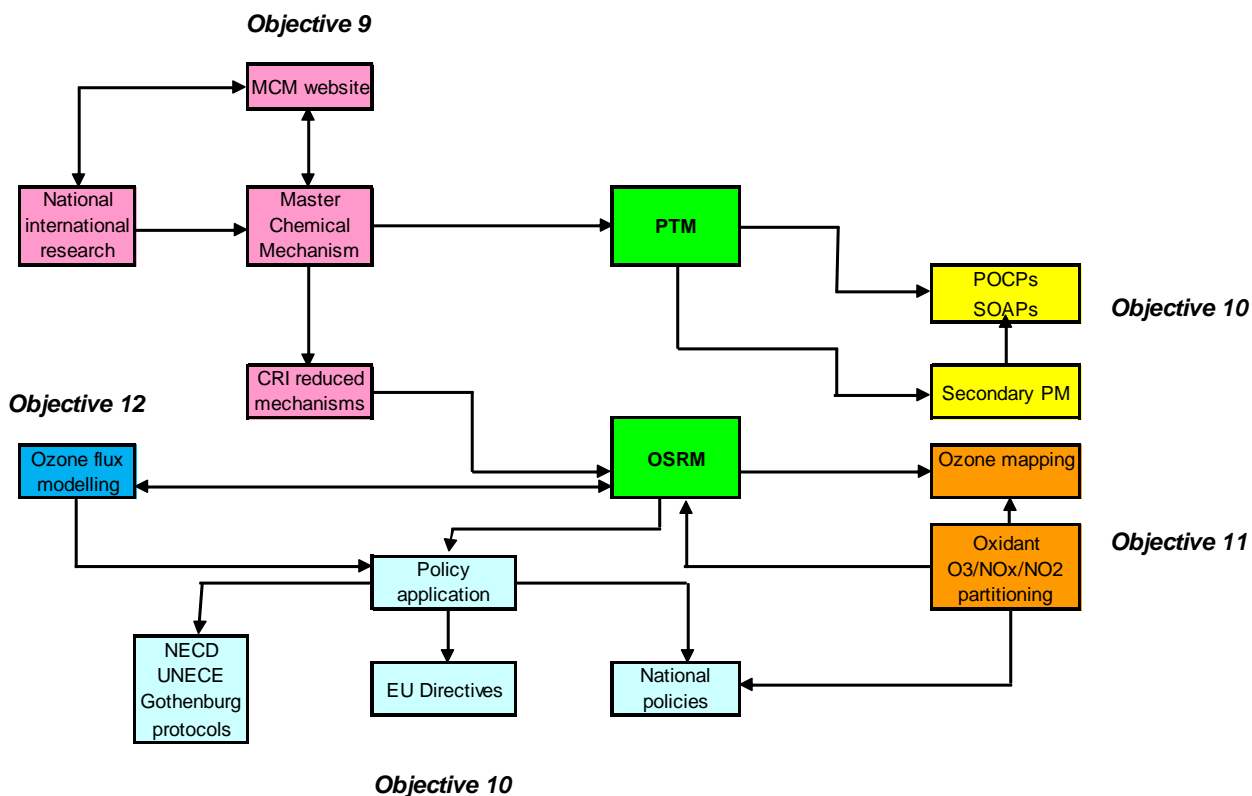
Thus the mechanism development work of Objective 9 feeds directly into the main ozone models used in this project, the OSRM and PTM, as well as other regional scale air pollution models used for Defra and EU policies. The PTM is involved in Objective 10 in evaluating models using new chemistry schemes and assessing the contribution of different sources to concentrations of ozone and secondary organic aerosols observed in the UK. The OSRM is involved in Objective 10 through describing the current and future ozone climate in the UK and modelling the impact of policies aimed at reducing precursor emissions in the UK and rest of Europe. The assessment of oxidant partitioning in Objective 11 helps to understand the spatial and temporal variability in hemispheric and regional components of background ozone and the effects of locally emitted NO$_x$ which helps to improve the mapping of ozone and NO$_2$ concentrations and improve local effects in air quality models used for Defra policy. The work of Objective 12 improves the treatment of ozone deposition in models such as the OSRM and the quantification of ozone flux to different vegetation species which in turn will help improve assessments on the impacts of ozone on crop damage for evaluating policies on ecosystem effects.

The work programme was carried out by a consortium of groups led by **AEA**. The other consortium partners were **Professor Dick Derwent (rdscientific), Dr Mike Jenkin (Atmospheric Chemistry Services) and Dr Andrew Rickard (University of Leeds)**. Each of these partners undertook specific tasks as shown in Table 2.1.

Table 2.1: Role of project partners

Project Member	Main activity
AEA	Project management.
	Modelling using the OSRM for policy support in Objective 10 and implementation of new ozone flux modelling methods in Objective 12.
rdscientific	Modelling using the PTM for policy support in Objective 10 and testing of new chemistry schemes in Objective 9
Atmospheric Chemistry Services	Development of chemistry schemes (Objective 9) and oxidant analysis (Objective 11)
University of Leeds	Development of chemistry schemes and maintenance of MCM website (Objective 9)

The project followed a schedule shown in Figure 2.2. There was some flexibility in some of the tasks to meet the policy needs of Defra, especially those relating to ad-hoc modelling and support in Objective 10. Progress was monitored through quarterly contract reports submitted to Defra and annual project meetings involving all the project partners and Defra officials.

Figure 2.2: Project schedule
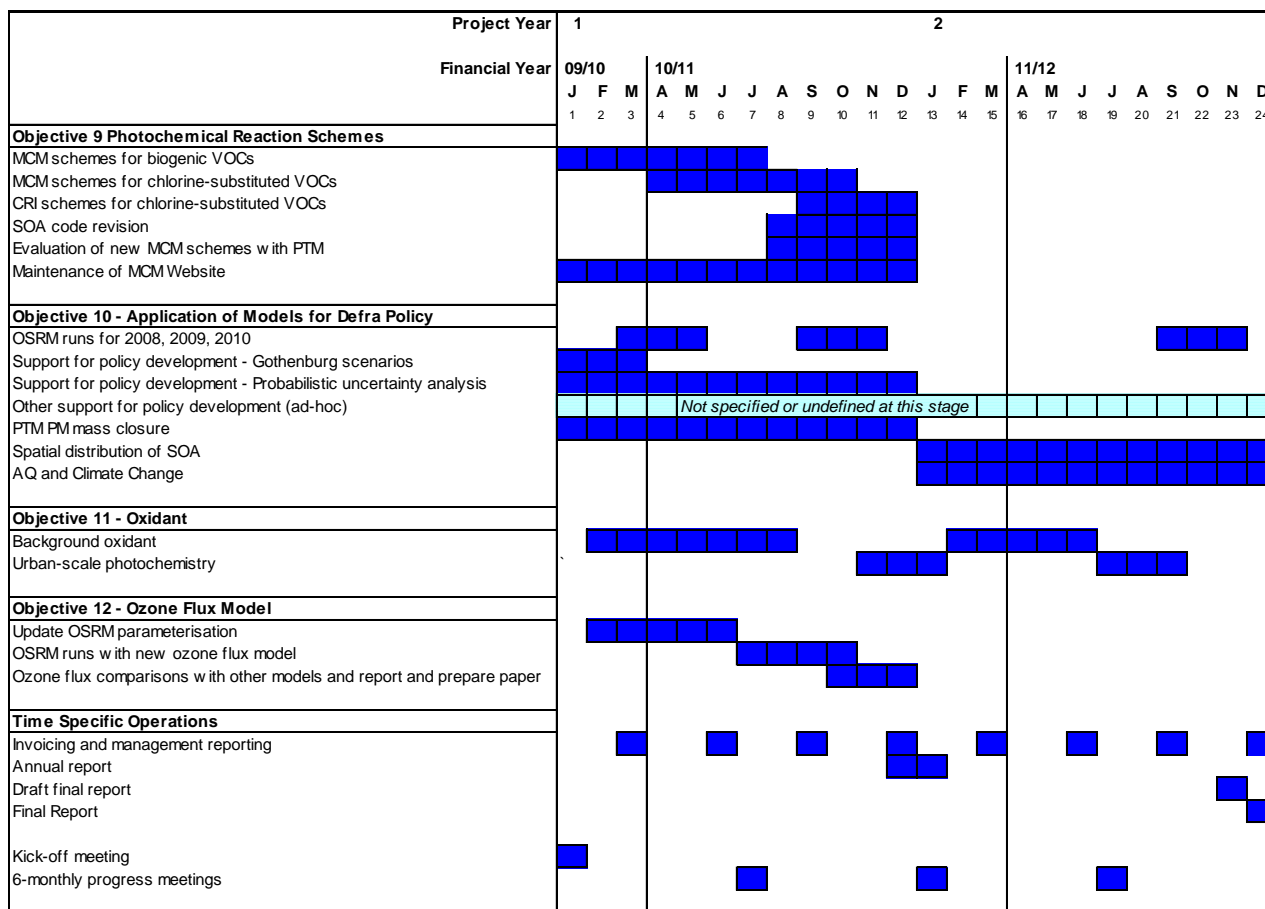
3 Improvements to Photochemical Reaction Schemes

3.1 Introduction

The **Master Chemical Mechanism (MCM)** is an internationally-recognised mechanism describing the detailed processes involved in the formation of ozone from the degradation of a large number of emitted precursor VOCs. Because of its detail in describing the intermediate organic oxidation products formed, it is also increasingly being applied to describe and understand the formation of particulates in the form of secondary organic aerosol (SOA), through gas-to-aerosol transfer of the organic oxidation products. The mechanism is thus regularly used in the scientific community as a benchmark in mechanism intercomparison and validation exercises, and in the development of reduced mechanisms.

Although the MCM is itself too large for direct use in many policy applications, traceable mechanism reduction activities carried out previously in the contract have included the development of a hierarchy of common representative intermediates (CRI) mechanisms which, for the first time, have provided a clear route for the implementation of reduced mechanisms into policy models with a demonstrably traceable link to the MCM (Jenkin et al., 2008; Watson et al., 2008; Utembe et al., 2009). This has established a platform and methodology for future advances in the scientific understanding of atmospheric chemistry to be transferred to policy models including the OSRM and PTM.

The work carried out in **Objective 9** during this phase of the project has focused on key development areas for the Master Chemical Mechanism (MCM), and for the traceable reduced mechanism, the Common Representative Intermediates (CRI) mechanism. This has included specific focuses on solvent and biogenic emissions. The work has also considered new advances in the understanding of chemistry under NO_x limited conditions which have only very recently been identified from field, laboratory and theoretical investigations and are currently not correctly described in any atmospheric chemistry mechanism. Given the trend in the UK ozone climatology towards NO_x limitation, correct representation and implementation of such processes in policy models is likely to become increasingly important for assessment of future scenarios.

Much of the work for this Objective was completed in the previous year of the project and reported in the 2010 Annual Report (Murrells et al, 2011). This report describes residual activity on this objective, which was carried out too late to appear in the 2010 annual report and was completed in 2011.

3.2 Revision of MCM schemes for chlorinated solvents and development of a reduced representation for use with the CRI mechanism

Following the general review of the chemistry of chlorine-substituted hydrocarbons reported previously, the MCM chemistry has been updated accordingly and the schemes have been released as part of MCM v3.2.

The chemistry has been used as a benchmark to consider whether it can be represented in a reduced form in the CRI mechanism. This was done using the same general procedure adopted for the original development and optimisation of CRI v2 (see Jenkin et al., 2008), and initially involved running a series of five-day box model reference simulations with

volatile organic compound (VOC) emissions in the form of each of the 15 chlorine-substituted hydrocarbons in turn, and with the chemistry represented by MCM v3.2.

A key assumption in the CRI v2 construction methodology is that the potential for ozone formation from a given volatile organic compound (VOC) is related to the number of reactive (i.e., C-C and C-H) bonds it contains. This procedure previously allowed a series of generic intermediates to be defined, with each being used as a "common representative" for a large set of species possessing the same index, as formed in the MCM. However, because the chlorinated hydrocarbons are comparatively small, and because they are a class of VOC which is distinct from those already considered in the mechanism, it was not possible to develop CRI-based chemistry with any substantial saving over that which appears in MCM v3.2. In practice, this is also the case for small VOCs in other classes (e.g., HCHO, CH_3CHO, CH_3OH), with the true saving in the CRI being for larger and more complex species.

In view of this, a compromise approach was investigated, in which the initial attack of OH on each chlorine-substituted hydrocarbon was assumed to generate a peroxy radical (or combination of peroxy radicals) already present in CRI v2 (see Table 3.1). The identities of the product peroxy radicals were adjusted to optimise the agreement with the MCM v3.2 reference simulations, using the formation of ozone as the sole criterion. This approach is therefore empirical and does not strictly follow that of CRI because the indices of the applied peroxy radicals bear no obvious or clear relationship with the bond structure of the parent VOC. However, it does provide a practical, empirical method for representing ozone formation from chlorinated hydrocarbons when using CRI v2.

The identified peroxy radical products (RO_2) which can be assigned to each of the 15 chlorine-substituted hydrocarbons are listed in Table 3.1. It must be emphasised that the use of these RO_2 species allows an acceptable description of ozone formation, but that this approach cannot be used to infer their impact on other secondary products, such as

Table 3.1: CRI peroxy radical products (RO_2) assigned to the 15 chlorine-substituted hydrocarbons

Parent VOC	MCM name	Representative RO_2 product in CRI
chloromethane (methyl chloride)	CH3CL	RN9O2
dichloromethane (methylene dichloride)	CH2CL2	RN15O2
trichloromethane (chloroform)	CHCL3	RN15O2
1,1,1-trichloroethane (methyl chloroform)	CH3CCL3	RN21O2
cis-1,2-dichloroethene	CDICLETH	RA16O2
trans-1,2-dichloroethene	TDICLETH	RA16O2
trichloroethene	TRICLETH	0.5 RA19AO2, 0.5 RA19BO2
tetrachloroethene (perchloroethylene)	TCE	RN24O2
1,2-dichloroethane	CH2CLCH2CL	RN21O2
1,1-dichloroethane	CHCL2CH3	RN21O2
1,1-dichloroethene	CCL2CH2	0.5 RA13O2, 0.5 RN18O2
1,2-dichloropropane	CL12PROP	RN12O2
chloroethane	CH3CH2CL	RN15O2
1,1,2,2-tetrachloroethane	CHCL2CHCL2	0.5 RN15O2, 0.5 RN18O2
1,1,2-trichloroethane	CH2CLCHCL2	RN18O2

oxygenated VOCs or secondary organic aerosol (SOA), because the degradation chemistry will generate organic products which cannot in practice be formed from these precursors. The performance of the approach is illustrated in Figure 3.1 for the example cases of chloromethane (methyl chloride) and 1,1,1-trichloroethane (methyl chloroform), showing that the description of ozone formation remains robust over a range of VOC/NOx emission ratios. **This therefore provides the possibility of using the CRI mechanism in solvent assessment activities which use methyl chloroform as a reference VOC**. A comparison of the average increment in ozone mixing ratio with MCM v3.2 and the empirical CRI method (compared with no VOC emissions) under base case conditions is shown in Figure 3.2 for all 15 chlorine-substituted hydrocarbons.

Figure 3.1: Comparison of ozone mixing ratios simulated from methyl chloride and methyl chloroform degradation over a five day period with MCM v3.2 (points) and CRI v2 with degradation to the existing RO$_2$ products identified in Table 3.1 (lines). Simulations were carried out for a range of 40 in VOC/NOx emission ratio (June 21 conditions, 51.5° Lat). The base case simulation was based on average 2001 UK emission densities for anthropogenic VOCs and NOx, the applied daily average densities being 15.4 kg km^{-2} day^{-1} for VOCs and 18.3 kg km^{-2} day^{-1} for NOx. The range in VOC/NOx was achieved by scaling the NOx emissions, with the figures shown (0.25 to 10) identifying the change relative to the base case.
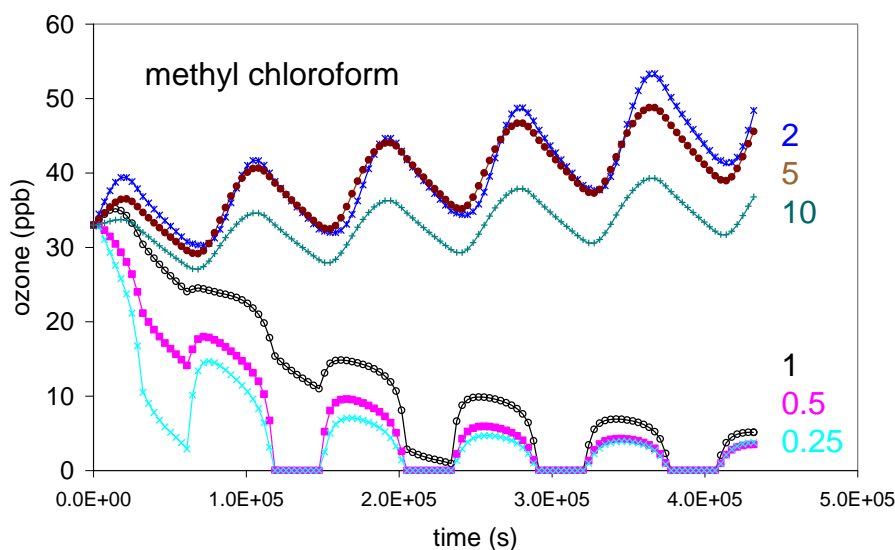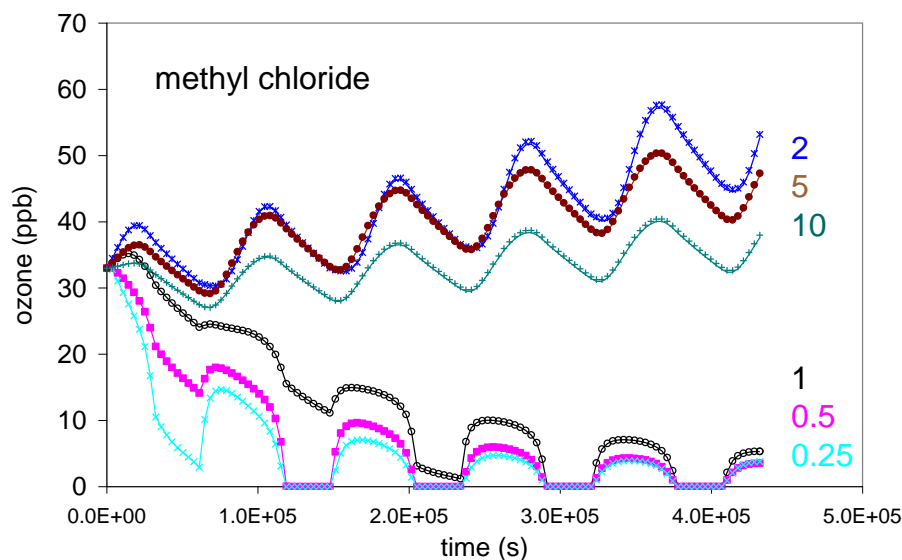
Figure 3.2: Comparison of average ozone mixing ratio increments simulated for the 15 chlorinated hydrocarbons over a five day period under base case conditions using the MCM v3.2 chemistry and the CRI v2 chemistry with degradation to the existing RO₂ products identified in Table 3.1.
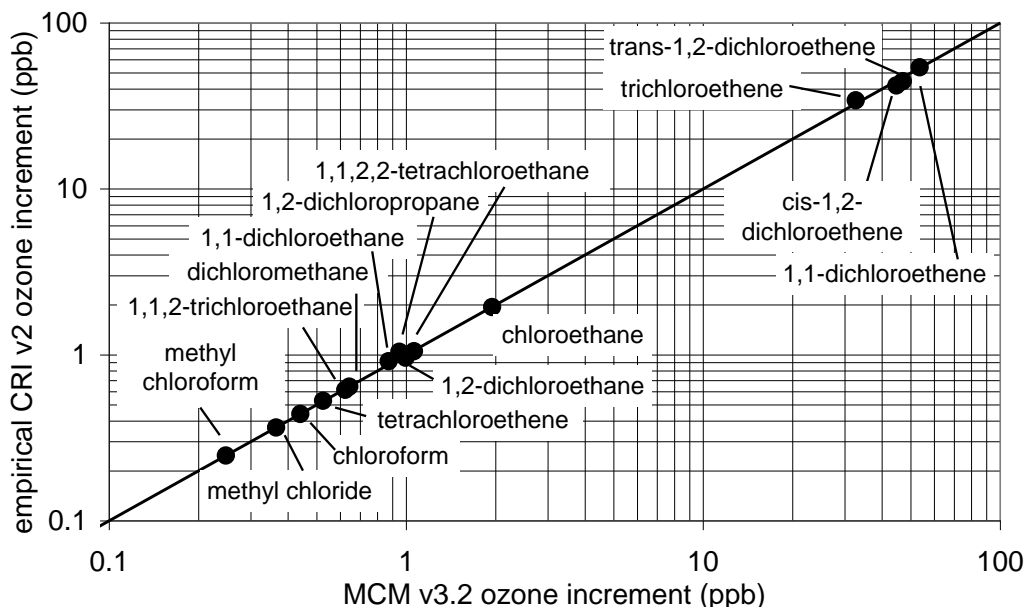
3.3 The MCM website and database

The targeted extensions and revisions to the gas phase chemical schemes within the current project (as described in the 2010 Annual Report) have been released as MCM v3.2, via the dedicated website facility (http://mcm.leeds.ac.uk/MCM/). The previous version, MCM v3.1, remains available via a link at the site.

Version 2.1 of the Common Representative Intermediates mechanism (CRI v2.1) has been released via a parallel, searchable and extractable facility. This can be accessed either via the main MCM v3.2 site, or directly at: http://mcm.leeds.ac.uk/CRI/. CRI v2.1 possesses the same reaction set at CRI v2, but has undergone some common rate coefficient revisions in parallel with those in the MCM v3.1 to v3.2 transition.

3.4 Summary and main conclusions

The main conclusions of the work of Objective 9 in 2011 on the improvements to photochemical reaction schemes are summarised as follows:

Summary:

- **The Master Chemical Mechanism (MCM) schemes for the atmospheric oxidation of chlorinated solvents have been revised and a reduced representation of the schemes in the CRI mechanism has been developed.**

- **The new schemes have been tested for a range of chlorinated VOCs and shown to perform well.**

- **This therefore provides the possibility of using models containing the new reduced schemes in future solvent assessment activities covering a wider range of solvent types.**

4 Modelling the UK Ground-Level Ozone Climate in 2009 and 2010

4.1 Ozone Source Receptor Model (OSRM)

Objective 10 involves the application of current models in support of Defra policy on ozone. One of these is the Ozone Source Receptor Model (OSRM) which has been used to model the UK's ground-level ozone climate for years 2008-2010 in Objective 10.1.

Details of the OSRM are given elsewhere in project reports and publications and only a brief description of the model is given here.

The OSRM (Hayman et al, 2010) is an established Lagrangian trajectory model that simulates the photochemical production of ozone in reactive air masses as they arrive at different receptor points in the UK. Essentially, each parcel of air picks up emissions from natural and man-made sources as it moves over land surfaces over a large spatial scale and these undergo a series of chemical reactions initiated by sunlight leading to the production of ozone. Gridded 1x1km emissions data for the UK are taken from the NAEI[1] (Bush et al, 2010) and 50x50km emissions data for the rest of Europe are taken from EMEP. Emission terms to describe natural biogenic emissions from European forests and agricultural crops are derived from the European PELCOM project. The model uses archived trajectory data from the Met Office NAME model providing boundary layer depth and other parameters. The chemical mechanism used to define the rate of ozone formation and loss is a modified version of the mechanisms used in the STOCHEM model, but an option is available to use the condensed CRIv2-R5 chemical scheme, linked to the MCM. Dry deposition processes are represented using a conventional resistance approach.

The OSRM calculates ozone concentrations at mid-boundary layer height at hourly intervals on a 10x10km grid covering the whole of the UK. These are corrected to account for loss of ozone due to reaction with local emissions of NO_x and deposition to land and sea surfaces in order to generate concentrations at ground-level.

The OSRM is also used in conjunction with a Surface Ozone Flux Model which can be used to model the uptake of ozone by different types of vegetation species under different meteorological conditions.

In conjunction with GIS-based tools, the OSRM is used to derive population- and area-weighted means of different ozone concentration metrics to provide the information necessary to Defra policy makers for cost-benefit analysis of emission reduction policies.

The previous phase of the tropospheric ozone modelling contract (2007-2009) had shown that the empirical modelling approach used in Defra's UK Ambient Air Quality Assessments (UKAAQA) model[2] traditionally gives results for ozone concentration metrics that, in model verification, are more representative of the measured concentrations than corresponding outputs provided by the OSRM. Hence, the UKAAQA modelling contract is used to provide the supplementary ozone modelling required for EU Air Quality Directive reporting on ozone to the European Commission each year on behalf of Defra. The OSRM, on the other hand, has a stronger role to play in scenario analysis and policy development as the OSRM can model future emission scenarios and the chemistry involved in forming and removing ozone over a large spatial scale from the emitted precursor gases, NO_x and VOCs. The OSRM is therefore maintained and evaluated each year using appropriate meteorology and emissions

---

[1] National Atmospheric Emissions Inventory, http://naei.defra.gov.uk/
[2] Previously referred as the Pollution Climate Mapping model (PCM)

data and comparing calculated ozone concentrations with those from the UKAAQA empirical model and with monitoring data at specific AURN sites.

The OSRM has been used to model the UK ground-level ozone climate based on meteorological conditions and emissions from 1999 to 2008 and for forecasting ozone under future UK and European-wide emission scenarios for different meteorological conditions represented by those of previous years. The model has been optimised for computational efficiency and has been a vital policy tool for Defra routinely used in quantifying the response of the UK's ground-level ozone climate to measures aimed at reducing emissions of the precursor species.

Both the UKAAQA and OSRM modelling techniques are verified against measured data to provide confidence in their performance. The two models have been compared in previous years, most recently for 2004, 2005 and 2007, which were noted as relatively "low ozone" years (Hayman et al, 2006a, Murrells et al, 2009b), 2006 which was a relatively "high ozone" year (Murrells et al, 2008) and 2008 which was a broadly moderate year for ozone concentrations (Murrells et al, 2011).

In this phase of the project for **Objective 10.1**, during 2011, the OSRM has been used to model UK ozone in 2009 and 2010. However, in order to do this, some modifications had to be made to the way the OSRM treated surface roughness to prevent model instabilities which initially occurred with the new meteorology data format provided by the Met Office. The Met Office used a new data delivery system to produce the 2009 and 2010 trajectory data required by the OSRM. This required some modifications to the OSRM meteorology data pre-processor to accommodate the new format, but led to some spurious results particularly in the maps for the AOT40 metric due to a number of locations and hours in the year where the ozone concentrations were beyond a reasonable range, either extremely high or extremely low. A series of diagnostics pinpointed the changes in surface roughness classification in the meteorology data as the cause of the problem. The Met Office explained that they had made some improvements in the way surface roughness length was represented in the Unified Model, but while these were suitable for their NAME model, they caused problems with the OSRM. The problem was resolved by modifying the new surface roughness data field to represent the traditional surface roughness in previous meteorology data provided for the OSRM.

4.2 Modelling the UK ozone climate in 2009

Monitoring data showed that ozone concentrations in 2009 were low-moderate overall as seen in Figure 4.1. This shows the annual maximum hourly ozone concentration reported at each AURN site in years between 2003 and 2009.

Figure 4.1: Annual maximum hourly ozone for all AURN sites with over 75%coverage.
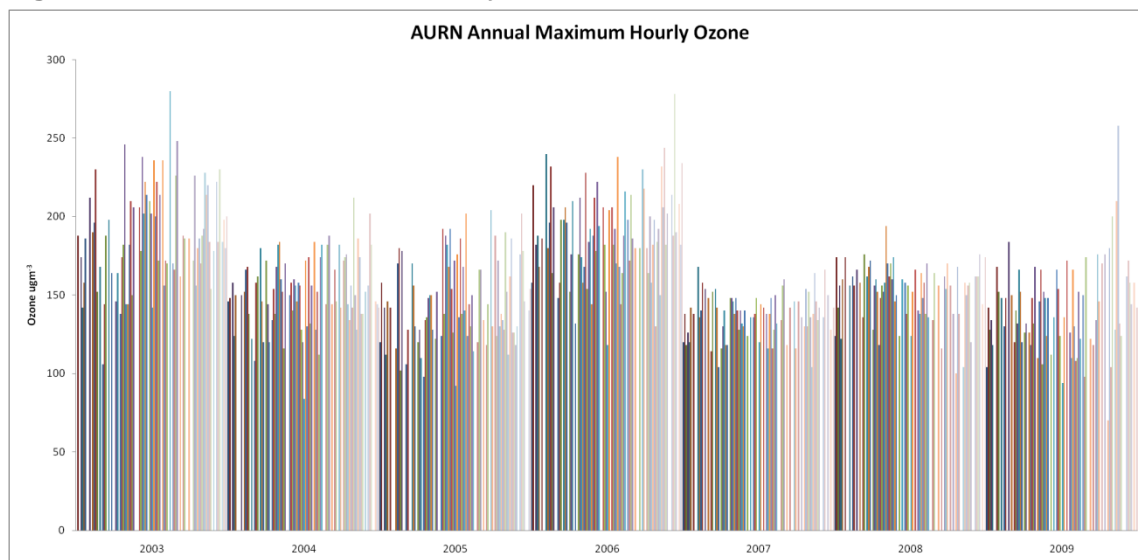
The maximum hourly concentration in the UK was 258µg m^{-3} at St Osyth (Essex) in 2009 but this was one site with relatively high values, the next highest being 200µg m^{-3}. This compares with the maximum hourly concentration value being 194µg m^{-3} (Hull) in 2008, 168 µg m^{-3} (Blackpool Marton) in 2007 and 278 µg m^{-3} (Wicken Fen) in 2006. Based on days greater than 120 µgm^{-3} and AOT40 metrics, 2009 would be better classed as a low ozone year.

The performance of the OSRM for 2009 was demonstrated for the two Long-Term Objective (LTO) metrics used in the EU Air Quality Directive reporting that correspond to the specific calendar year 2009:

- Days greater than 120 µg m^{-3} as a maximum daily running mean (Long Term Objective for Human Health)

- AOT40 (Long Term Objective for Vegetation)

The multi-year Target Value metrics will not be as good an indicator of model performance during a specific year as the Long-Term Objective metrics because averaging over several years will lessen the contribution of ozone concentrations associated with a particular year. For this reason, the metrics that the evaluation concentrated on are the single year (2009) metrics for human health and vegetation.

OSRM runs for 2009 were made by implementing 6-hourly meteorological data from the Met Office NAME model and using UK emissions inventory data for 2009. The NAEI 1x1 km emissions data for 2008 were implemented and scaled to 2009 using the NAEI emission projections (UEP38) for each pollutant and source sector. The latest EMEP emissions data for other European countries were used, re-scaled to 2009. The latest initialisation adjustment data for 2009 have been obtained from Prof Derwent based on measurements at Mace Head. Ozone concentration metrics were calculated on a 10x10 km grid and at specific AURN sites.

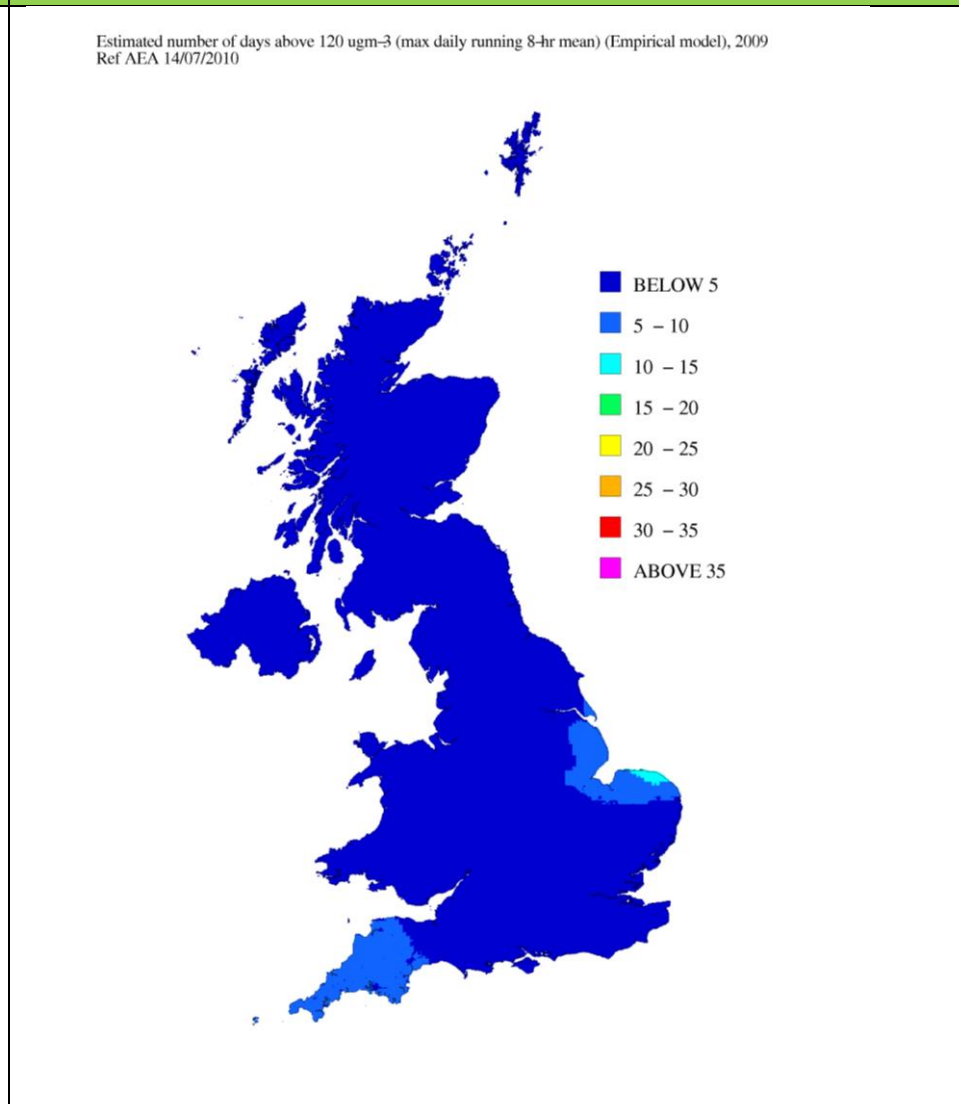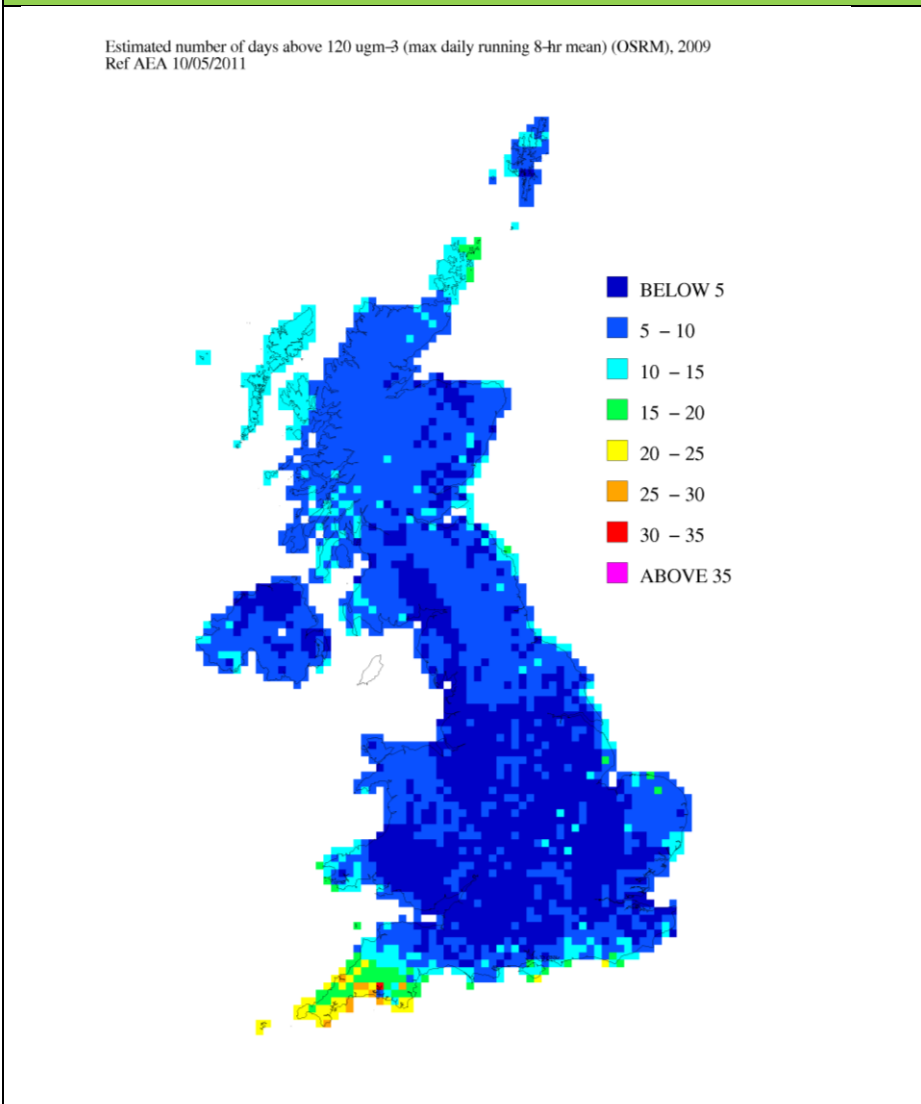### 4.2.1 Comparison of maps of OSRM and UKAAQA outputs for ozone metrics in 2009

The maps that have been generated from the outputs of the OSRM and empirical UKAAQA model for both the health and vegetation Long-Term Objective metrics are presented in Figures 4.2 to 4.5. Figure 4.2 presents the map of the number of days exceeding 120 µg m^{-3} in 2009 from the OSRM and Figure 4.3 shows the same metric output from the UKAAQA empirical model. Figure 4.4 shows the OSRM map for the AOT40 metric in 2009 and Figure 4.5 shows the corresponding map from the UKAAQA empirical model.

With 2009 being a low/moderate year for ozone, the NO$_x$ titration effect is not as apparent as it had been in 2006. Only the OSRM and UKAAQA AOT40 maps identify areas of ozone depletion due to NO$_x$ titration in large city areas and major roads. The number of days above 120 µg m^{-3} metric maps do not show the NO$_x$ titration effect as the values are too low. The UKAAQA model has a finer resolution (1km) than the OSRM (10km), so it identifies areas such as larger cities and major roads more readily than the OSRM. The empirical model utilises a modelled NO$_x$ map (described in Kent and Stedman, 2008) with a coefficient to describe the decrement in ozone concentrations with increased NO$_x$. The process also uses the latest NO$_x$-NO$_2$-O$_3$ relationships developed in Objective 11 of this project (Section 8). The OSRM uses the surface conversion post-processor in conjunction with NAEI NO$_x$ emission maps to account for the effects of NO$_x$ titration on local ozone concentrations.

The typical gradient seen in previous years, decreasing from higher concentrations in the south to lower concentrations in the north is not as clear as it was in 2006. In both the OSRM and UKAAQA maps for the number of days above 120 µg m^{-3} most of the UK is below 10 days. In 2009 the higher ozone concentrations are in the South and coastal areas. The usual pattern is a natural feature of the increase frequency and magnitude of photochemical

Figure 4.2: Number of days exceeding 120 µg m⁻³ (2009) (OSRM map)

Figure 4.3: Number of days exceeding 120 µg m⁻³ (2009) (UKAAQA empirical map)

Estimated number of days above 120 ugm-3 (max daily running 8-hr mean) (OSRM), 2009
Ref AEA 10/05/2011

Estimated number of days above 120 ugm-3 (max daily running 8-hr mean) (Empirical model), 2009
Ref AEA 14/07/2010

Figure 4.4: AOT40 (µg m^{-3}.hours) (2009) (OSRM map)	Figure 4.5: AOT40 (2009) (µg m^{-3}.hours) (UKAAQA empirical map)
Estimated AOT40 metric (OSRM), 2009 (ugm-3.hours) Ref AEA 09/05/2011	Estimated AOT40 metric (Empirical model), 2009 (ugm-3.hours) Ref AEA 15/07/2010
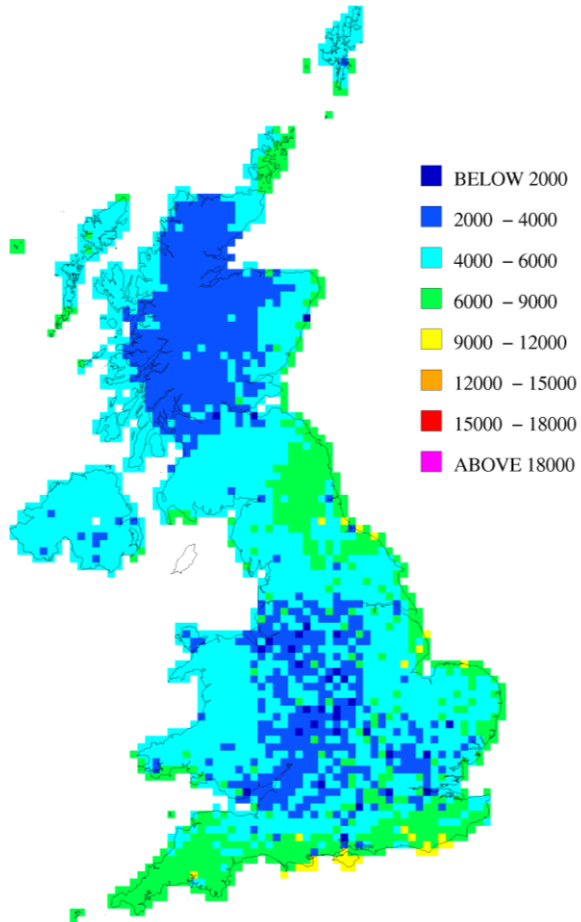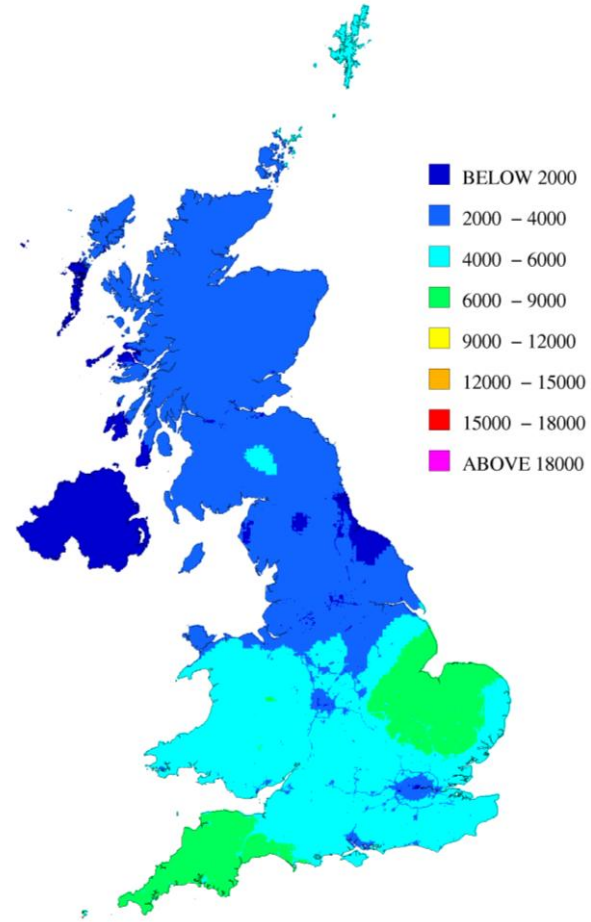
events in the more southerly and easterly areas of the UK. In previous years there have been relatively high concentrations of ozone in the north of Scotland. It has been suggested (Hayman et al, 2006b) that this may be the result of higher hemispheric background ozone concentrations here being represented in the model or intrusions of stratospheric ozone. This has not been seen in 2009.

The OSRM shows broadly similar patterns to the empirical maps, however there are some specific spatial differences. The OSRM maps estimate notably higher concentrations of ozone in the south west of the country over Cornwall that has not been captured to such an extent as in the corresponding empirical maps though these do show elevated concentrations in the south-west. The low values for the number of days greater than 120 µg m^{-3} show little spatial variation. The majority of the higher ozone concentration areas identified by OSRM in 2009 are in south and coastal fringe areas. This is consistent with OSRM outputs from previous years. This effect had been seen in previous OSRM modelled years and it has been suggested by Hayman et al (2006b) that this coastal 'edge effect' might be the result of the lack of ozone deposition over the sea surface or limitations of meteorological datasets. 2009 was a moderate ozone year and this effect is even more visible than in the higher ozone year (2006).

The highest modelled value of both the AOT40 and the days greater than 120 µg m^{-3} metrics in the empirical map were located in Cornwall. The OSRM map for the AOT40 metric is quite different to the UKAAQA map. The highest concentrations are in south west England and coastal areas. The UKAAQA identifies East Anglia as having relatively high ozone but this is not apparent in the OSRM.

4.3 Modelling the UK ozone climate in 2010

In 2010, the maximum hourly concentration in the UK was 376 µgm^{-3} measured at Weybourne. This was one site with relatively high concentrations, the next highest being at Sibton, Leamington Spa and Yarner Wood with values of 174, 170 and 168 µgm^{-3} respectively. These maximum concentrations along with the annual mean values for AOT40 and days greater than 120 µgm^{-3} would class 2010 as being a relatively low ozone year.

The OSRM was used to model ozone concentrations in the UK in 2010 in the same way as for previous years, but using 6-hourly meteorological data from the Met Office NAME model and UK emissions inventory data for 2010. The NAEI 1x1 km emissions data for 2009 were implemented and scaled to 2010 using the NAEI emission projections (UEP38) for each pollutant and source sector. The latest EMEP emissions data for other European countries were used, re-scaled to 2010. The latest initialisation adjustment data for 2010 were obtained from Prof Derwent based on measurements at Mace Head.

The only other difference between the simulations done for 2009 and 2010 is that a more streamlined version of the OSRM was used for the 2010 simulations. The streamlining merely involves more efficient use of input data such as the Mace Head boundary conditions correction factors and was introduced to bring the version of the OSRM in line with the experimental version developed with secondary organic aerosol chemistry included in it (Section 5). The streamlined version was tested in detail as described in Section 4.5.

4.3.1 Comparison of maps of OSRM and UKAAQA outputs for ozone metrics in 2010

The maps that have been generated from the outputs of the OSRM and empirical UKAAQA model for both the health and vegetation Long-Term Objective metrics are presented in Figures 4.6 to 4.9. Figure 4.6 presents the map of the number of days exceeding 120 µg m^{-3} in 2010 from the OSRM and Figure 4.7 shows the same metric output from the UKAAQA empirical model. Figure 4.8 shows the OSRM map for the AOT40 metric in 2010 and Figure 4.9 shows the corresponding map from the UKAAQA empirical model.

Figure 4.6: Number of days exceeding 120 µg m^{-3} (2010) (OSRM map)

Estimated number of days above 120 ugm−3 (max daily running 8-hr mean) (OSRM), 2010
Ref AEA 20/12/2011

BELOW 5
5 – 10
10 – 15
15 – 20
20 – 25
25 – 30
30 – 35
ABOVE 35

Figure 4.7: Number of days exceeding 120 µg m^{-3} (2010) (UKAAQA empirical map)
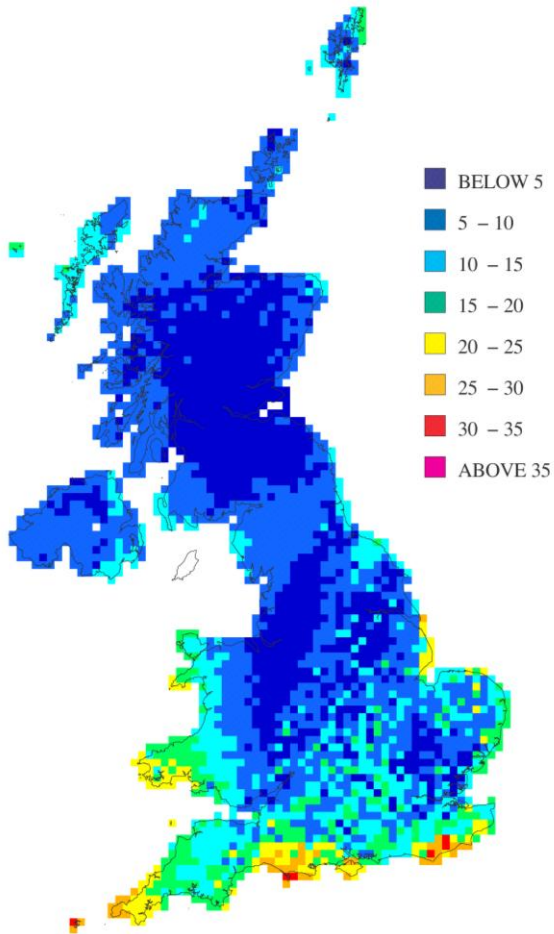
Estimated number of days above 120 ugm−3 (max daily running 8-hr mean) (Empirical model), 2010
Ref AEA 22/07/2011

BELOW 5
5 – 10
10 – 15
15 – 20
20 – 25
25 – 30
30 – 35
ABOVE 35
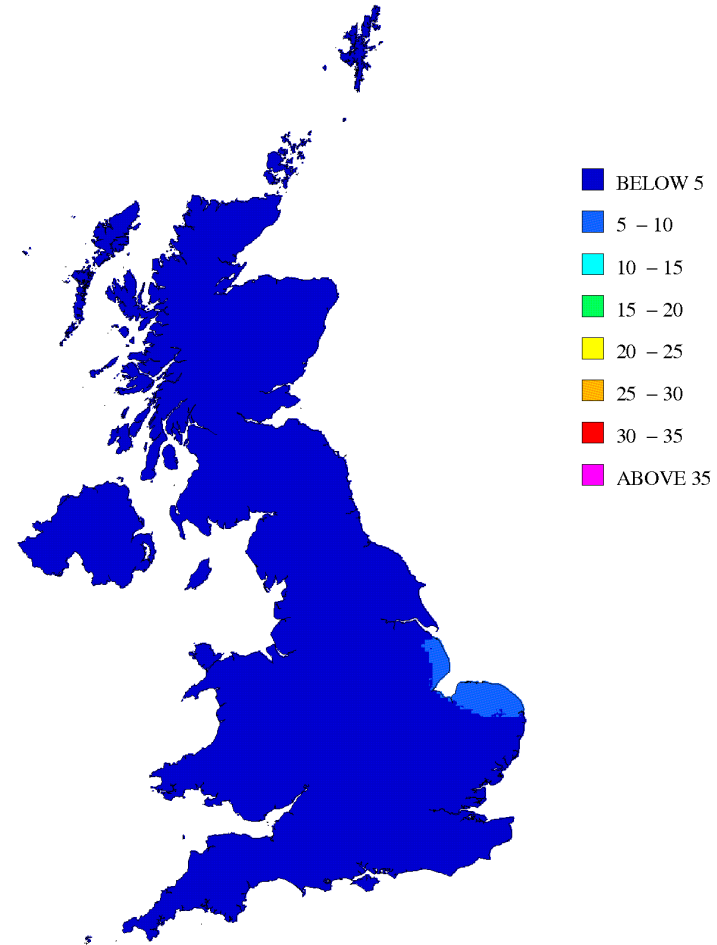
Figure 4.8: AOT40 (µg m⁻³.hours) (2010)

(OSRM map)

Estimated AOT40 metric (OSRM), 2010
(ugm-3.hours) Ref AEA 29/12/2011

BELOW 2000
2000 – 4000
4000 – 6000
6000 – 9000
9000 – 12000
12000 – 15000
15000 – 18000
ABOVE 18000
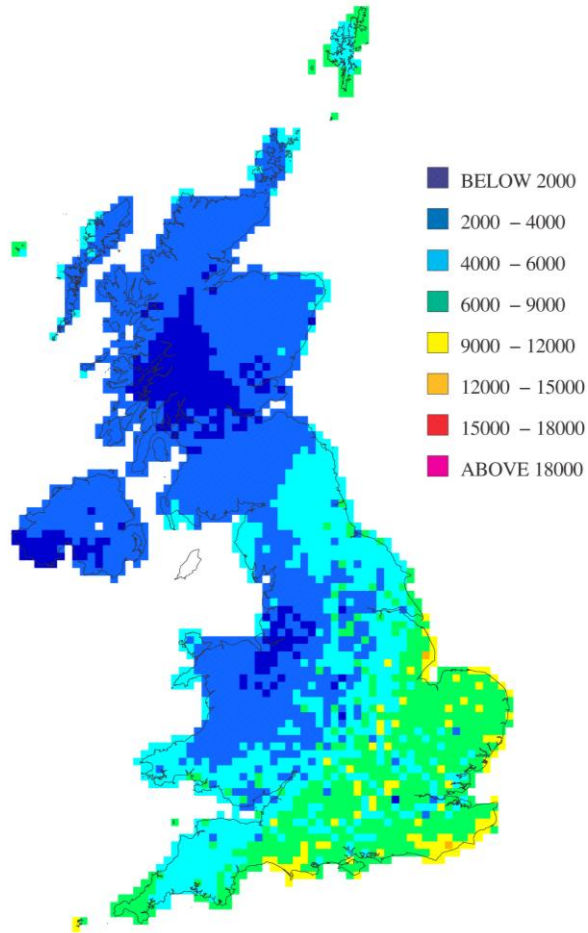
Figure 4.9: AOT40 (2010) (µg m⁻³.hours)

(UKAAQA empirical map)

Estimated AOT40 metric (Empirical model), 2010
(ugm-3.hours) Ref AEA 19/07/2011

BELOW 2000
2000 – 4000
4000 – 6000
6000 – 9000
9000 – 12000
12000 – 15000
15000 – 18000
ABOVE 18000
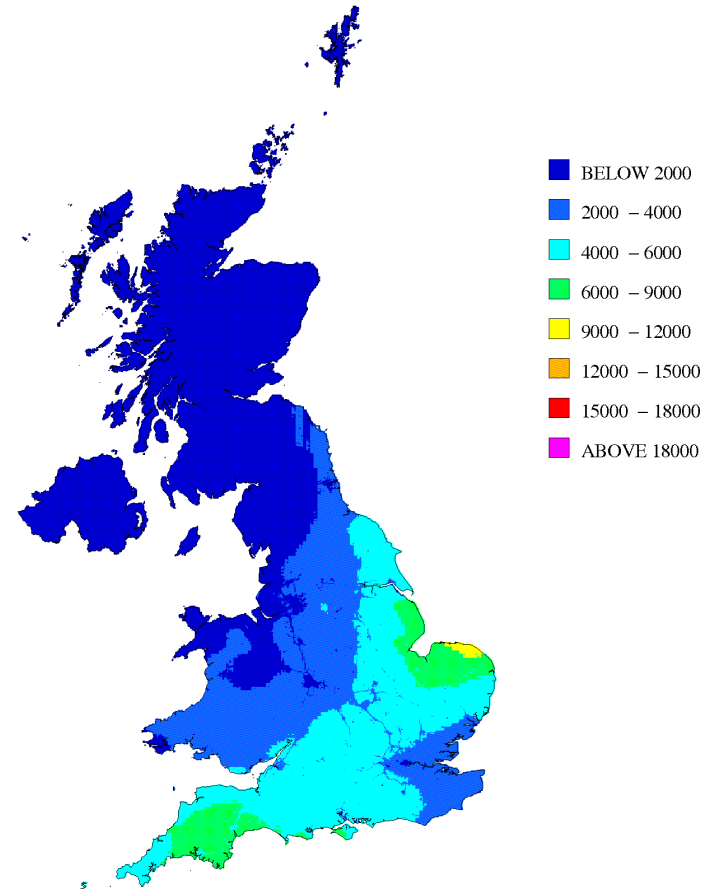
Again, with 2010 being a low year for ozone, the NO_x titration effect is not so apparent and only the OSRM and UKAAQA AOT40 maps identify areas of ozone depletion due to NO_x titration in large city areas and major roads.

The typical gradient seen in previous years, decreasing from higher concentrations in the south to lower concentrations in the north is clearly identifiable in the AOT40 maps. The highest ozone is in the south and coastal areas. For the number of days above 120 μgm^{-3} metric, the UKAAQA maps report less than 5 days for most of the UK. The OSRM predicts more days above 120 μgm^{-3} particularly around the coastal areas of Wales and Southern England. As for the 2009 simulations, the relatively high concentrations of ozone in the north of Scotland seen in previous simulations are not apparent. This may be a feature of the new meteorology data.

Again, the OSRM shows broadly similar patterns to the empirical maps, but there are some specific spatial differences. The OSRM maps estimate notably higher concentrations of ozone in the south east of the UK that have not been captured in the corresponding empirical maps. The low values for the number of days greater than 120 $\mu g\ m^{-3}$ show little spatial variation in the empirical maps. The majority of the higher ozone concentration areas identified by the OSRM in 2010 are in south and coastal fringe areas.

The highest modelled values of the AOT40 metric in the empirical map were located in East Anglia and south west of England. The OSRM map for the AOT40 metric is different showing a strong gradient with the highest concentrations in the south east and lowest in the north west. The increased ozone as a result of the coastal effect is more apparent on the days greater than 120 $\mu g\ m^{-3}$ maps.

4.4 Verification of OSRM and UKAAQA outputs for ozone metrics in 2009 and 2010

An evaluation of OSRM and UKAAQA model performance has been undertaken, comparing model results for 2009 and 2010 with measured concentrations from monitoring campaigns around the UK and against each other.

The model verification is represented in scatter plots comparing the model outputs with the corresponding measured metrics at ozone monitoring sites around the UK. Verification plots are shown for the AOT40 metric for the OSRM and UKAAQA empirical model in Figures 4.10 and 4.11, respectively, for 2009 and Figures 4.12 and 4.13, respectively, for 2010. The verification statistics for the days greater than 120 $\mu g\ m^{-3}$ metric have not been included because in both years the mean number of days were so low (around 1 day) that the statistical parameters become meaningless.

Two groups of sites are presented in the verification charts and summary tables:

- national network (AURN) monitoring sites
- verification sites

The AURN sites were used as a direct input to the UKAAQA empirical model and therefore provide a useful check during the verification process, but are not able to provide a completely independent representation of model performance. For this reason there is a separate group of sites labelled 'verification sites' that are completely independent from the UKAAQA model. These typically come from local authorities, research institutions and *ad-hoc* monitoring campaigns for which AEA holds and ratifies the data. These monitoring data are ratified to the same standard as the AURN. Both groups of sites provide an independent verification of the OSRM because this is a process model which does not use monitoring data as an input or a calibration method. A data capture threshold of 75% has been applied to the monitoring data prior to analysis.

Figure 4.10: OSRM verification: 2009 (AOT40, µg m^{-3}.hours)

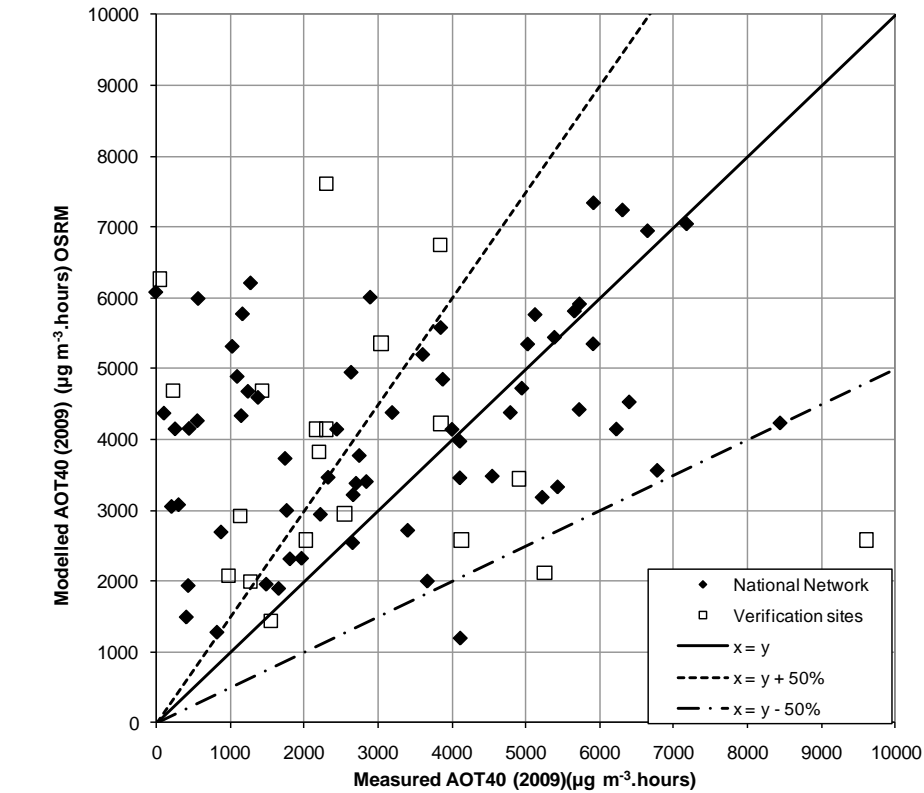**Figure 4.11: UKAAQA empirical model verification: 2009 (AOT40, µg m^{-3}.hours)**
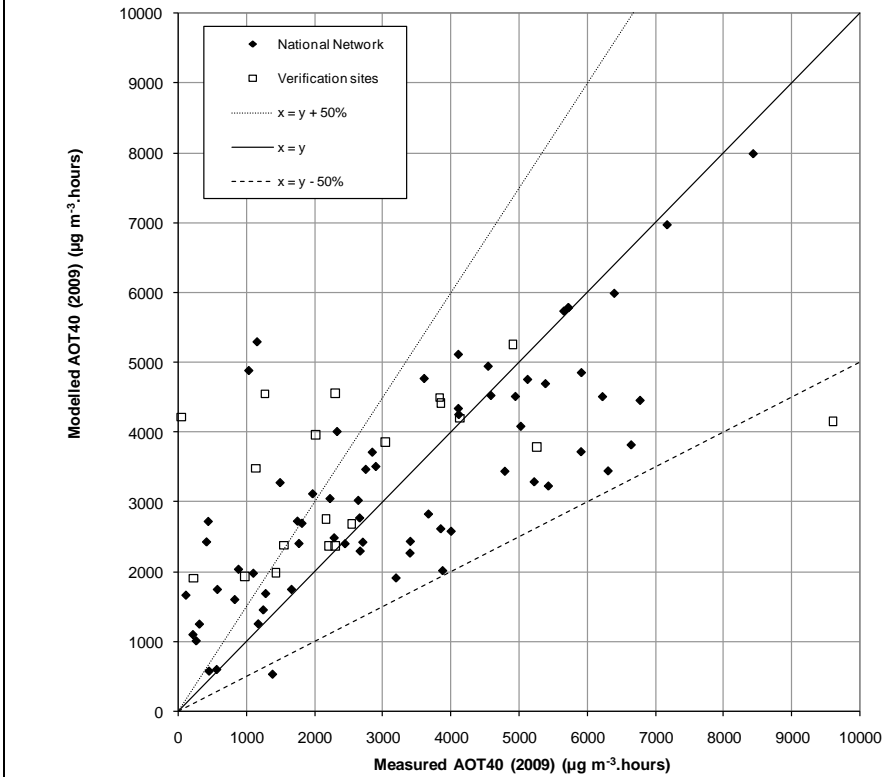
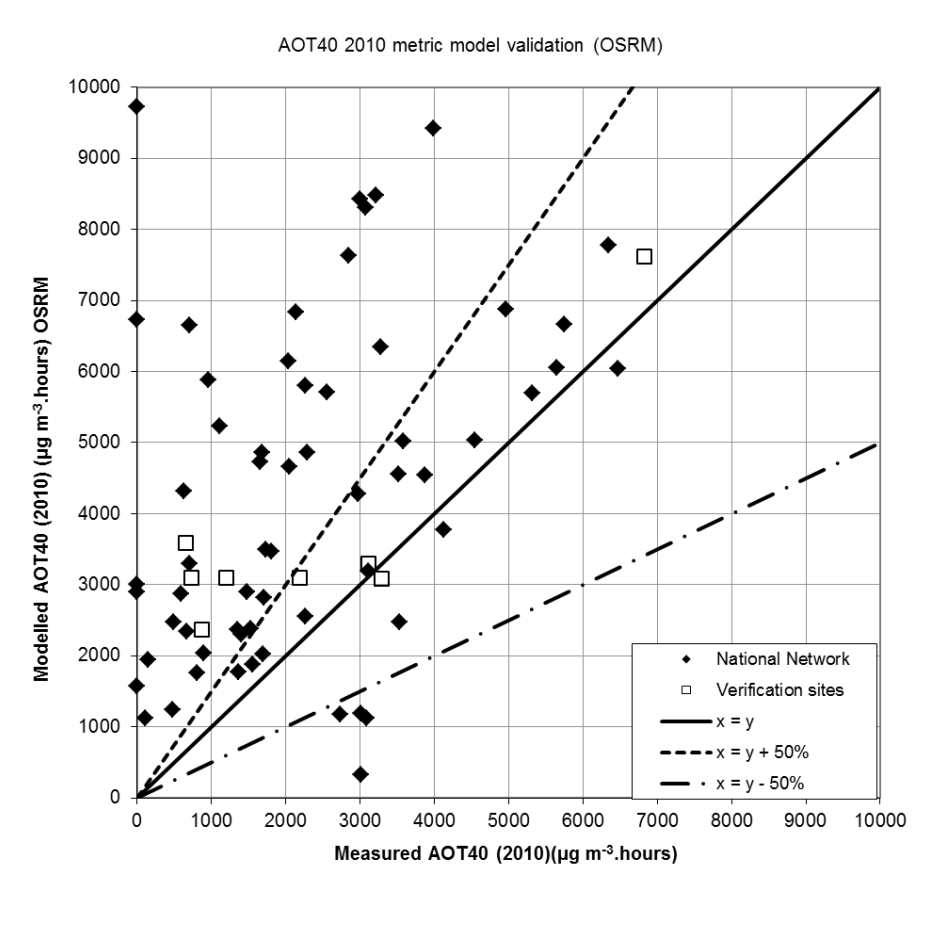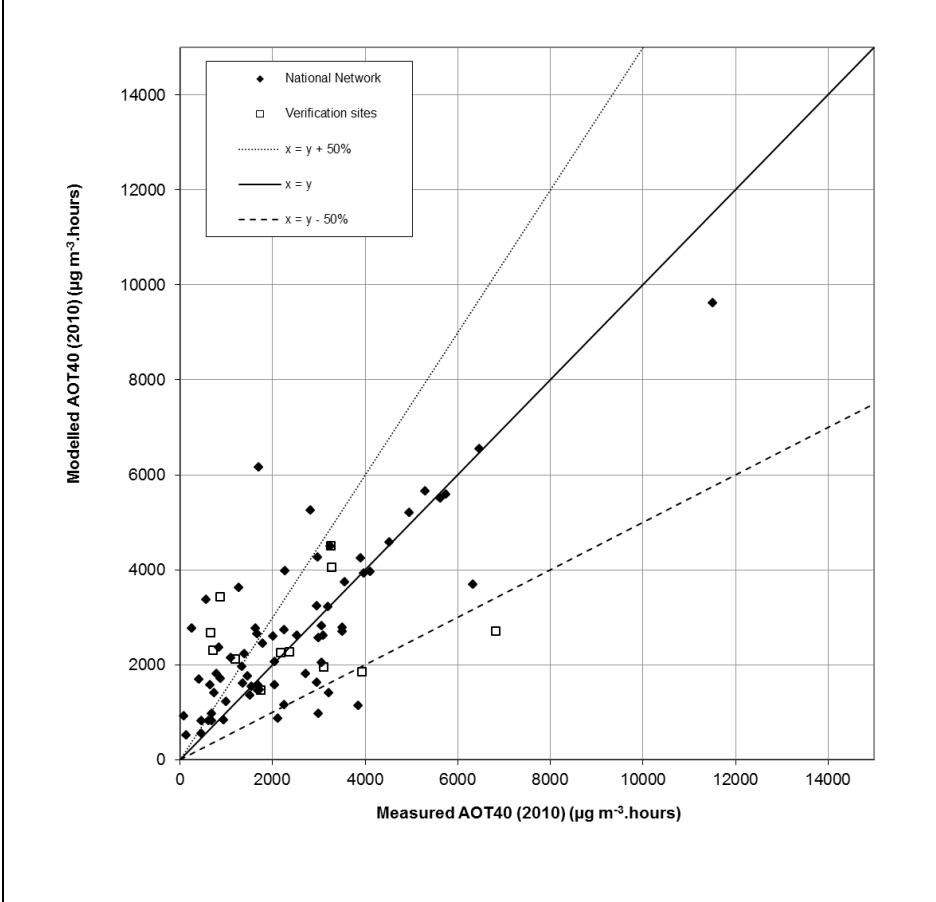**Figure 4.12: OSRM verification: 2010 (AOT40, µg m⁻³.hours)**

AOT40 2010 metric model validation (OSRM)

Figure 4.13: UKAAQA empirical model verification: 2010 (AOT40, µg m⁻³.hours)

The verification charts also present a 1:1 line and lines representing the data quality objectives (DQO) defined in the EU Air Quality Directive (+/- 50%).

Corresponding summary tables (Tables 4.1 and 4.2) are also provided which display the average of the measured AOT40 concentrations, the average of the modelled estimates, the R^2 of the fit line, the number of monitoring sites used and the percentage of these monitoring sites that fall outside the DQO.

Table 4.1: OSRM verification summary – AOT40 metric

AOT40 metric	Year	Mean of measurements (µg m^{-3}.hours)	Mean of model estimates (µg m^{-3}.hours)	R^2	% outside DQO	No. sites used in assessment
National network	2009	3182	4274	0.12	35.8	67
Verification sites	2009	2738	3818	0.03	70.0	20
National network	2010	2244	4404	0.11	61.4	57
Verification sites	2010	2518	4150	0.17	50.0	12

Table 4.2: UKAAQA empirical model verification summary – AOT40 metric

AOT40 metric	Year	Mean of measurements (µg m^{-3}.hours)	Mean of model estimates (µg m^{-3}.hours)	R^2	% outside DQO	No. sites used in assessment
National network	2009	3182	3262	0.60	23.9	67
Verification sites	2009	2738	3463	0.21	45.0	20
National network	2010	2244	2620	0.41	24.6	57
Verification sites	2010	2518	2619	0.02	50.0	12

For the AOT40 metric, the OSRM generally over predicted concentrations and the UKAAQA empirical map performed better.

Past analysis (Hayman et al, 2006b) has shown that the OSRM has slightly under predicted measured concentrations in some cases and slightly over predicted measured concentrations in others. In general, it has under predicted ozone metrics in high ozone years (e.g. 2003 and 2006) and slightly overpredicted ozone metrics in low ozone years (2004, 2005 and 2007, Murrells et al, 2009b). In 2008 which was considered a moderate ozone year, the OSRM generally underpredicted AOT40 concentrations.

Tables 4.3 and 4.4 below present the average measured and averaged modelled results from OSRM for the years 2004-2010. These illustrate the model performance during high (2006) and low (2004, 2005, 2007) years for both metrics. The difference between the concentrations predicted by the OSRM and the measured concentrations is larger for 2006 than for 2004, 2005, 2007 and 2008. In 2010, the AOT40 result would indicate a low ozone year similar to 2007, but there were more days greater than 120 µg m^{-3} predicted than measured. The 2009 and 2010 OSRM results are not directly comparable with earlier years because of model improvements to emissions, boundary conditions and changing to the new meteorology data format.

The results tend to show that the OSRM overestimates ozone concentrations more in 2010 than in 2009.

Table 4.3: Days greater than 120 μg m^{-3}. OSRM results from 2004-2010

Year modelled	NAEI Year	National network		Verification sites	
		Mean of measured	Mean of modelled	Mean of measured	Mean of modelled
2004	2004	13	12	7	6
2005	2004	3	6	4	5
2005	2005	3	6	4	5
2006	2005	13	8	8	8
2007	2006	2	4	2	6
2008	2007	5	6	5	7
2009	2008	1	4	1	4
2010	2009	1	8	2	9

Table 4.4: AOT40 (μg m^{-3}.hours). OSRM results from 2004-2010

Year modelled	NAEI Year	National network		Verification sites	
		Mean of measured	Mean of modelled	Mean of measured	Mean of modelled
2004	2004	2888	2056	3681	2256
2005	2004	3650	4165	3810	3088
2005	2005	3650	4099	3810	3372
2006	2005	10497	5043	5061	6574
2007	2006	2281	4503	3061	5211
2008	2007	6025	4444	4913	4559
2009	2008	3182	4274	2738	3818
2010	2009	2244	4404	2518	4150

4.5 Further evaluation of restructured versions of the OSRM

During the 2011 reporting year of the project, a version of the OSRM was developed with a new chemical mechanism (CRI-SOA) derived from the MCM to model secondary organic aerosol formation (SOA). This work is described in Section 5, but the version developed had not kept in line with further developments in the original version used for the 2009 ozone simulation such as the way the Mace Head corrections to the boundary conditions were treated. Both OSRM codes which are in effect the same except in the chemical mechanism (OSRM original and OSRM-CRI) were restructured to bring them to the same level of development in all other respects and provide a format to keep them in line in future. As a result, the Mace Head correction factors are read in as input data without the need to create a new version of the OSRM each year with new hard-wired correction factors, so any future

developments of the OSRM can be incorporated into just the two versions (original and CRI versions) going forward.

An evaluation of the restructured versions of the OSRM was undertaken using the tools and methods developed as part of the Defra Model Intercomparison Protocol to test that the restructuring did not change the OSRM predictions of ozone formation in the original model and to show how the two versions differing only in terms of chemical mechanism compared with respect to ozone predictions. This exercise was in itself a useful model performance evaluation of the original OSRM.

Four versions of the OSRM were actually compared:

1. OSRM.orig   - the original version of OSRM (v24b) used for the 2009, 2008 (and preceding years) simulations
2. OSRM.new   - the restructured code with Mace Head boundary correction (v26o)
3. OSRM.xMH   - the restructured code without Mace Head boundary correction (v26o)
4. OSRM.CRI   - the restructured code using CRI-SOA chemical mechanism with Mace Head boundary correction (v26c, i.e. the OSRM-CRI version)

The correlation coefficient (r) is used to measure the strength of the linear relationship in ozone concentrations between the original version of the OSRM and the new restructured versions. The correlation coefficients were derived for relationships at individual sites (Table 4.5) and across each month of the year (Table 4.6) in 2009. The values of r = 1 for OSRM.new indicate perfect linear relationships.

The differences between OSRM.orig and OSRM.xMH reflect the effect of the Mace Head boundary correction. However, the relationship remains linear with r=0.98-1.00.

As described before the OSRM.CRI tends to predict higher ozone concentrations, but the correlation coefficient remains strong with r=0.89-1.00. The correlation is lowest during the summer months where the differences in modelled ozone concentrations between the original and CRI versions of the OSRM are greatest. This may be due to the inclusion of the more explicit biogenic VOC chemistry in the CRI version which was required for SOA processing.

Figures 4.14-4.18 are other evaluation plots for comparing the different OSRM versions. Figure 4.14-4.16 show Mean Bias for hourly ozone concentration ranges, FAC2 (model values within a factor of 2 of the observation) and Mean Bias for the 8hr rolling mean at different sites. Figures 4.17 and 4.18 show plots of AOT40 and the weekend-weekday variation in concentrations, respectively.

The performance statistics are very similar for OSRM.new and OSRM.orig. The version without Mace Head correction performs slightly worse. The CRI version tends to overestimate ozone in 2009 and does not perform as well as the original version.

Figure 4.14 shows that the bias is different at different sites and is most apparent for the highest ozone concentration range. Figure 4.15 shows that all versions perform relatively well with more than 50% of paired model-observation values within a factor of 2 for all sites. Figure 4.16 shows that the mean bias of the rolling 8 hr mean is more variable with some sites, e.g. Bush Estate, performing well and others, e.g. Harwell, not so well.

The overestimation of the OSRM.CRI is amplified in the AOT40 comparison shown in Figure 4.17 with none of the sites performing within the 1:2 and 2:1 range. This also shows up slight differences in the OSRM.orig and OSRM.new versions. Taking all the data into account the differences in the two versions is within the bounds of mathematical variation although the differences between these versions are greater for the AOT40 metric.

Figure 4.18 shows that there is no difference between the models for weekend and weekday variation in ozone concentrations.

Table 4.5: Correlation coefficient between the original and the new versions of the OSRM at 15 rural sites relative to OSRM.orig.

Site	OSRM.new	OSRM.xMH	OSRM.CRI
Aston.Hill	1.00	0.99	0.97
Bottesford	1.00	0.99	0.97
Bush.Estate	1.00	0.98	0.96
Eskdalemuir	1.00	0.98	0.97
Glazebury	1.00	0.99	0.97
Harwell	1.00	0.99	0.97
High.Muffles	1.00	0.99	0.97
Ladybower	1.00	0.99	0.97
Lough.Navar	1.00	0.98	0.96
Lullington.Heath	1.00	0.99	0.97
Rochester	1.00	0.99	0.97
Sibton	1.00	0.99	0.95
Strath.Vaich	1.00	0.98	0.97
Wicken.Fen	1.00	0.99	0.96
Yarner.Wood	1.00	0.99	0.97
All sites	**1.00**	**0.99**	**0.97**

Table 4.6: Correlation coefficient between the original and the new versions of the OSRM for each month of 2009 relative to OSRM.orig.

	OSRM.new	OSRM.xMH	OSRM.CRI
January	1.00	1.00	1.00
February	1.00	1.00	0.99
March	1.00	1.00	0.99
April	1.00	1.00	0.94
May	1.00	1.00	0.93
June	1.00	0.98	0.89
July	1.00	0.99	0.91
August	1.00	0.98	0.90
September	1.00	0.99	0.96
October	1.00	1.00	0.97
November	1.00	0.99	0.99
December	1.00	1.00	0.99
2009	**1.00**	**0.99**	**0.96**

Figure 4.14: Mean Bias of hourly ozone for concentration ranges.
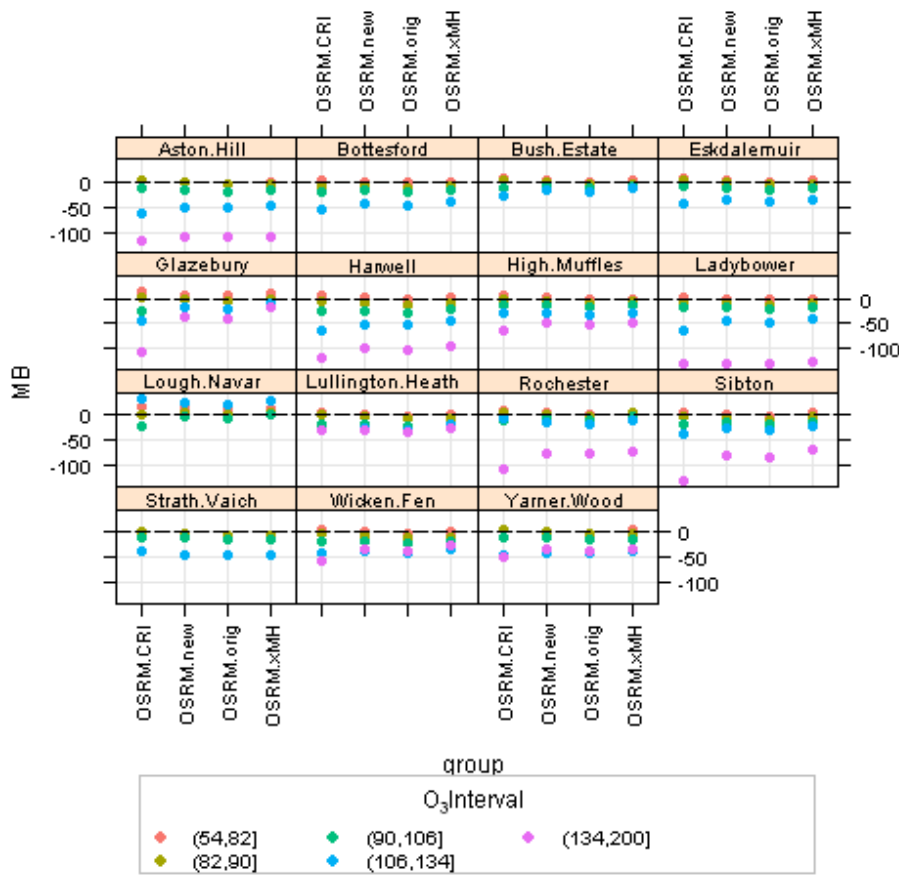

Figure 4.15: Proportion of model values within a factor of 2 of the observation.
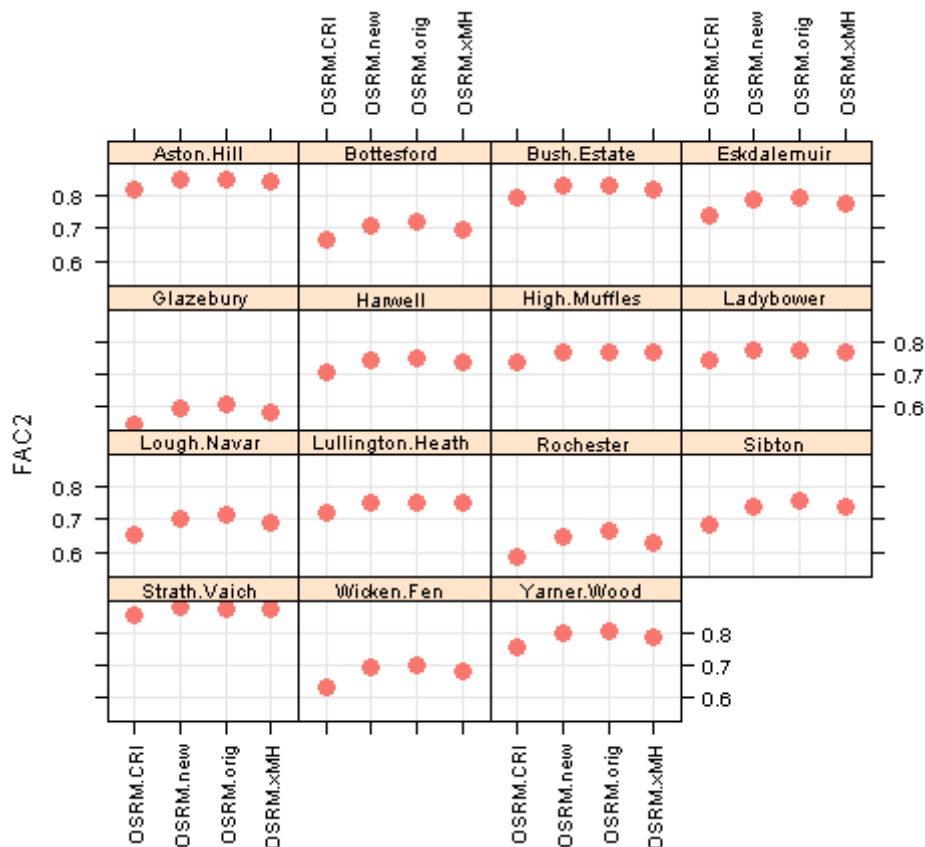
Figure 4.16: Ozone - Mean Bias of the rolling 8hr
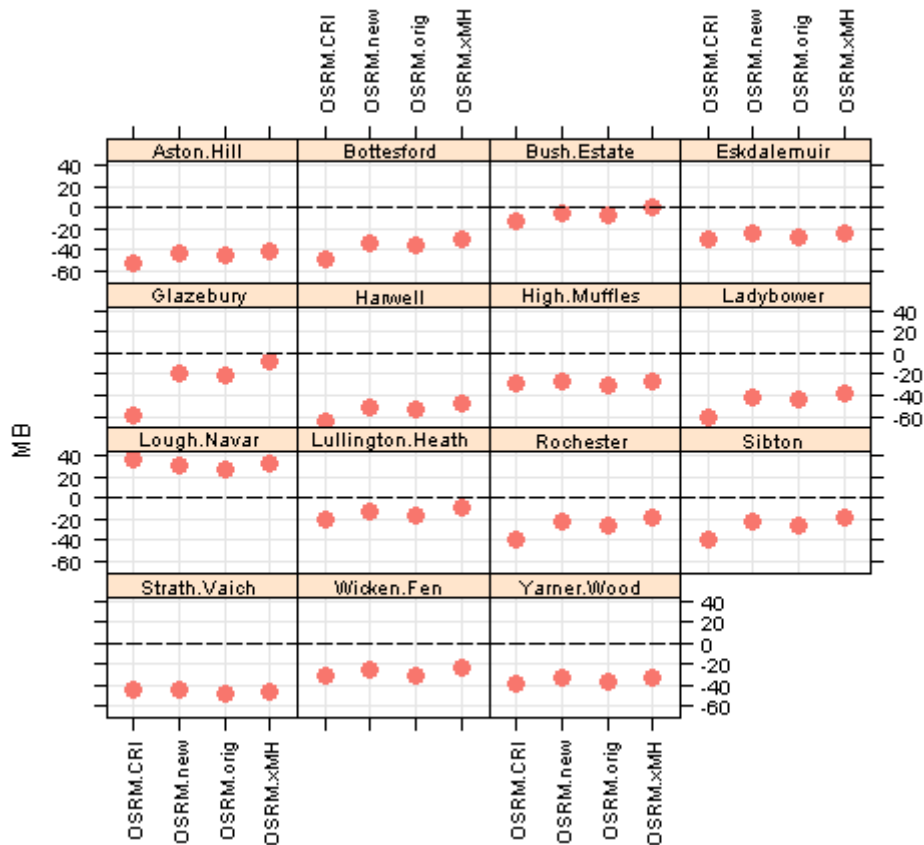
Figure 4.17: AOT40 for each model.
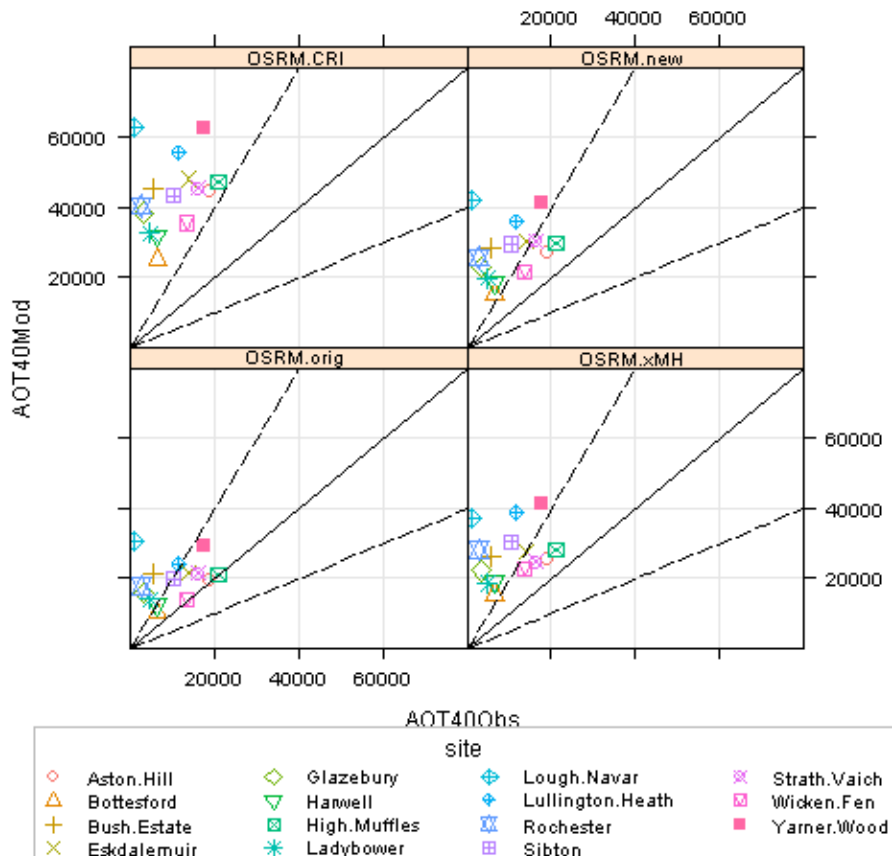
Figure 4.18: Ozone - Weekend-Weekday variation for each model.
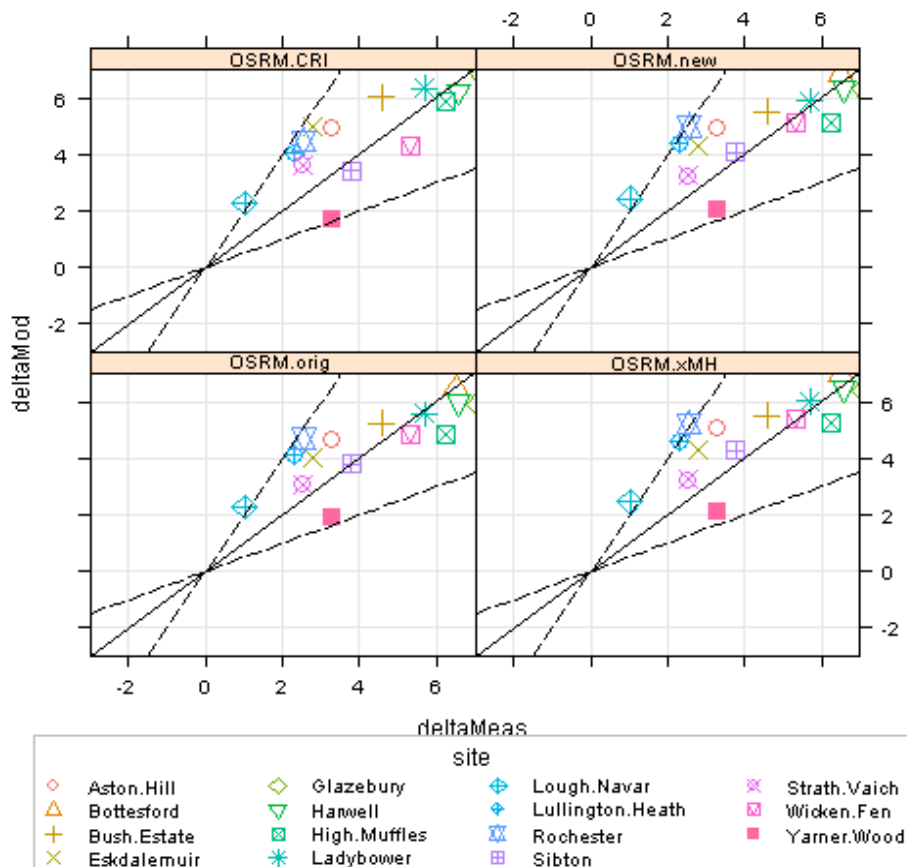
The tests have demonstrated that the new, restructured OSRM code (v26o) which was used for the 2010 simulation performs almost identically to the original version used for the 2009 simulation.

4.6 Summary and main conclusions

The main conclusions of the work of Objective 10.1 on modelling the UK ozone climate for 2009 and 2010 using the OSRM are summarised as follows:

Summary:

- **Both 2009 and 2010 were predominantly low ozone, but showed some characteristics of being moderate ozone years.**

- **When comparing the OSRM results for 2009 and 2010 with measured data for the two EU Air Quality Directive metrics the OSRM generally overestimated concentrations in both years. The OSRM overestimates ozone concentrations more in 2010 than in 2009.**

- **This is consistent with the way the OSRM has overestimated these ozone metrics in previous low ozone years (2004, 2005 and 2007)**

- **The model code for the original version of the OSRM and the CRI-SOA version have been restructured to bring them to the same level of development, and provide a format to keep the versions in line in the future. The difference between the two versions is in terms of the chemical schemes used.**

- **The original version was used for the 2009 simulation, but the new version**

was used for the 2010 simulation. Performance evaluations showed that the original and new versions of the OSRM performed the same within acceptable limits.

5 Modelling Secondary Organic Aerosol Formation with the OSRM

5.1 Introduction

Secondary organic aerosols (SOA) are an important secondary component of PM_{10} and $PM_{2.5}$ mass concentrations. They are formed by a series of gas phase reactions in the atmosphere analogous to those involved in forming ozone followed by gas to particle conversion processes. Modelling SOA formation therefore requires the same type of chemical transport models used for regional ozone modelling.

A chemical mechanism for SOA formation was developed previously in Phase I of this project for the MCM and its reduced derivative chemical schemes, the CRIv2. These have been used with the Photochemical Trajectory Model to calculate SOA concentrations at specific receptors. Work in **Objective 10.3** has also involved implementing the latest reduced chemical mechanism for SOA into the OSRM and testing the performance of the model in predicting SOA by comparing with results from other models and with measurements.

This section describes the setting up of the chemical scheme in the OSRM and an assessment of model results at specific sites in 2006, 2007 and 2008. It also includes the development of maps showing the spatial distribution of SOA concentrations in 2009.

5.2 Implementing the CRIv2-R5 chemical scheme for SOA in the OSRM

As described in detail previously (Utembe et al., 2009), the formation of SOA is represented in terms of the equilibrium partitioning of oxidation products between the gas and condensed organic phases, according to the following relationship (Pankow, 1994):

$$C_a/C_g = K_p C_{om} \tag{1}$$

where C_a and C_g are the concentrations of a given species in the condensed organic and gas phases, respectively, C_{om} is the total mass concentration of condensed organic material in units of $\mu g\ m^{-3}$, and K_p is the species-dependent partitioning coefficient ($m^3\ \mu g^{-1}$). Phase partitioning is represented for the 14 species in the most reduced form of the CRI mechanism, CRI v2-R5, shown in Table 5.1. These comprise ten terpene-derived biogenic species, one isoprene-derived biogenic species, and three aromatic hydrocarbon-derived species. Each species acts as a surrogate, used to represent a set of species in the MCM code (also identified in Table 5.1), which were found to make major contributions to each class of SOA in case study scenarios over the wide range of pollution conditions that were considered in the original MCM simulations (see Utembe et al., 2009). The values of K_P assigned to the surrogate species are based on those of the closest MCM v3.1 analogue species (determined as described by Johnson et al. 2006 and optimised empirically as described by Utembe et al., 2009), with those for the sets of aromatic, terpene-derived biogenic and isoprene-derived biogenic species being scaled independently, in order to optimise agreement with results from the MCM v3.1 reference simulations (see Utembe et al., 2009).

Table 5.1: Summary of species used to represent SOA formation from CRI v2-R5 in OSRM.

CRI v2 species	Description	Closest MCM analogue(s)
Biogenic species		
RTN28OOH	First-generation α−pinene product containing -*OH* and -*OOH* groups	APINAOOH, APINBOOH, APINCOOH
RTN28NO3	First-generation α−pinene product containing -*OH* and −*ONO$_2$* groups	APINANO3, APINBNO3, APINCNO3
RTX28OOH	First-generation β−pinene product containing -*OH* and -*OOH* groups	BPINAOOH, BPINBOOH, BPINCOOH
RTX28NO3	First-generation β−pinene product containing -*OH* and -*ONO$_2$* groups	BPINANO3, BPINBNO3, BPINCNO3
RTN26OOH	Second-generation α−pinene product containing -*C(=O)-* (x2) and -*OOH* groups	PINALOOH, PERPINONIC
RTN26PAN	Second-generation α−pinene product containing -*C(=O)-* and -*C(=O)OONO$_2$* groups	C10PAN2
RTN25OOH	Second-/third-generation α−pinene product containing -*C(=O)-* and -*OOH* groups	C96OOH
RTN24OOH	Second-/third-generation α−pinene product containing -*OH, -C(=O)-* and -*OOH* groups	C97OOH
RTN23OOH	Second-/third-generation α−pinene product containing -*OH, -C(=O)-* (x2) and -*OOH* groups	C98OOH
RCOOH25	First-/second-generation α−pinene product containing -*C(=O)-* and -*C(=O)OH* groups	PINONIC
RU12OOH	Second-generation isoprene product containing -*OH* (x2), -*C(=O)-* and -*OOH* groups	C57OOH, C58OOH, C59OOH
Anthropogenic species		
ARNOH14	Second-generation benzene product containing -*OH* and -*ONO$_2$* groups	HOC6H4NO2
ARNOH17	Second-generation toluene product containing -*OH* and -*ONO$_2$* groups	TOL1OHNO2
ANHY	Second-generation cyclic anhydride product of aromatic oxidation	MALANHY and substituted analogues

The CRIv2-R5 mechanism containing SOA chemistry had previously been incorporated into a new version of the OSRM, but the model had not been activated and optimised for producing SOA outputs. This version of the OSRM was activated and the biogenic emissions updated and the final version (CRI-SOA) standardised by introducing other recent improvements made to the main OSRM version used for ozone modelling as described in Section 4.5.

The SOA code was incorporated and activated using the instructions sent by Dr Mike Jenkin and Steve Utembe who had developed the code and also implemented it to other models including the PTM. The initial experimental version of the OSRM with the CRIv2-R5 mechanism had been tested for modelling ozone and had categorised all biogenic emissions as isoprene. However, as 10 of the 11 biogenic SOA species were formed from $\alpha-$ and $\beta-$pinene this version of the OSRM had to be updated to account for the extra biogenic emissions.

The SOA module describes the organic aerosol (OA) mass loading in terms of three components. These are Primary Organic Aerosol (POA), Secondary Organic Aerosol (SOA) and Background Organic Aerosol (BGOAM). These are summed to calculate the total Mass concentration of Organic Aerosol (referred to here as TMOA, but referred to in previous reports as MOM). All values are mass concentrations in μgm^{-3}. The SOA can be subdivided into biogenic (BSOA) and anthropogenic (ASOA) derived components. POA represents the OA emitted directly into the atmosphere from anthropogenic sources. The emissions are defined as relative to those of NO_x according to observed correlations between NO_x mixing ratios and mass concentrations of fine organic PM at several urban locations.

5.3 OSRM organic aerosol results for 2006, 2007 and 2008 at different sites

As a preliminary check, OA results from the OSRM for the site at Harwell (Table 5.2) were compared to the original test results from the pre-optimised version of the OSRM without the biogenic terpenes treated explicitly. The figures in the table to the left are from the optimised version of the OSRM (CRI-SOA), the results to the right are from the pre-optimised version. The table shows the hourly minimum, hourly maximum and the annual mean of the concentrations in each year.

The POA results are the same for 2007 in both versions, as would be expected. Including the $\alpha-$ and $\beta-$pinene emissions explicitly in the optimised version increases the SOA concentrations. The increases in the annual mean are roughly the same for 2006 and 2007 and in fact at Harwell the average concentrations show little variation between 2006, 2007 and 2008. However, there is a wide variation in the hourly maximum in SOA each year. In 2007 the maximum daily concentration of total OA (TMOA) is more than twice that of 2006, but the average for 2007 is less than 2006.

Figure 5.1 shows the annual mean component OA at 17 rural sites in the UK. Over a series of years the characteristics of each site remain similar. POA is the main component contributing to the variation in OA between sites. This is due to the primary OA contribution from emissions.

Figure 5.2 shows the maximum OA concentrations at each site for each year. This shows more variation between the sites for the different years. For example, Sibton is the site with the second highest annual mean TMOA in 2006, but it has a lower hourly maximum than other sites and in 2006 the maximum POA (the main component) was less than a third that of 2008 at this site.

The results indicate that when averaged over a year there is little inter-year variation in the OA concentration, but this masks a large range in spatial and temporal variation.

Table 5.2: Comparison of OA simulated at Harwell for 2006, 2007 and 2008

Optimised version of OSRM using $\alpha-$ and $\beta-$pinene emissions				Pre-optimised version of OSRM not using $\alpha-$ and $\beta-$pinene emissions		
	POA µgm^{-3}	SOA µgm^{-3}	TMOA µgm^{-3}		POA µgm^{-3}	SOA µgm^{-3}	TMOA µgm^{-3}
2006				**2006**			
min	0.03	0.00	0.73	min	0.03	0.00	0.73
max	30.28	5.11	31.53	max	30.28	2.56	31.51
average	1.44	0.24	2.39	average	1.44	0.13	2.28
2007				**2007** (S. Utembe test data)			
min	0.03	0.00	0.73	min	0.03	0.00	0.75
max	67.56	13.07	68.36	max	67.56	1.01	68.34
average	1.37	0.22	2.29	average	1.37	0.13	2.20
2008							
min	0.03	0.00	0.74				
max	42.19	4.81	42.99				
average	1.29	0.23	2.22				

Figure 5.1: Annual hourly average TMOA in µgm^{-3} broken down by components (POA, ASOA, BSOA and BGOAM) for 17 rural monitoring sites for a) 2006, b) 2007 and c) 2008.
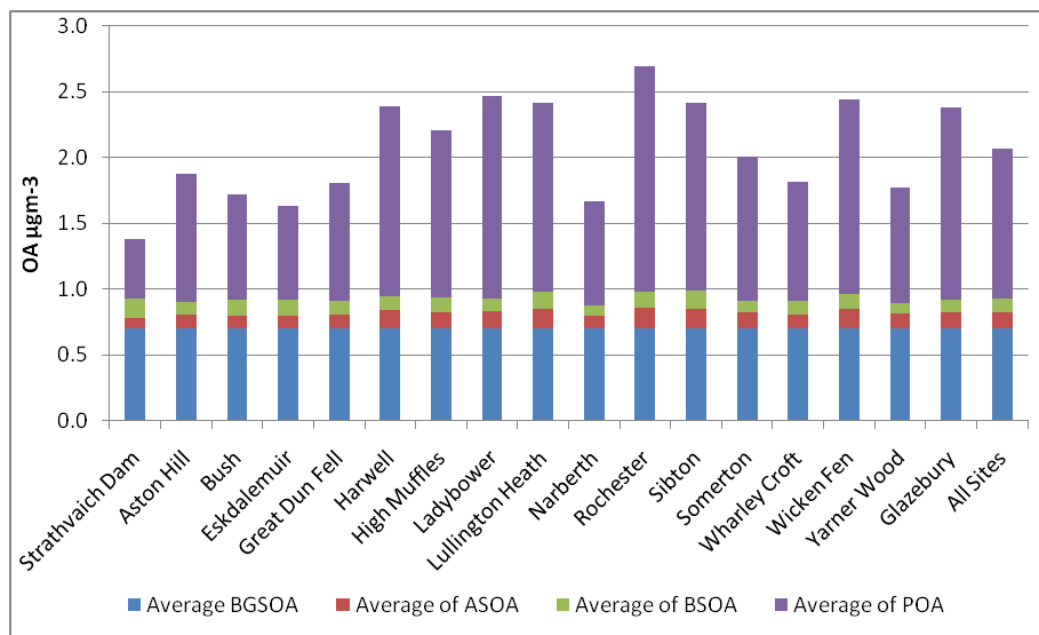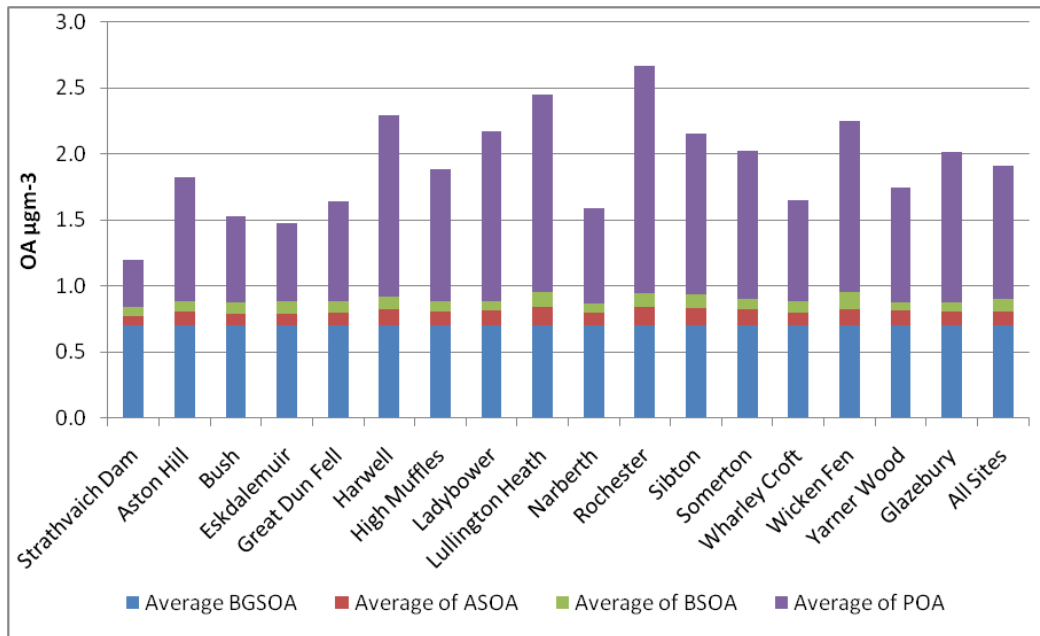
a) 2006

b) 2007

c) 2008

Figure 5.2: Annual hourly maximum for POA, ASOA and BSOA in μgm⁻³ for 17 rural monitoring sites a) 2006, b) 2007 and c) 2008.

a) 2006
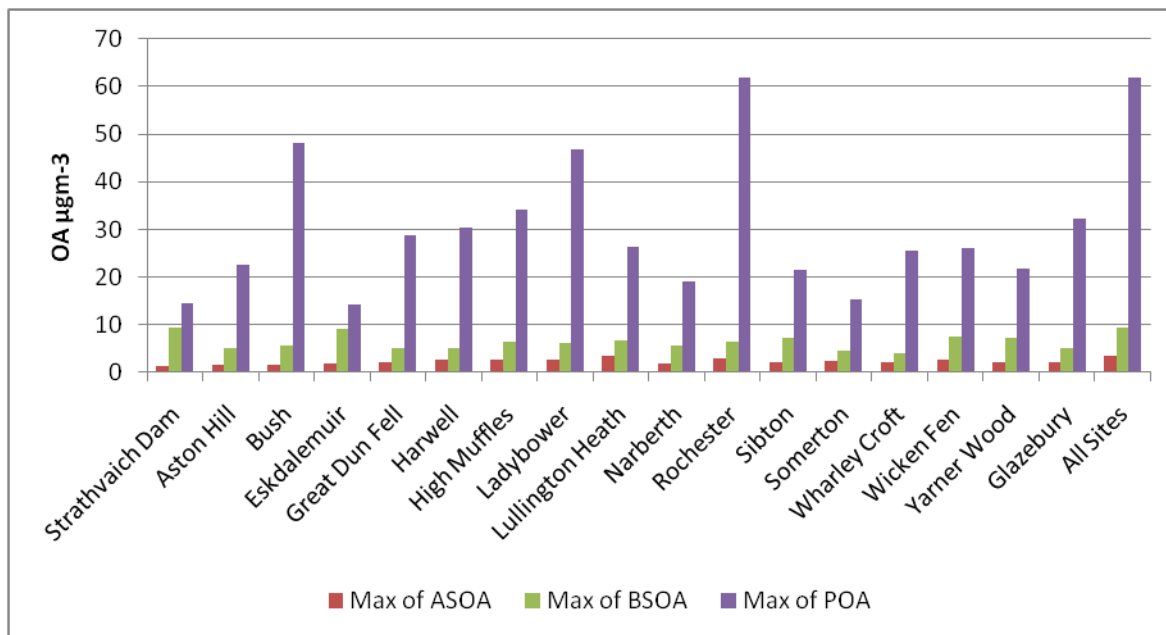
b) 2007
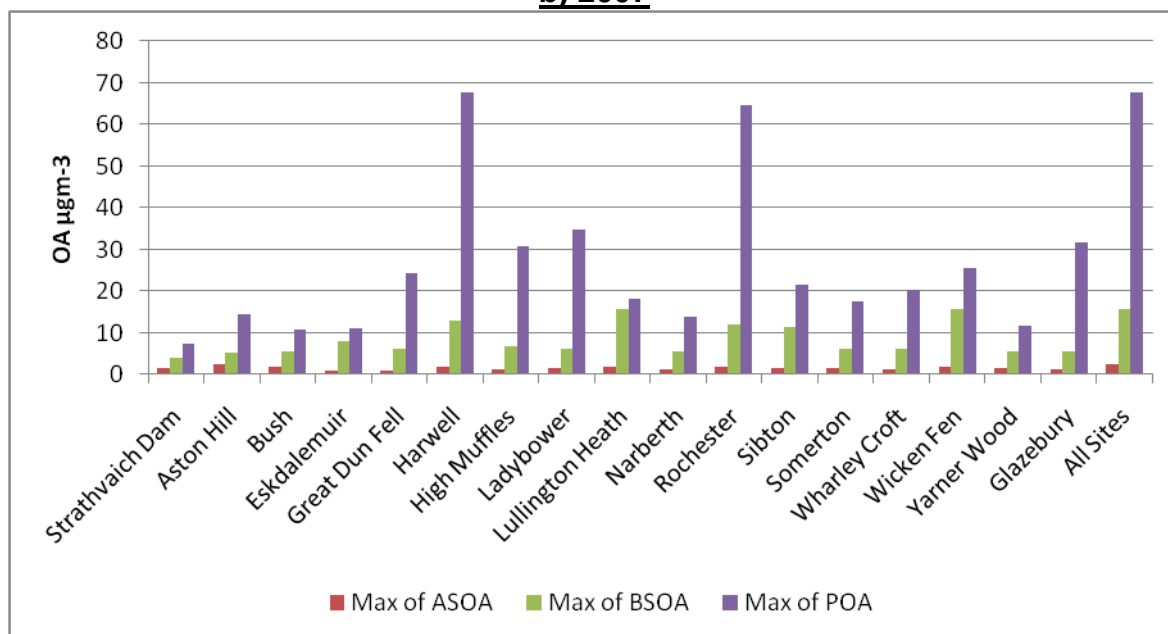
c) 2008
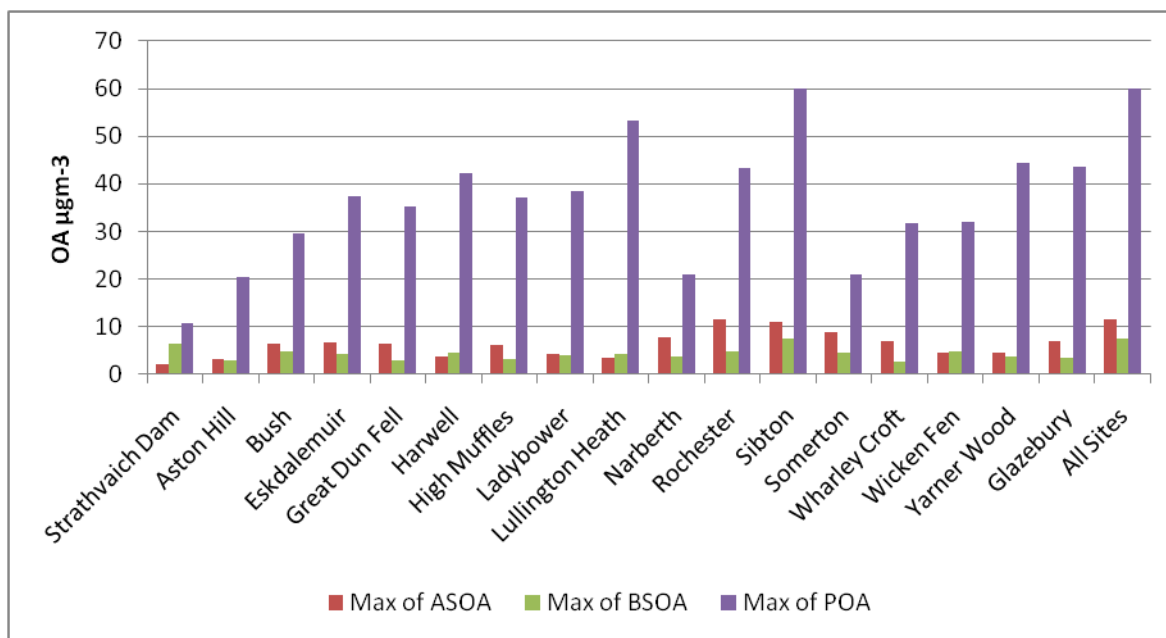
The monthly variations in OA concentrations are shown in Figures 5.3 (monthly hourly average) and 5.4 (monthly hourly maximum). POA is the main component of TMOA and shows the greatest monthly variation, but there is no particular seasonal trend consistent across all years. For example, in 2006 and 2008, there is a tendency to have raised POA concentrations in winter, but in 2007, POA was particularly low in January and high in May. There is a tendency for higher SOA levels in summer for 2006 and 2007 whereas concentrations tended to be lower between June-August during 2008, bucking the trend seen in 2006 and 2007. In all years there is a higher concentration of BSOA in summer than winter.

Figure 5.3: Monthly hourly average TMOA in µgm^{-3} broken down by components (POA, ASOA, BSOA and BGOAM) for 17 rural monitoring sites for a) 2006, b) 2007 and c) 2008.
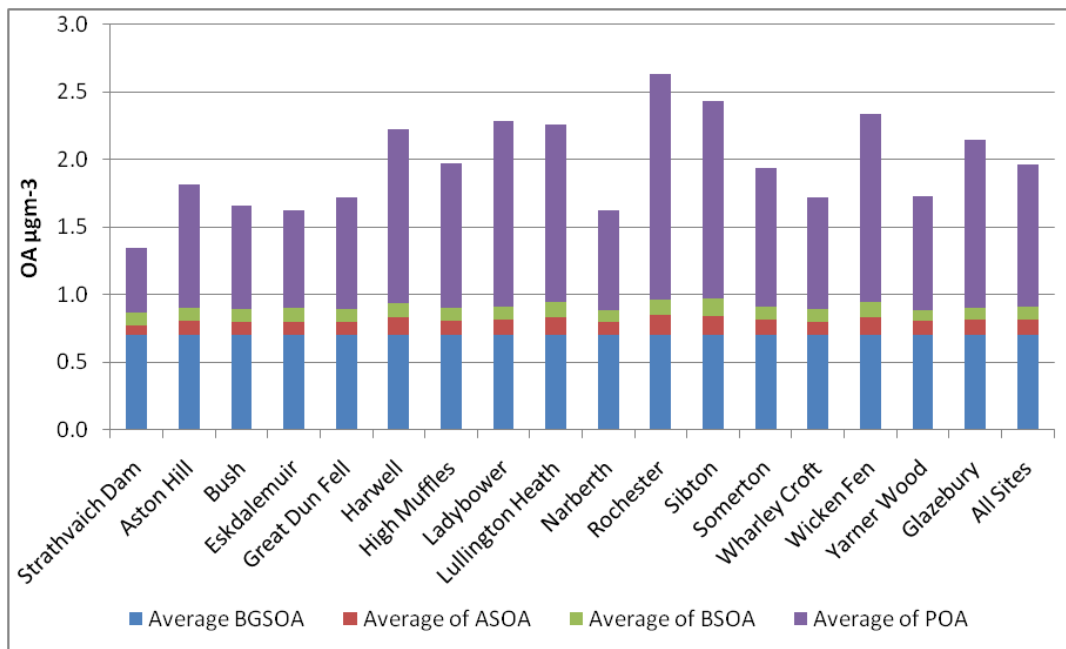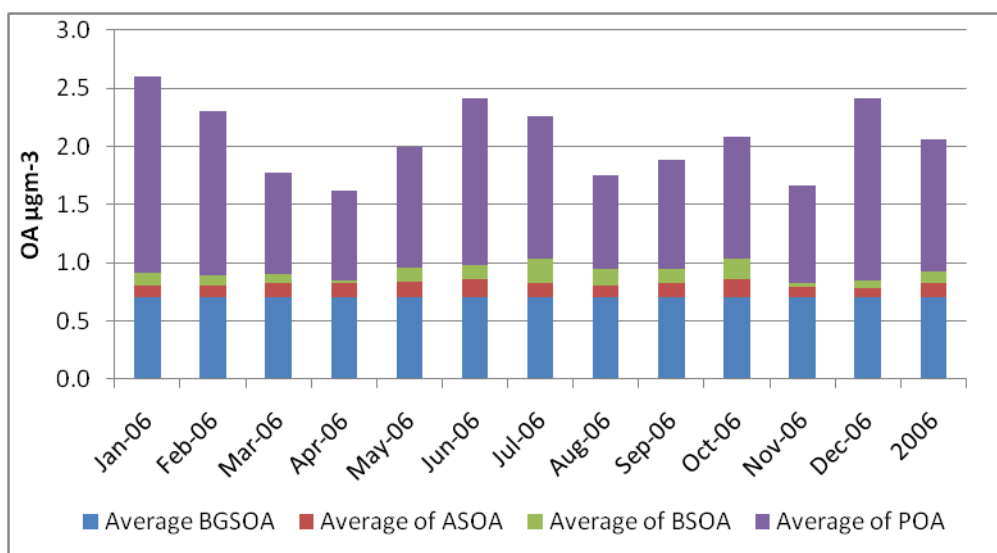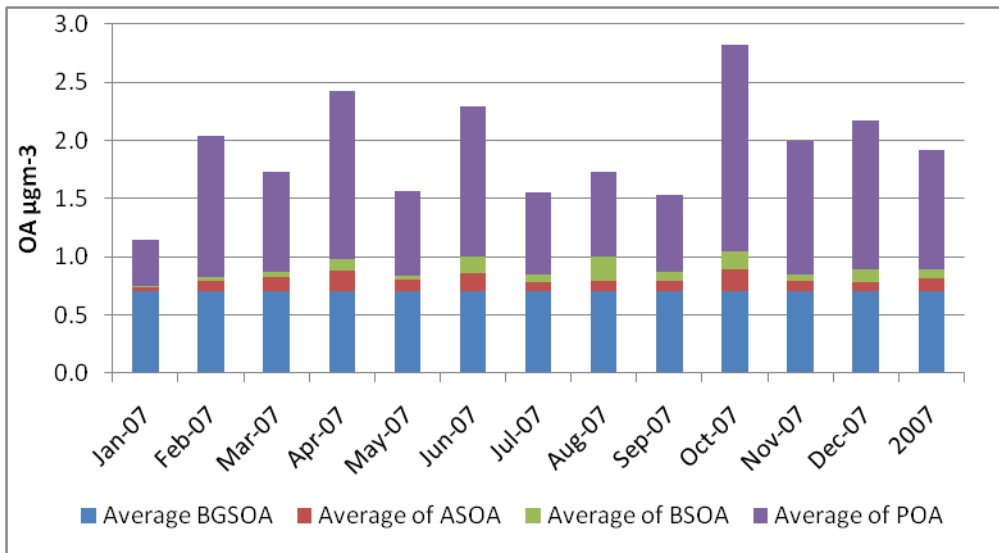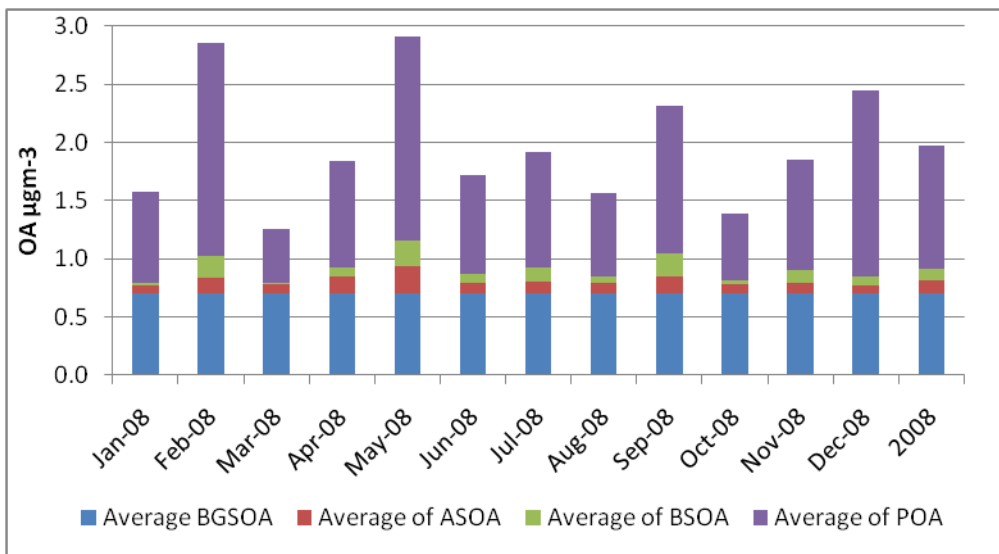
a) 2006

b) 2007

c) 2008

Figure 5.4: Monthly hourly maximum for POA, ASOA and BSOA in µgm⁻³ for 17 rural monitoring sites a) 2006, b) 2007 and c) 2008.

a) 2006
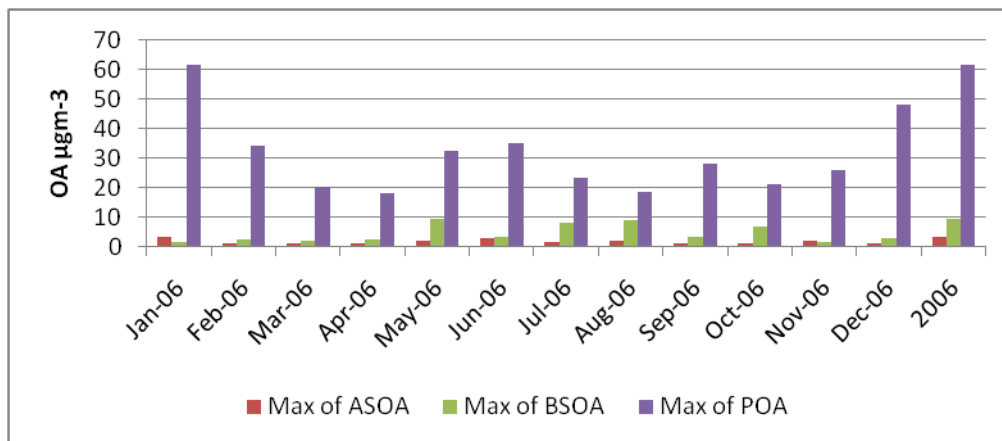
b) 2007
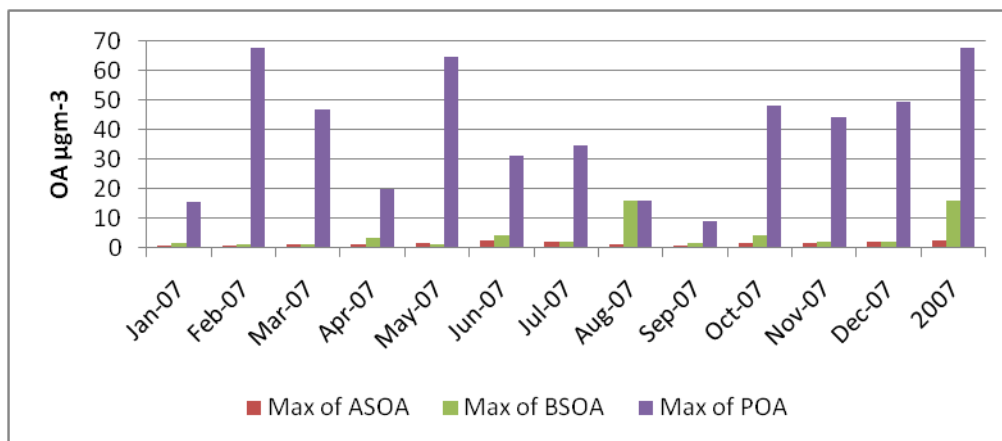
c) 2008
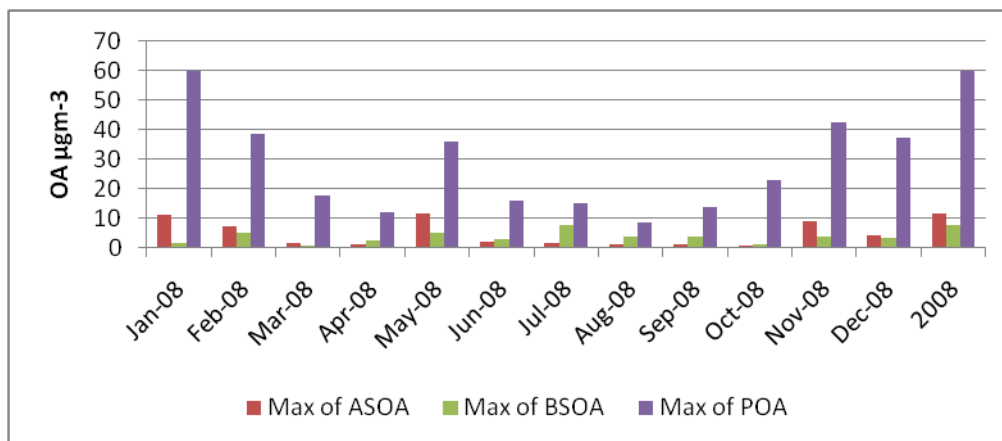
Figure 5.5 shows a more detailed breakdown in the SOA components on the total OA in 2008 between anthropogenic and biogenic sources. Figure 5.5(a) shows the annual average SOA in 2008 at each site. The sites in the more remote north and west show lower

ASOA concentrations, the higher concentrations being at the sites closer to polluted areas in the south-east of England. Figure 5.5(b) shows the hourly SOA in 2008 averaged over all sites for each month. In terms of the monthly maximum, February, May and September have the greatest contribution from biogenic OA. This is consistent with trends found from PTM modelling reported previously in the 2010 project annual report (Murrells et al, 2011), although the magnitude of the SOA concentrations derived from the OSRM are lower than those derived from the PTM. One significant difference is that the PTM simulates mid afternoon conditions whereas the OSRM simulates concentrations each hour.

Figure 5.5: Hourly SOA in µgm⁻³ for 2008 broken down by components (ASOA and BSOA) for 17 rural monitoring sites averaged for a) each site and b) each month.

   a)   Hourly SOA averaged over all months for each site
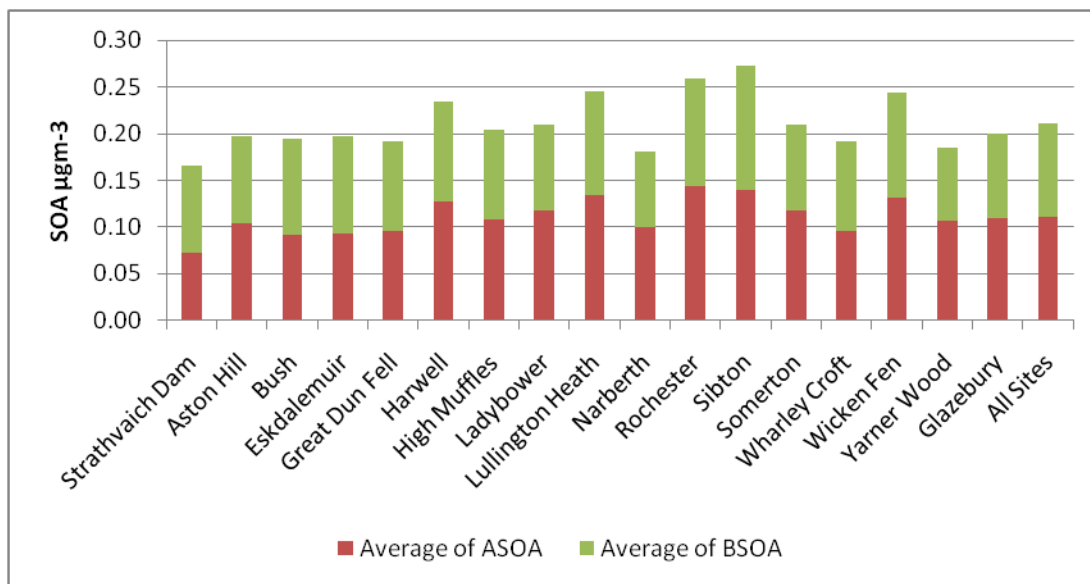
   b)   Hourly SOA averaged over all sites for each month
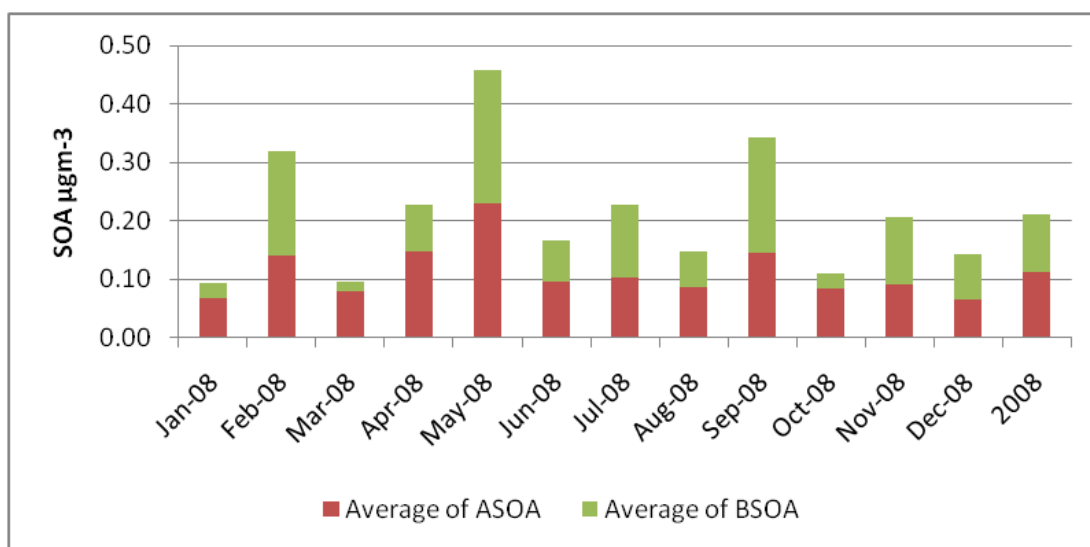
5.4 Comparison of the OSRM model results with the PTM model results and observations from the Birmingham area

Figure 5.6 is a copy of Figure 4.24 from the 2010 project Annual Report (Murrells et al, 2011) showing a comparison of the PTM model results for SOA with measurements from the Churchill Pumping Station site near Birmingham for the first half of 2006. The OSRM was used to model SOA at the Birmingham Centre and Birmingham East AURN sites over the same period and the results are shown in Figure 5.7.

Of particular note is how the OSRM model results in Figure 5.7 for these sites in Birmingham replicate the elevated organic carbon PM observed at the Churchill Pumping Station site near Birmingham at the end of February and early May also shown by the PTM. The results from the PTM and the OSRM are of the same magnitude. The higher concentrations of the occasional spikes e.g. 2nd March 2006 reflect increase in POA. The OSRM simulates each hourly concentration and will detect more of these spikes then the PTM which simulates mid afternoon values only.

Figure 5.6: Time series of observed organic carbon concentrations shown as plus signs at the Churchill Pumping Station site near Birmingham for the first half of 2006, together with the PTM model 95%-ile, 84%-ile, 50%-ile, 16%-ile and 5%-ile points. Taken from 2010 project Annual Report (Murrells et al, 2011*)*
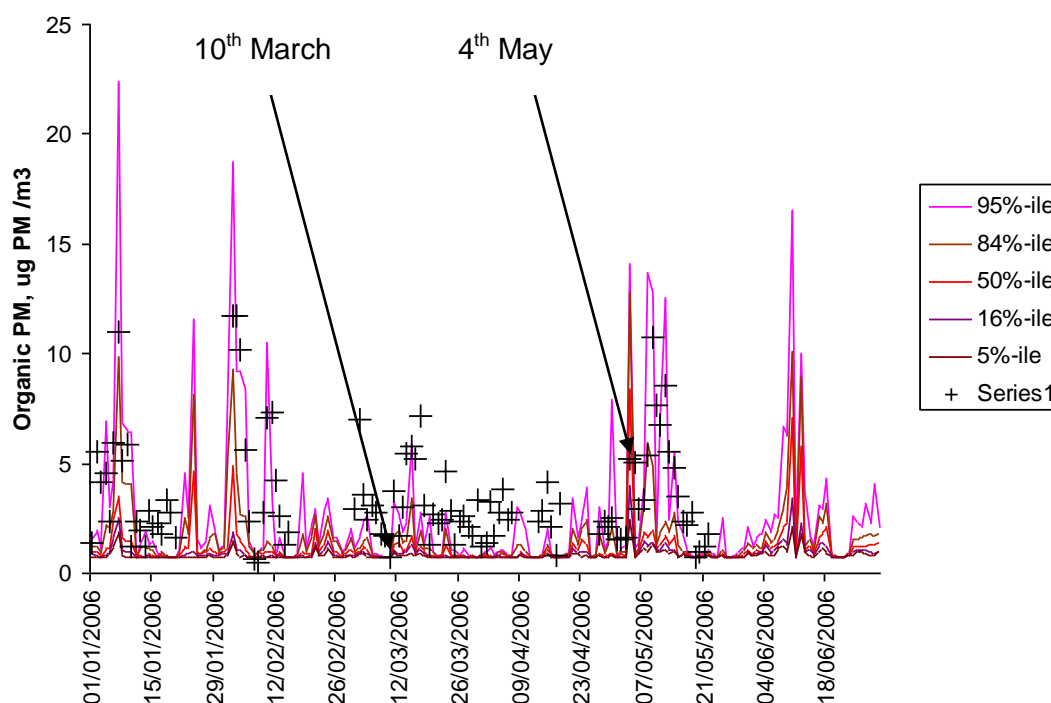
Figure 5.7: Time series of total organic aerosol modelled by the OSRM for two sites in Birmingham in 2006
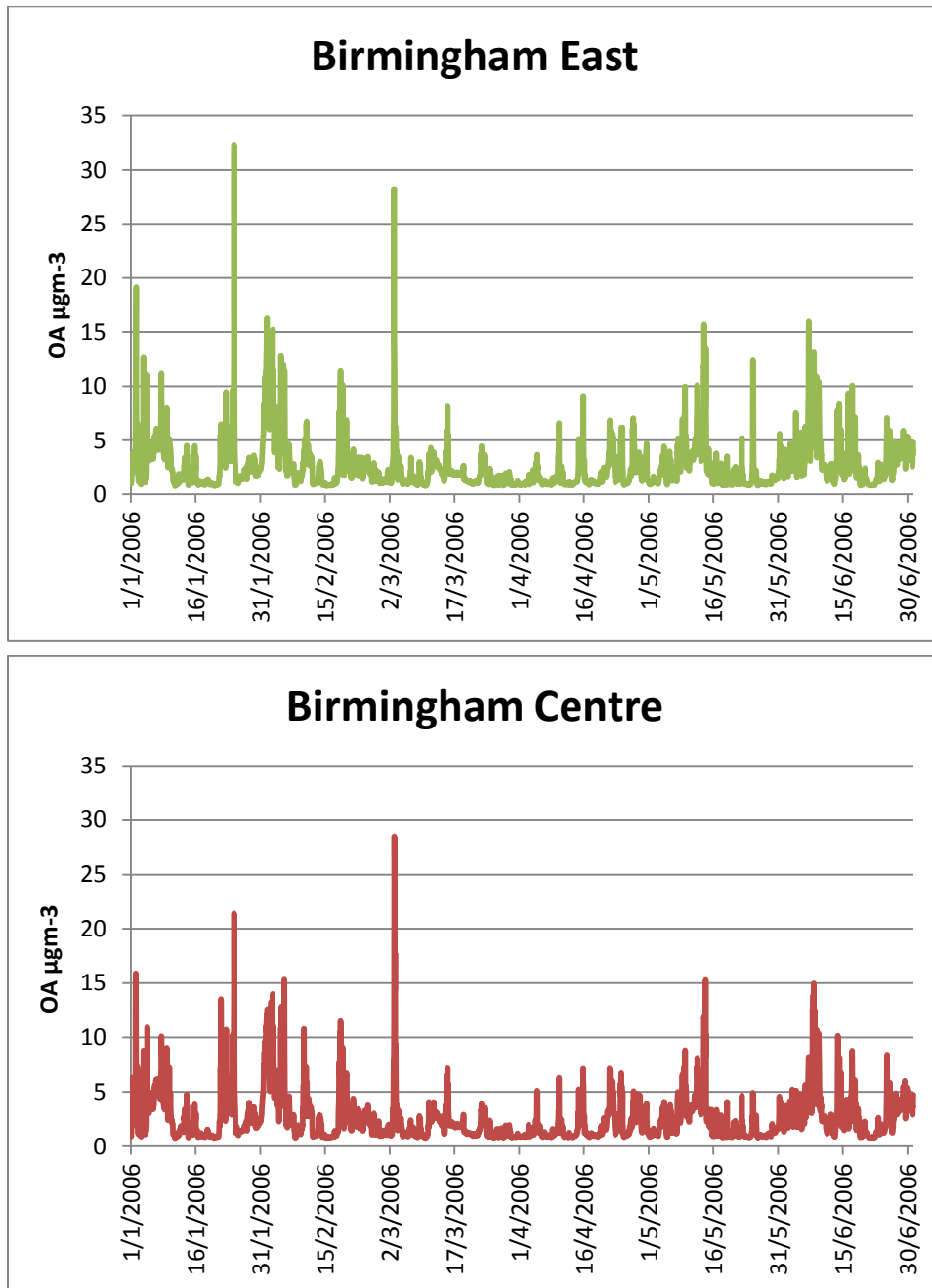
5.5 Spatial distribution of secondary organic aerosol in the UK modelled using the OSRM

The OSRM was used to carry out a full UK simulation in order to produce 10x10km maps of SOA showing the spatial variability in 2009. The simulation took 18 days to run compared with 4 days to run the standard (non-CRI-SOA) version.

Maps of annual averages of POA and SOA are shown in Figures 5.8 and 5.9, respectively. The maps are plotted on different scales with higher concentrations coming from POA than SOA. However, both maps show a general south-east to north-west reduction in POA and SOA. These concentrations are annual averages of an air mass that has followed a 96hr back trajectory. The south-east to north-west reduction in OA that is observed will be related to the prevailing weather directions, the north-west having more days when the air mass is representative of clear air moving in from the west. The south-east will include more days when the air mass has moved over areas of higher emissions in the UK or Europe.

The Primary Organic Aerosol (POA) represents the OA emitted directly into the atmosphere from anthropogenic sources. Figure 5.8 shows the highest concentrations in the south-east, around London and the industrial areas of the East Midlands and Yorkshire with the concentration decreasing towards the north and west.

In Figure 5.9 the SOA follow a similar but less defined south-east to north-west reduction. The SOA in the south-east is concentrated along the east coast and not centred on London as the POAs are.

 The SOA can be subdivided into anthropogenic (ASOA) and biogenic (BSOA) derived components and these are shown in Figures 5.10 and 5.11, respectively. The ASOA shows a well defined south-east to north-west gradient in concentrations. This may reflect the contribution of 'aged' air mass. The BSOA have a high contribution in areas of vegetation. The lower contribution in the south-west reflects the relatively short amount of time the biogenic emissions have contributed to the OA mass with the prevailing westerly weather conditions.

This is the first organic aerosol maps that have been produced from the OSRM-CRI and it has raised a number of questions the most interesting being the relative contribution to SOA from sources from the UK and from Europe. Further work would be required to investigate this, but the OSRM clearly has potential for assessing the impact of UK and European precursor emissions on the spatial distribution of SOA concentrations in the UK.

Figure 5.8: Map of Primary Organic Aerosol for 2009 (annual mean)	**Figure 5.9: Map of Secondary Organic Aerosol for 2009 (annual mean)**
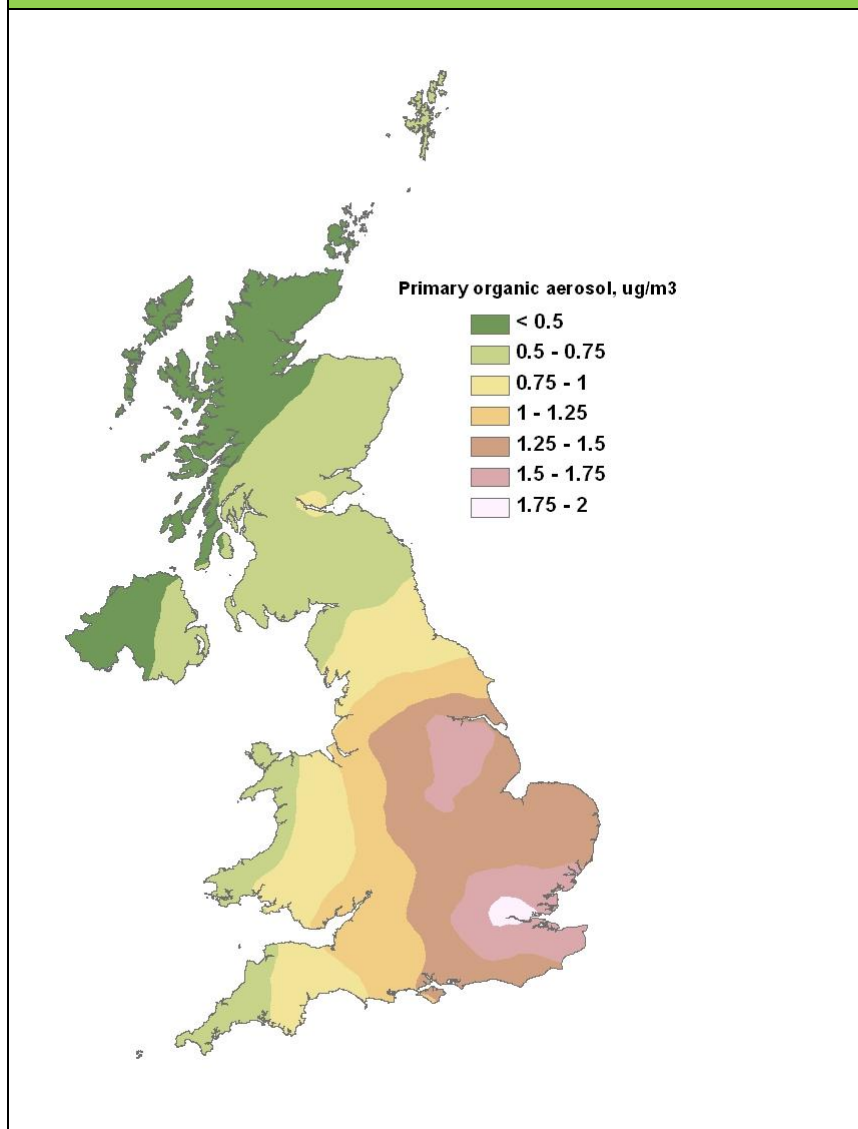
Primary organic aerosol, ug/m3

- < 0.5
- 0.5 - 0.75
- 0.75 - 1
- 1 - 1.25
- 1.25 - 1.5
- 1.5 - 1.75
- 1.75 - 2

Secondary organic aerosol, ug/m3

- <0.125
- 0.125 - 0.15
- 0.15 - 0.175
- 0.175 - 0.2
- 0.2 - 0.225
- 0.225 - 0.25

AEA
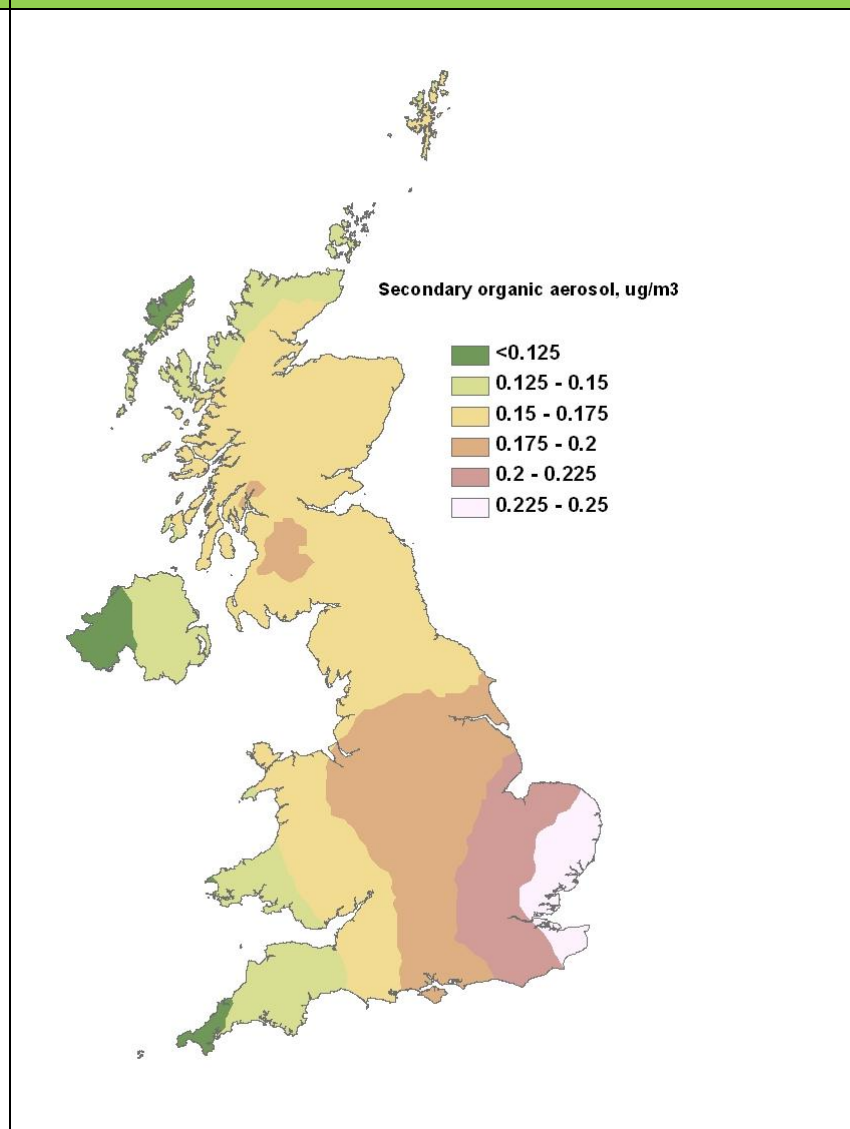
Figure 5.10: Map of Anthropogenic Secondary Organic Aerosol for 2009 (annual mean)	Figure 5.11: Map of Biogenic Secondary Organic Aerosol for 2009 (annual mean)

Anthroprogenic secondary organic aerosol, ug/m3
- < 0.075
- 0.075 - 0.1
- 0.1 - 0.125
- 0.125 - 0.15

Biogenic secondary organic aerosol, ug/m3
- <0.05
- 0.05 - 0.075
- 0.075 - 0.1
- 0.1 - 0.125
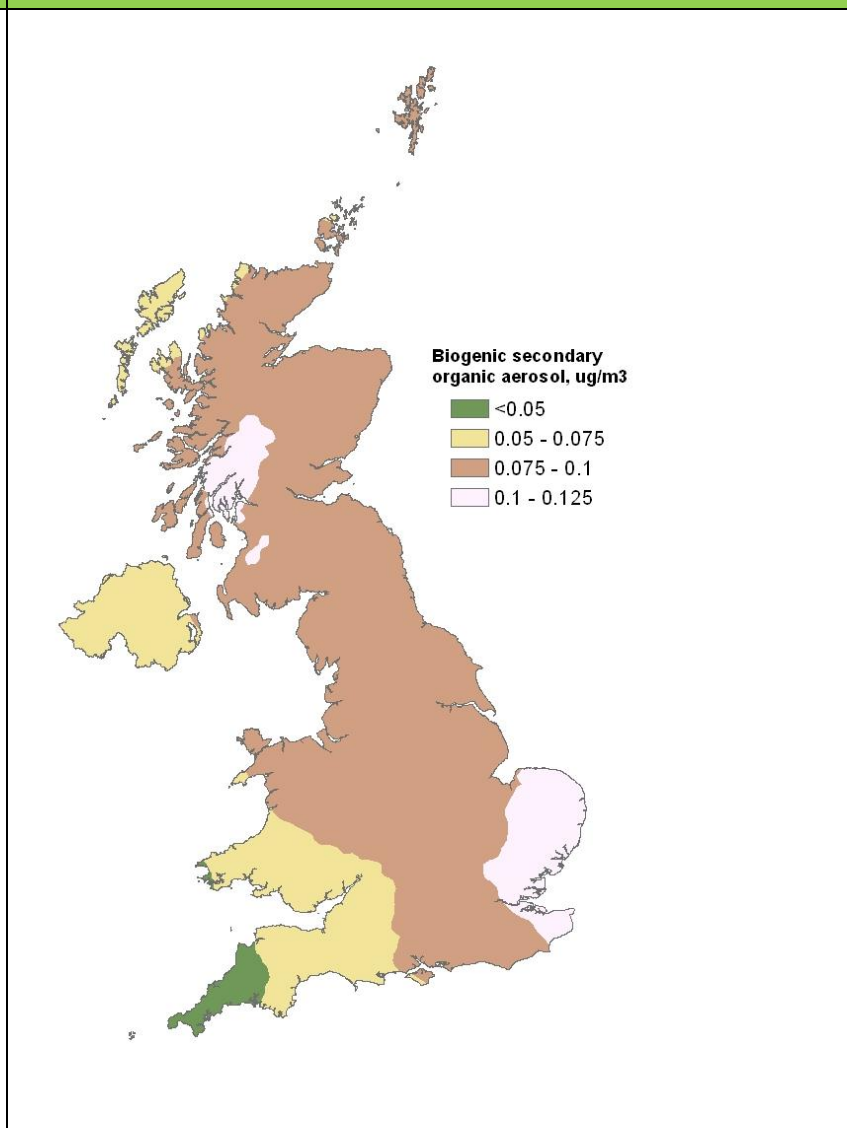
5.6 Summary and main conclusions

The main conclusions of the work of Objective 10.3 on modelling secondary organic aerosol formation with the OSRM are summarised as follows:

Summary:

- **The SOA code from the CRIv2-R5 reduced chemical scheme has been successfully incorporated into the OSRM allowing this model to simulate organic aerosol formation for the first time. The new version has been optimised by upgrading biogenic emissions to account for the role of $\alpha-$ and $\beta-$pinene in SOA formation**

- **The results from the OSRM show that when averaged over a year, total organic aerosol mass concentrations are similar at different sites and show little inter-year variability, with annual mean concentrations falling within a range of 1-3 μgm^{-3} OA.**

- **However this masks a large range in spatial and temporal variation as can be seen by the range of maximum concentrations at different sites, months and years which vary over a range of 10-80 μgm^{-3} OA**

- **Seasonal trends in SOA in 2008 modelled by the OSRM are similar to those reported for the PTM, although the OSRM estimates lower concentrations.**

- **Maps have been developed at 10x10km resolution showing the spatial distribution of different components of SOA. Biogenic SOA components show a different distribution to the anthropogenic components**

- **The OSRM has potential for assessing the impact of UK and European precursor emissions on the spatial distribution of SOA concentrations in the UK**

6 Modelling Support for Ozone Policy Using the OSRM

Objective 10.2 aims to support Defra's development and implementation of policy relating to ozone on an ad-hoc basis by running simulations with the OSRM.

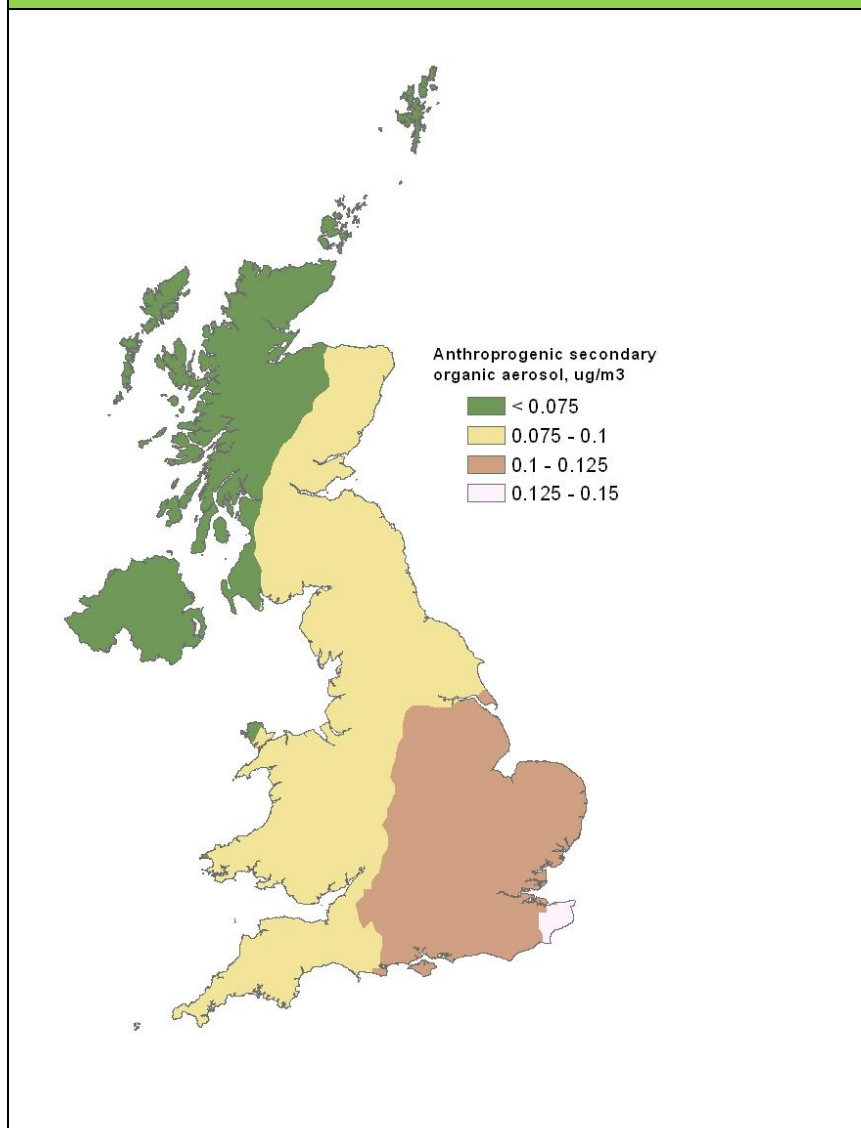The general approach is to model future ozone concentrations in the UK in 2020 or other future year based on the current emission projections and assuming meteorological conditions for one or two previous years. Alternative emission scenarios are defined by Defra and the OSRM is run to show what impact the emission changes have on future ozone concentrations expressed in terms of the current Air Quality Directive metrics (AQD). The ozone metrics are provided for policy applications as population or area-weighted means for the UK as a whole and for different parts of the UK.

A total of 22 model simulations were performed with the OSRM in 2011, mostly to inform Defra of the impacts of different national emission reduction scenarios under consideration by the UNECE for revisions to the Gothenburg Protocol and the EU National Emissions Ceilings Directive and taking into account the latest DECC (UEP) energy projections for the UK. The OSRM was run for scenarios where just the UK emissions were changed or where emissions were changed for the UK and other groups of countries in Europe. The changes in emissions for different countries in Europe would usually be taken from the UNECE PRIMES baseline projections.

Of the 22 model simulations, 18 were for different combinations of emission changes, model years and meteorology years. This report provides details and results from the last batch of 10 simulations modelled in late 2011. These are intended for direct comparison with each other and included results for SOA as well as ozone and the scenarios were also modelled by the Photochemical Trajectory Model focusing on the impacts on peak ozone rather than the AQD metrics. The previous 8 scenarios modelled in the Spring of 2011 will only be referred to briefly in this report as these scenarios were largely superceded by the later batch. However, details of these 8 earlier model runs were reported in the project's spring quarterly progress report and are available on request.

The remaining 4 scenarios modelled with the OSRM were hypothetical NO_x and VOC emission reduction scenarios requested for Defra's Model Intercomparison Exercise. Detailed results on ozone and other species were sent to Defra's Air Quality Modelling Review Steering Group and will be reported in this Group's main findings during 2012.

6.1 OSRM Simulations for 2020, 2025 and 2030 for different UK emission scenarios

The focus of these model runs was the impact of changes in UK emissions of ozone precursors for different years against a backdrop of constant emissions for a given model year from other countries in Europe. The UK emissions were projected to 2020, 2025 and 2030 based on the 2009 NAEI projections using different energy projections developed by DECC referred to as UEP43 CCC, UEP43 HFF and UEP43 LFF[3]. UEP43 CCC is DECC's central case energy scenario and is the scenario that underpins the baseline NAEI emission projections for the UK. UEP43 HFF is for a high fuel price scenario and UEP43 LFF is for a low fuel price scenario.

---

[3] http://www.decc.gov.uk/media/viewfile.ashx?filetype=4&filepath=11/about-us/economics-social-research/3134-updated-energy-and-emissions-projections-october.pdf&minwidth=true

The UK NO_x and VOC emission projections for these different UEP energy scenarios are summarised in Table 6.1

Table 6.1: UK NO_x and VOC emission projections for different UEP43 energy scenarios

		NO_x (ktonnes)	NMVOCs (ktonnes)
UEP43 CCC	2020	666.1	702.3
	2025	576.9	706.0
	2030	563.2	712.3
UEP43 HFF	2020	681.4	701.6
UEP43 LFF	2020	656.9	703.1

The 2008 NAEI emission maps were used to represent the spatial distribution of emissions in the UK (Bush et al, 2010).

For emissions from other countries in Europe, the 2008 EMEP inventory was used to represent the spatial distribution of emissions. Emissions were projected to 2020, 2025 and 2030 using the UNECE PRIMES REF 2010 projections for these years generated by IIASA using the GAINS integrated assessment model[4]. Where these were not available for certain countries EMEP 2008 projections for 2020 were used. EMEP 2008 projections were also used for CO projections for all European countries as this pollutant was not covered by the UNECE PRIMES REF projections.

For each emission scenario, the OSRM was run using 2006 and 2007 meteorology as years representing "high ozone" (2006) and "low ozone" (2007) forming meteorology years.

A total of 10 simulations were carried out and these are listed in Table 6.2.

Ozone concentrations were derived for each scenario for the Air Quality Directive ozone metrics:

- Number of days greater than 120 μg m^{-3} as a maximum daily running mean (DGT120), metric for protection of human health
- AOT40 (crops) metric for protection of vegetation

Maps were produced for each ozone metric and population-weighted means of the DGT120 metric and area-weighted means of the AOT40 metric were derived for different areas of the UK and the UK as a whole.

For the UEP43 CCC and UEP43 HFF 2020 runs, the OSRM was also used to provide annual means of SOA concentrations.

---

[4] http://gains.iiasa.ac.at/gains/docu.EUR/index.menu

Table 6.2: Details of scenarios run and meteorology used

UK Inventory	Meteorology year	Non-UK UNECE inventory	Projected Inventory Year
UEP 43 CCC (2009)	2006	PRIMES REF (2010)	2020
UEP 43 CCC (2009)	2007	PRIMES REF (2010)	2020
UEP 43 CCC (2009)	2006	PRIMES REF (2010)	2025
UEP 43 CCC (2009)	2007	PRIMES REF (2010)	2025
UEP 43 CCC (2009)	2006	PRIMES REF (2010)	2030
UEP 43 CCC (2009)	2007	PRIMES REF (2010)	2030
UEP 43 HFF (2009)	2006	PRIMES REF (2010)	2020
UEP 43 HFF (2009)	2007	PRIMES REF (2010)	2020
UEP 43 LFF (2009)	2006	PRIMES REF (2010)	2020
UEP 43 LFF (2009)	2007	PRIMES REF (2010)	2020

Note: CCC = central case scenario, HFF = high fuel price scenario, LFF = high fuel price scenario

6.1.1 Ozone concentration metrics for each UEP43 emission scenario

Table 6.3 shows the projected area-weighted means of the AOT40 ozone metric in Scotland, Wales, Northern Ireland, Inner London, Outer London and rest of England and for the UK as a whole for each model year (2020, 2025 and 2030) and UEP43 emission scenario. Results are shown for 2006 and 2007 meteorology years.

Table 6.3: Area-Weighted AOT40 - Crops ozone metric (µgm^{-3}.hours) for each UEP43 emission scenario

Met year		Scenario	Scotland	Wales	Northern Ireland	Inner London	Outer London	Rest of England	All UK
2006	2006	Base	5389	6458	5593	4148	4222	6869	6259
2006	2020	UEP43 CCC	8855	10814	8912	12967	12414	12217	10789
	2020	UEP43 HFF	8830	10757	8880	12916	12354	12150	10738
	2020	UEP43 LFF	8874	10856	8934	12973	12434	12261	10823
	2025	UEP43 CCC	9809	11887	9850	15031	14338	13668	12016
	2030	UEP43 CCC	10958	13192	10957	16603	15870	15201	13377
2007	2020	UEP43 CCC	9893	9755	7623	10195	9788	10238	9929
	2020	UEP43 HFF	9877	9695	7599	10149	9742	10184	9889
	2020	UEP43 LFF	9906	9797	7641	10206	9808	10277	9957
	2025	UEP43 CCC	10835	11033	8407	12197	11578	11561	11093
	2030	UEP43 CCC	11942	12350	9406	13715	13044	12942	12356

The results indicate an increase in AOT40 values for all years and scenarios relative to the values for 2006. They also indicate increasing ozone metrics as NO_x emissions decrease and VOC emissions increase across the years from 2020 to 2030, although the increase in ozone across this time-series is less than the initial rise between 2006 and 2020. It is also apparent that less ozone is estimated for the high fuel price (HFF) scenario and higher ozone is estimated for the low fuel price (LFF) scenario relative to the central case (CCC) scenario, but again the differences are small between these scenarios compared with the differences between years. The same pattern is seen for both the 2007 and 2006 meteorology years, although the AOT40 metrics are lower assuming 2007 meteorology than those assuming 2006 meteorology, as would be expected.

Table 6.4 shows the corresponding data for the population-weighted means of the DGT120 ozone metric. These show the same general pattern of change as the AOT40 metrics.

Table 6.4: Population-weighted number of days greater than 120 μg m^{-3} as a maximum daily running mean for each UEP43 emission scenario

Met year		Scenario	Scotland	Wales	Northern Ireland	Inner London	Outer London	Rest of England	All UK
2006	2006	Base	3.6	9.2	5.8	5.8	5.1	8.4	7.6
2006	2020	UEP43 CCC	7.0	15.6	11.5	14.3	13.7	13.8	13.3
	2020	UEP43 HFF	7.0	15.3	11.4	13.8	13.6	13.7	13.1
	2020	UEP43 LFF	7.1	15.6	11.5	14.3	13.7	13.9	13.3
	2025	UEP43 CCC	8.8	17.9	13.4	16.1	15.7	15.8	15.2
	2030	UEP43 CCC	11.7	20.9	15.8	17.3	18.7	18.3	17.8
2007	2020	UEP43 CCC	10.4	8.1	2.6	11.6	11.0	8.5	8.8
	2020	UEP43 HFF	10.4	8.0	2.4	11.6	11.0	8.4	8.7
	2020	UEP43 LFF	10.4	8.2	2.6	11.6	11.0	8.6	8.9
	2025	UEP43 CCC	11.9	11.1	3.9	13.9	13.3	10.7	11.0
	2030	UEP43 CCC	13.5	14.8	5.4	15.8	15.6	13.2	13.4

Table 6.5 shows the corresponding data for the area-weighted annual mean ozone concentrations. These also show the same pattern of change across the scenarios and years although for this metric the changes are relatively smaller and the means are higher for the 2007 meteorology year than for 2006.

Table 6.5: Area-Weighted annual mean ozone metric (μgm⁻³) for each UEP43 emission scenario

Met year		Scenario	Scotland	Wales	Northern Ireland	Inner London	Outer London	Rest of England	All UK
2006	2006	Base	63.5	64.5	63.9	46.2	46.6	56.6	59.9
2006	2020	UEP43 CCC	68.9	71.5	69.4	63.2	62.5	66.2	67.7
	2020	UEP43 HFF	68.9	71.5	69.3	63.1	62.4	66.1	67.6
	2020	UEP43 LFF	68.9	71.6	69.4	63.2	62.5	66.3	67.8
	2025	UEP43 CCC	70.0	72.9	70.5	65.5	64.6	67.9	69.1
	2030	UEP43 CCC	71.0	74.0	71.3	66.5	65.7	69.0	70.2
2007	2020	UEP43 CCC	72.1	72.3	71.8	62.6	62.1	66.7	69.3
	2020	UEP43 HFF	72.1	72.3	71.7	62.5	62.0	66.6	69.2
	2020	UEP43 LFF	72.1	72.4	71.8	62.6	62.1	66.8	69.3
	2025	UEP43 CCC	73.2	73.8	72.9	65.1	64.4	68.5	70.7
	2030	UEP43 CCC	74.1	75.0	73.8	66.2	65.6	69.6	71.8

6.1.2 Maps of AOT40 ozone metric for UEP43 CCC basecase scenario

Figures 6.1-6.3 show maps of the AOT40 metric in 2020, 2025 and 2030 for the same UEP43 CCC emission scenario. For comparison with each other, all maps are based on 2006 meteorology. There are little differences in the maps for the different HFF and LFF scenarios, so these are not shown. These maps illustrate the increasing extent of the higher AOT40 ranges across the UK as NO_x emissions reduce across the years and the dominance of high AOT40 values in the south and east of the country.

Maps of the DGT120 show similar spatial patterns as the AOT40 maps so are not shown. The maps using 2007 meteorology show a markedly different spatial variation, but a similar pattern of increasing extent of higher DGT120 ranges as NO_x emissions decrease across the years.

6.1.3 Maps of organic aerosols for UEP43 CCC basecase scenario

Figures 6.4 and 6.5 show maps of annual mean organic aerosol concentrations in 2020 for the UEP43 CCC baseline scenario under 2006 and 2007 meteorological conditions. The maps are shown for primary organic and total secondary organic aerosols and biogenic and anthropogenic secondary organic aerosols. The spatial variation in organic aerosol concentrations is significantly different for the two meteorology years, especially for secondary organic aerosols.

Figure 6.1: Map of AOT40 ozone metric for 2020 using the UEP43 central scenario and 2006 meteorology
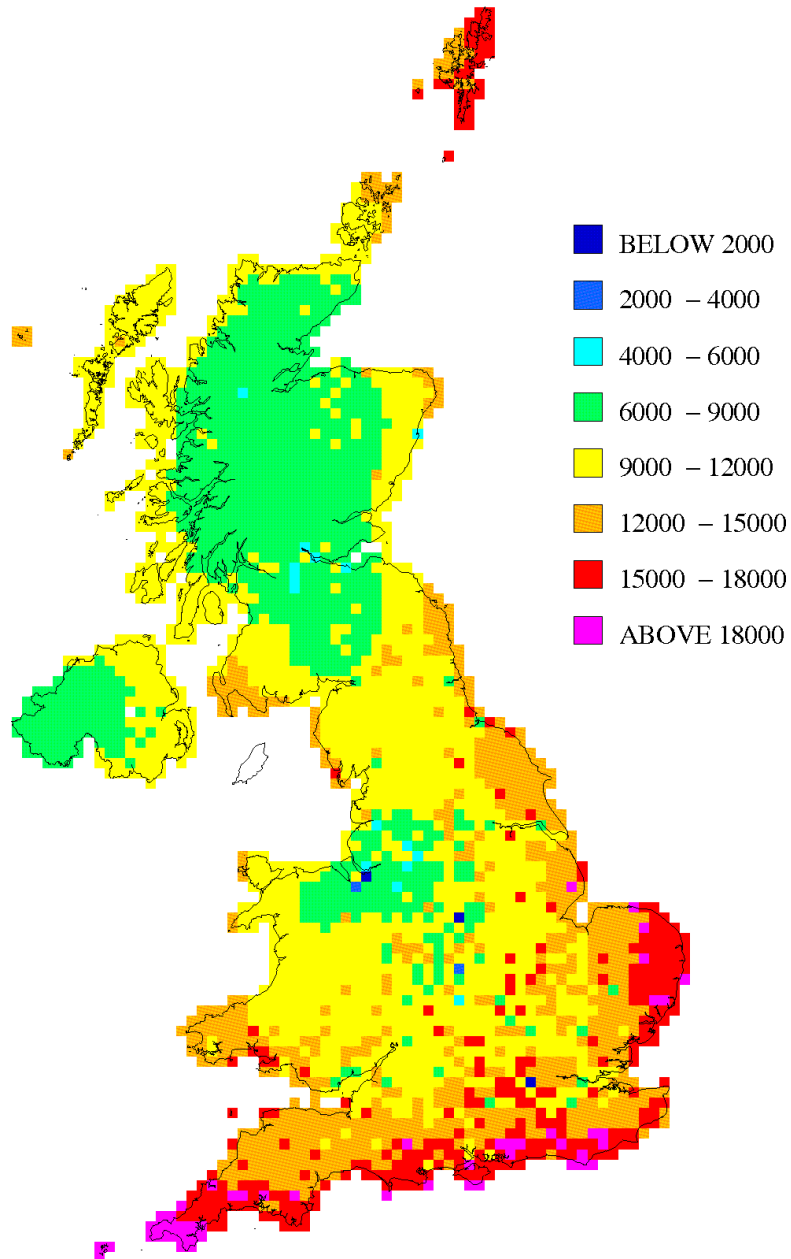
Figure 6.2: Map of AOT40 ozone metric for 2025 using the UEP43 central scenario and 2006 meteorology
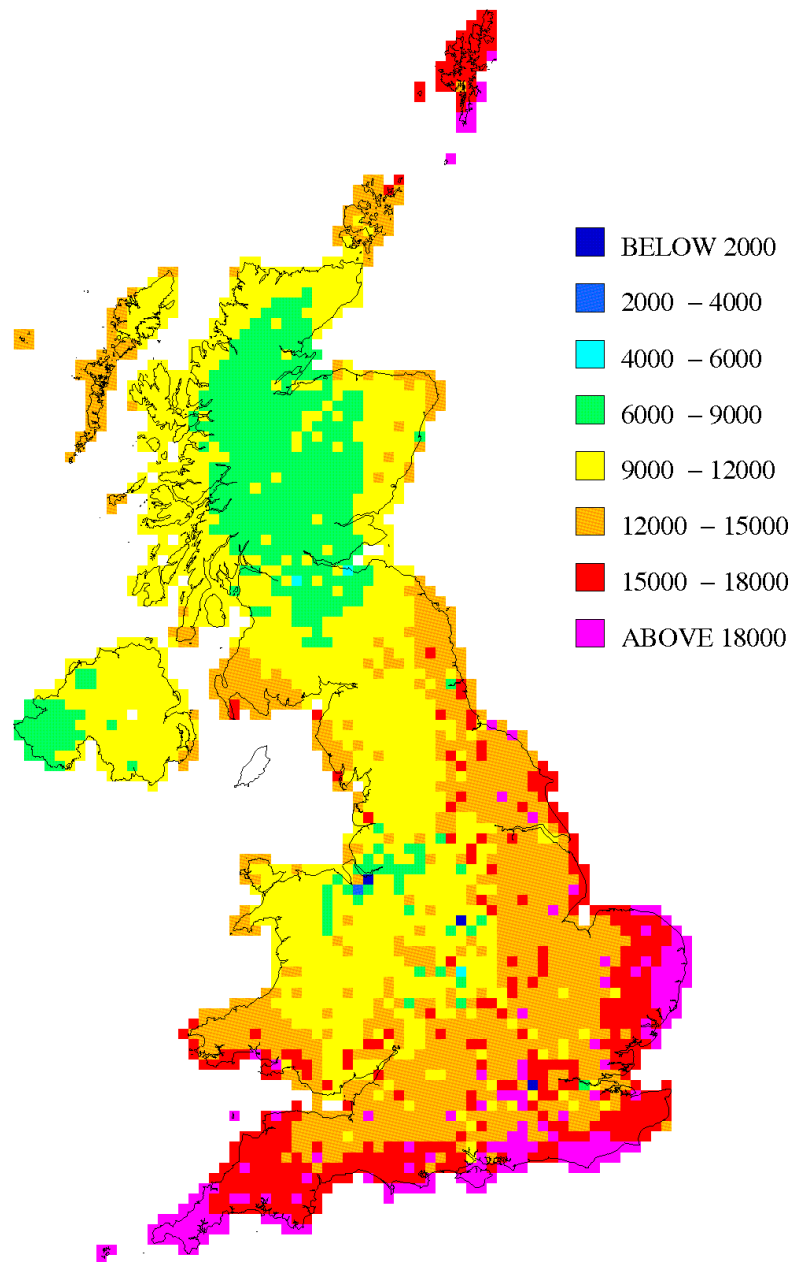
Figure 6.3: Map of AOT40 ozone metric for 2030 using the UEP43 central scenario and 2006 meteorology
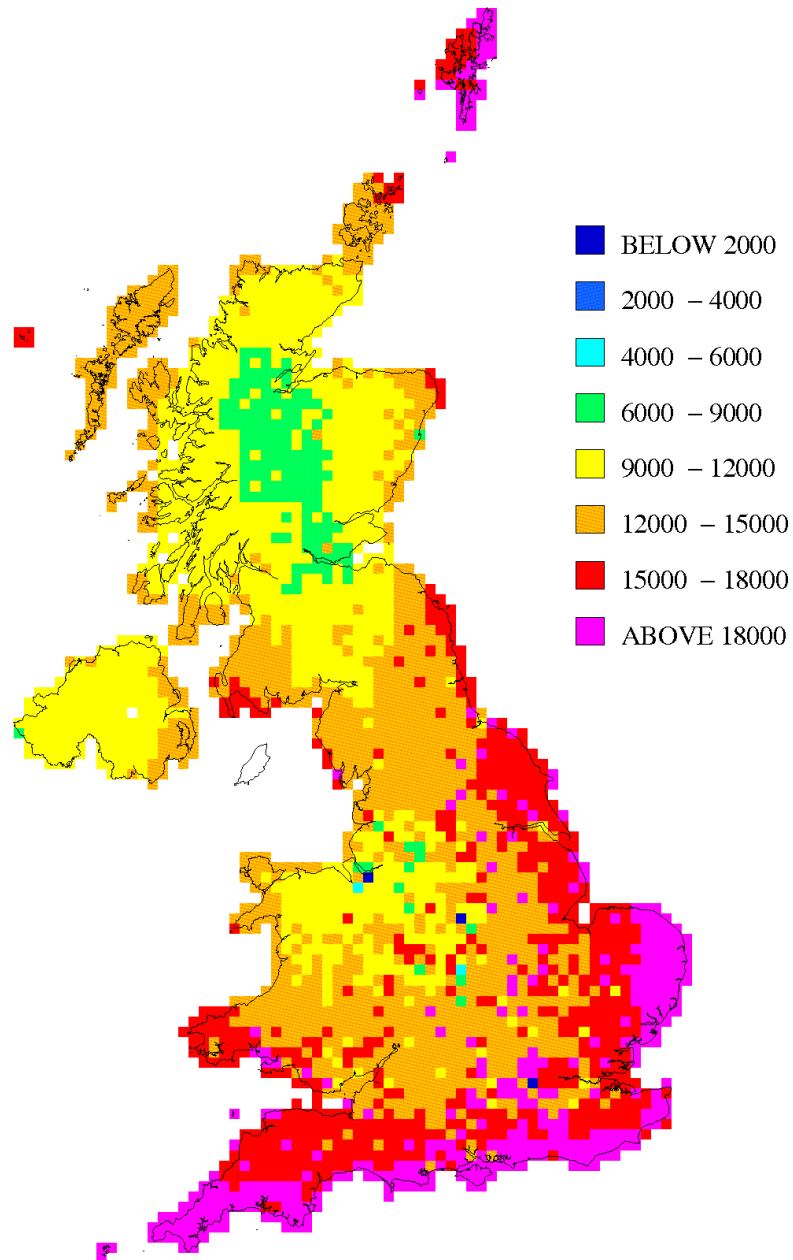
Figure 6.4: Maps of organic aerosol concentrations (µgm⁻³ annual means) for 2020 using the UEP43 central scenario and 2006 meteorology

(a) Primary organic aerosol

(b) Total secondary organic aerosol
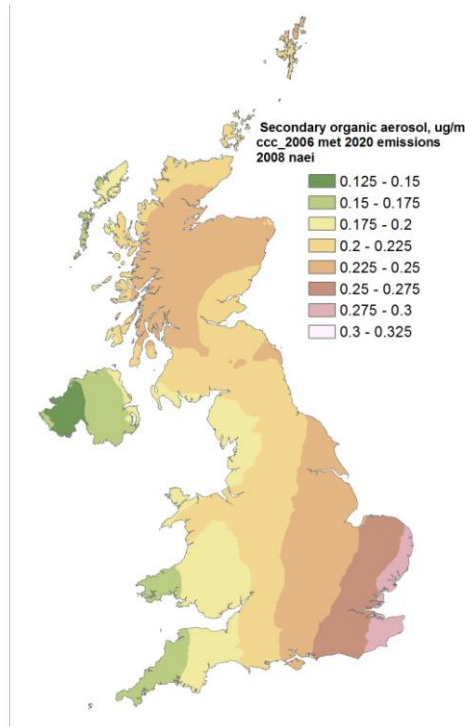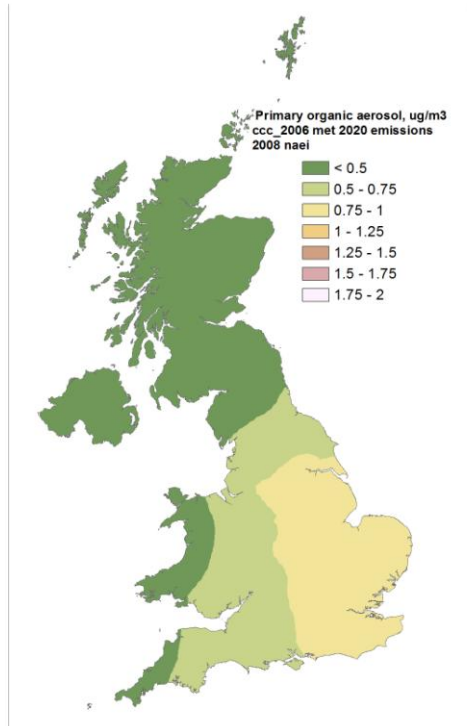
(c) Biogenic organic aerosol

(d) Anthropogenic organic aerosol

Figure 6.5: Maps of organic aerosol concentrations (µgm^{-3} annual means) for 2020 using the UEP43 central scenario and 2007 meteorology

(a) Primary organic aerosol   **(b) Total secondary organic aerosol**

(c) **Biogenic organic aerosol**   (d) **Anthropogenic organic aerosol**

6.2 OSRM Simulations for 2020 under different UNECE PRIMES Emission Scenarios

A number of OSRM simulations for 2020 were run in 2011 for alternative future emission scenarios relating to possible national emission ceilings considered for the UK and other parts of Europe.

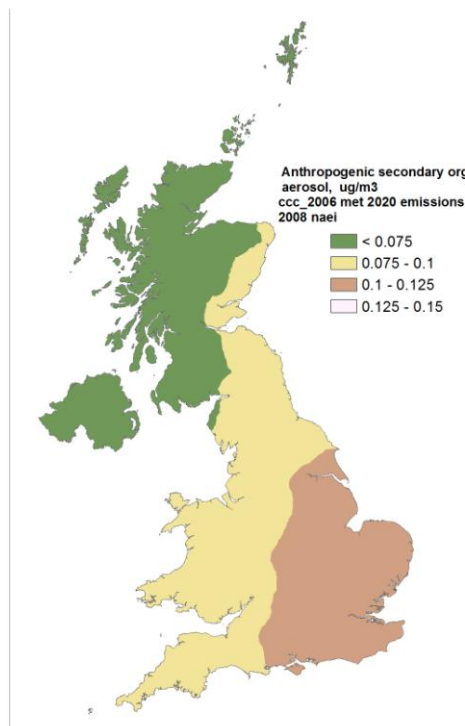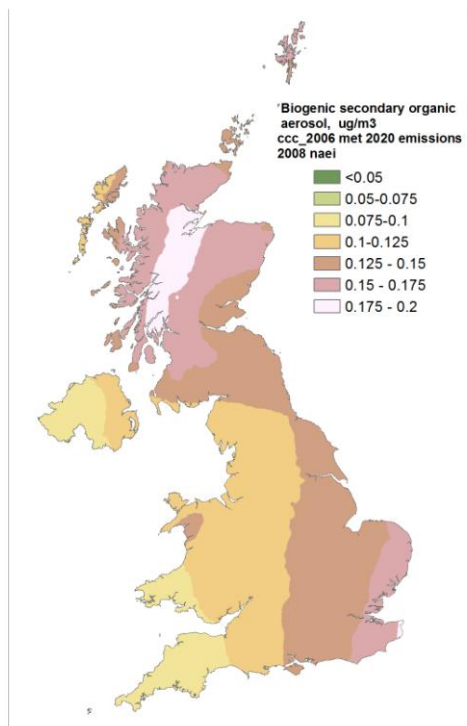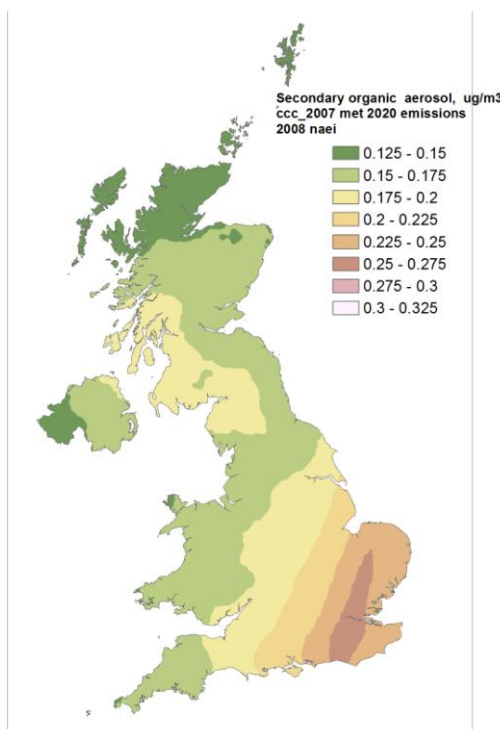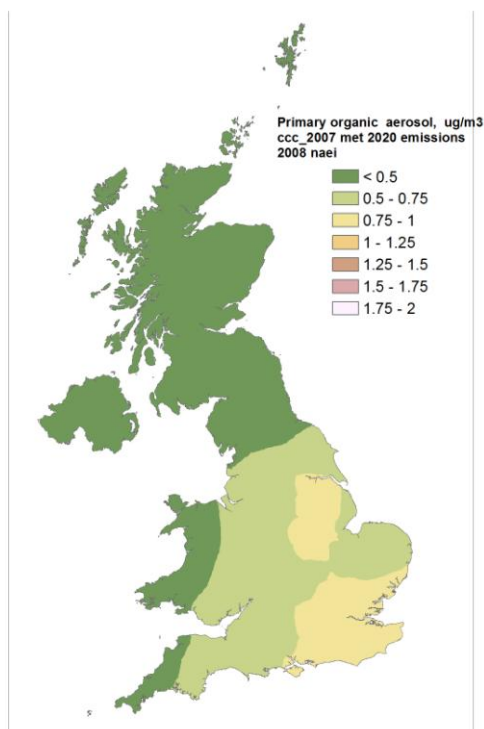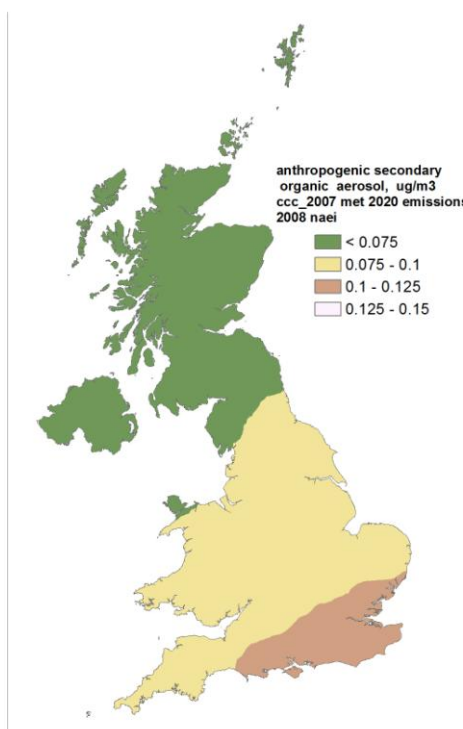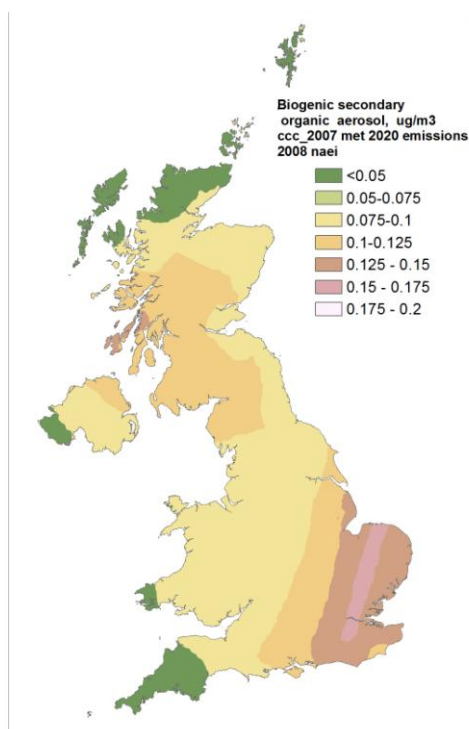Five alternative emission scenarios were specified by Defra and three of these were modelled assuming two different meteorology conditions using data held for the 2006 and 2007 calendar years. The other two were modelled only for 2006 meteorology conditions. This required a total of 8 simulations. Some of the scenarios were based around emission figures developed by Dr Mike Holland (EMRC – hereafter called the EMRC scenario) presented at an IAPSC meeting as a broad indication of where the revised Gothenburg Protocol and NEC Directive may head to so far as the UK is concerned.

The scenarios are summarised as follows:

- **For the base case**, the NAEI 2008 projections for 2020 were used for the UK emissions and UNECE PRIMES baseline projections for 2020 were used for other countries in the UNECE. EMEP 2008 projections for 2020 were used where UNECE PRIMES baseline projections were not available for certain countries. The EMEP projections were also used for the pollutant CO in all countries (except the UK) as this pollutant is not covered in the UNECE PRIMES baseline.

- **Scenario 1** whereby the NAEI 2008 projections for the UK in 2020 were scaled to EMRC predicted values for NO_x, VOC and SO_2, with CO remaining constant. Baseline UNECE PRIMES baseline projections for 2020 were used for other countries in the UNECE.

- **Scenario 2**, whereby the NAEI 2008 projections for the UK in 2020 were scaled to EMRC predicted values for NO_x, VOC and SO_2, with CO remaining constant. For all other countries in the UNECE, emissions were scaled from the PRIMES baseline so that emissions were reduced between PRIMES and the more ambitious PRIMES MTFR 2020 projections with the same level of ambition as the EMRC values for the UK. Values for CO were maintained at the EMEP baseline.

- **Scenario 3,** whereby the NAEI 2008 projections for the UK in 2020 were scaled to EMRC predicted values for NO_x, VOC and SO_2, with CO remaining constant. For all other EU countries, emissions were scaled from the PRIMES baseline so that emissions were reduced between PRIMES and the more ambitious PRIMES MTFR 2020 projections for these countries with the same level of ambition as the EMRC values for the UK. For non-EU countries in the UNECE, baseline UNECE PRIMES baseline projections for 2020 were used. Values for CO were maintained at the EMEP baseline. This scenario therefore involves changes in Scenario 2 applied only to the EU sub-set of countries in the UNECE.

- **Scenario 4** is the same as the base except that the NAEI 2008 projections for NMVOCs in the UK in 2020 were scaled to the more ambitious UNECE PRIMES MTFR 2020 values for this pollutant in the UK and the UNECE PRIMES Maximum Technically Feasible Reduction (MTFR) projections for NMVOCs were used for all other countries in the UNECE. Emissions for all other pollutants (NO_x, SO_2 and CO) were retained at the levels in the basecase.

- **Scenario 5** is the same as the base except that the NAEI 2008 projections for NMVOCs and SO_2 in the UK in 2020 were scaled to the more ambitious UNECE PRIMES MTFR 2020 values for this pollutant in the UK and the UNECE PRIMES MTFR projections for NMVOCs and SO_2 were used for all other countries in the

UNECE.   Emissions for all other pollutants (NO_x and CO) were retained at the levels in the basecase. This scenario is the same as Scenario 4 except that the more ambitious emission reductions are extended to SO_2.

The combination of emission scenarios and met years modelled are shown in Table 6.6:

Table 6.6: Emission scenarios and meteorology years modelled by the OSRM for UK ozone in 2020

Emission Scenario	Meteorology year
Base case	2006
Base case	2007
Scenario 1 (EMRC UK)	2006
Scenario 1 (EMRC UK)	2007
Scenario 2 (EMRC UK and UNECE)	2006
Scenario 2 (EMRC UK and UNECE)	2007
Scenario 3 (EMRC UK and EU)	2006
Scenario 3 (EMRC UK and EU)	2007
Scenario 4 (MTFR UK and UNECE – NMVOCs)	2006
Scenario 5 (MTFR UK and UNECE – NMVOCs and SO_2)	2006

Population and area-weighted ozone metrics were derived for the 2020 basecase and each scenario in different areas of the UK. Details of the results are available on request, but some general observations can be made.

- **Scenario 1** generally leads to an increase in ozone metrics relative to the 2020 base, especially in London, and this is most likely to be due to reductions in the NO_x titration effect as a consequence of further reductions in NO_x emissions in the UK.

- **Scenario 2** introduces further reductions in NO_x and VOC emissions across UNECE countries and this has the effect of reducing ozone metrics relative to Scenario 1 and in some cases even reduces ozone metrics below the 2020 base. This highlights the significance of precursor emissions in Europe to ozone concentrations in the UK. The reduction in UNECE emissions reduces ozone production. The effect of Scenario 2 in reducing UK ozone is generally stronger when using 2006 meteorology than when using 2007 meteorology and probably reflects the greater significance of European emissions to UK ozone in 2006 when there were more episodic days with meteorological conditions more favourable for transfer of emissions from continental Europe.

- The pattern of changes for **Scenario 3** relative to the base is similar to Scenario 2. The results for Scenario 3 sit between the results for Scenarios 1 and 2, but are closer to Scenario 2. This is to be expected and is because the extent of emission reductions across Europe is reduced by limiting the emission reductions to only the EU countries instead of all UNECE countries. The fact that ozone concentrations in Scenario 3 sit closer to those for Scenario 2 indicates the relatively small impact of the non-EU countries to the change in ozone observed in the UK.

- **The two MTFR scenarios (4 and 5)** lead to far more significant reductions in UK ozone than any other scenario reflecting the important role played by VOC emissions across Europe to production of ozone in air transported to the UK. All the metrics show reductions relative to the 2020 base. Scenario 5 leads to slightly lower ozone concentrations than Scenario 4 indicating that reducing SO_2 emissions as well as VOC emissions reduces ozone, but that the effect of SO_2 emission changes is considerably smaller than the effect of reducing VOC emissions.

In conclusion, the results indicate that it will be important for comparable reductions in emissions to be achieved across Europe as well as in the UK to prevent ozone concentrations in the UK rising. It also showed the benefits to be achieved by reducing VOC emissions across Europe.

6.3 OSRM results for the Defra Model Intercomparison Exercise Phase 2

Defra's Air Quality Modelling Review Steering Group specified the scenarios and outputs requested for the Phase 2 study of the Model Intercomparison Exercise. Hourly results from the OSRM were provided for 23 receptor sites for four different emissions scenarios:

  1. Reduce total anthropogenic NOx and VOC by 30% across the UK + Europe

  2. Reduce total anthropogenic NOx and VOC by 30% across the UK only

  3. Reduce anthropogenic NOx by 30% across UK + Europe

  4. Reduce anthropogenic VOC by 30% across UK + Europe

The base year was 2006 (emissions and meteorology). Hourly ground-level concentrations were provided for ozone and other indicator species, namely NO, NO_2, NO_y, HNO_3 and H_2O_2.

The results for each scenario were sent to David Carslaw (King's College London) for statistical analysis and comparison with results from other regional scale models. The results will be published by the Review's Steering Group in 2012.

6.4 Summary and main conclusions

The main conclusions of the OSRM ozone modelling work for Objective 10.2 are summarised as follows:

Summary:

- **The OSRM has been used to model the future UK ground-level ozone climate for a number of different UK and European emission scenarios assuming meteorological conditions representative of 2006 and 2007**

- **Some of these referred to changes in UK emissions according to the latest DECC energy scenarios up to 2030. All scenarios led to increases in the AOT40 and Days Greater than 120 µgm^{-3} ozone metrics for 2020-2030 relative to values calculated for 2006. The differences in the values of the metrics between different model years (2020-2030) were greater than they were between different emission scenarios**

- **Maps of annual mean organic aerosol concentrations were calculated for 2020 showing different spatial patterns using 2006 and 2007 meteorology**

- **Further simulations were carried out for different UK and European emission scenarios with different levels of ambition for 2020. The analysis indicated**

> **that it will be important for comparable reductions in emissions to be achieved across Europe as well as in the UK to prevent ozone concentrations in the UK rising.**
>
> - **It also shows the benefits to be achieved by reducing VOC emissions across Europe. These results will help inform Defra's policy relating to potential future national emission ceilings**

7 Modelling Support for Ozone Policy Using the PTM

A range of different investigative activities was carried out with the Photochemical Trajectory Model, but with an emphasis on modelling peak ozone concentrations at specific receptors, rather than annual simulations covering the whole of the UK, and in conjunction with probabilistic uncertainty analysis and sensitivity to choice of chemical reaction scheme used in the model. The PTM was used to investigate ozone responses to precursor emission changes, including changes in isoprene emissions as a consequence of climate change.

A description of the activities and results from the PTM runs are provided in this section.

The PTM was used to model the impacts of the same UEP43 CCC emission scenarios modelled with the OSRM and described in Section 6.1, but with a different emphasis, focusing on changes in the daily maximum ozone concentrations at the rural Harwell site in southern England. The results from this study complement those from the OSRM. The PTM was also used to model the impact of these emission changes on secondary inorganic aerosol concentrations at the Harwell site.

The other activities described in this section are summarised as follows.

For **Objective 10.2** Support for Policy Development and Implementation with respect to ozone:

- Impact of chemical mechanism choice on air quality policy development
- Probabilistic uncertainty analysis of the impact of emission scenarios on ozone

For **Objective 10.3** Specific Modelling and Assessments for Policy Development on Secondary Air Pollutants:

- Secondary pollutant air quality and climate change

7.1 The Photochemical Trajectory Model (PTM)

The PTM has been used to describe photochemical ozone formation as well as secondary inorganic and organic aerosol formation in north-western Europe. Details are given in Derwent et al (1996, 1998, 2009), Abdalmogith et al. (2006) and Johnson et al. (2006). The model describes the chemical development within an air parcel that follows a trajectory for up to 10 days. For each mid-afternoon of each day a large number of equally probable and randomly selected 96-hour air parcel trajectories are generated using the Met Office Numerical Atmospheric dispersion Model Environment (NAME) model. The PTM uses NAEI and EMEP gridded emissions data and inventories for natural biogenic emissions. Initial and background species concentrations are taken from the EMEP site at the Valentia Observatory and the atmospheric baseline station at Mace Head, Ireland. The model has the option of using different chemical mechanisms. Dry deposition processes are represented using a conventional resistance approach.

The PTM has been used for a variety of purposes to support Defra policy on ozone and secondary PM. These include the estimation of photochemical ozone creation potentials (POCPs) of individual VOCs (Derwent et al., 1998) and more recently in this project to estimate secondary organic aerosol formation potentials (SOAPs, Derwent et al, 2010a). It has also been used to evaluate the effectiveness of current precursor emission controls in Europe on levels of ground-level ozone in the UK (Derwent et al, 2010b) and the effectiveness of future potential emission controls.

7.2 PTM Simulations for 2020, 2025 and 2030 for future UK emission scenarios

The UEP43 CCC emission projections modelled by the OSRM (Section 6.1) were also modelled by the PTM for the rural location of Harwell in Oxfordshire.

An uncertainty analysis framework has been developed for the PTM model, based on the Monte Carlo sampling of predefined model input uncertainty ranges for all model input parameters. As part of this framework, each model run had a randomly selected chemical mechanism from the following: CBM-4, CB-05, SAPRC-99 and SAPRC-07. A large number, 488,000, of PTM model runs were performed for the 2008 base case for mid-afternoon conditions for the 122-day period from 1st April to 31st July 2008, for Harwell, Oxfordshire. Only those parameter sets that performed well against the AURN observations were deemed 'acceptable' and were used again for the 2020, 2025 and 2030 scenario cases. The results from the 'acceptable' base case run were paired up with the corresponding scenario case and the impact of the scenario was found by taking the differences in the daily maximum ozone concentrations for each day from the 2008 base case. The differences found for each day were sorted and ranked and the percentiles and 1-σ confidence ranges were estimated.

7.2.1 Probabilistic Results for the Highest Ozone Day

The highest daily maximum 1-hour ozone concentration was observed (76 ppb) and modelled on the 11th May 2008 (Day 40) at Harwell, Oxfordshire. Out of the 4,000 model runs performed for this day, 158 were deemed 'acceptable', of which 24 utilised the CB05 chemical mechanism, 31 CBM4, 35 SAPRC-07 and 68 SAPRC-99. In the majority of the 'acceptable' model runs, ozone levels on the 11th May decreased between the 2008 base case and the 2020 scenario case under the influence of the emission projections. The differences, defined by $O_3^{2008} - O_3^{2020}$, $O_3^{2008} - O_3^{2025}$ and $O_3^{2008} - O_3^{2030}$ were largely positive, implying a reduction in episodic peak ozone levels and hence an improvement in ozone air quality. However, there were 18 runs out of the 158 in 2020 where the differences were negative, implying a deterioration in ozone air quality. There was therefore a high probability, better than 88 chances out of 100, that the emission projections to 2020 would lead to an improvement in **peak ozone** air quality. This probability rose to 92 chances out of 100 in the 2025 scenario case and to 94 chances in 2030.

Figure 7.1 shows the box-and-whisker plot of the impact of the emission projections to 2020 on the highest daily ozone maximum concentration, relative to the peak ozone in 2008. The median differences, shown as a black squares, were 10 ppb, 12.5 ppb and 14 ppb, respectively, in 2020, 2025 and 2030. All these differences from the base case were highly statistically significant. The interquartile range of the differences, shown by the shaded boxes, extended from 7 to 14 ppb and the 1-σ confidence interval covered the range from 1.8 to 17.3 ppb in 2020. The extreme maximum difference found in any model run, shown as a hexagon, was 19.8 ppb in 2020. This extreme maximum difference brought the highest daily maximum ozone concentration down to 49 ppb on the highest ozone day in 2020.

There was therefore an extremely low probability, less than 1 chance in a 100, that the emission projections to 2020 would have achieved enough of a reduction in ozone precursor emissions to have reduced episodic peak ozone levels on the highest ozone day so that the World Health Organisation (WHO) Air Quality Guideline for ozone of 50 ppb maximum 8-hour mean concentration was met. This makes due allowance for the difference in averaging time periods between the WHO Air Quality Guidelines (8-hour) and the model results (1-hour). This probability was unchanged in 2025 and 2030.

7.2.2 Probabilistic Results for Ozone Air Quality for the Whole 122-day Period

Median daily maximum ozone levels decreased on 108 days and increased on 14 days relative to the 2008 base case in response to the emission projections to 2020. The whole period average daily maximum 1-hour ozone concentrations decreased from 41.8 ppb in

AEA

Figure 7.1: Probabilistic predictions of the influence of the 2020, 2025 and 2030 emission projections relative to 2008 on the highest daily maximum ozone mixing ratios from the Monte Carlo uncertainty analysis, showing the median values (black squares), interquartile range (shaded boxes), range from maxima to minima (lines with bars), outliers (hexagons) and extremes (stars).
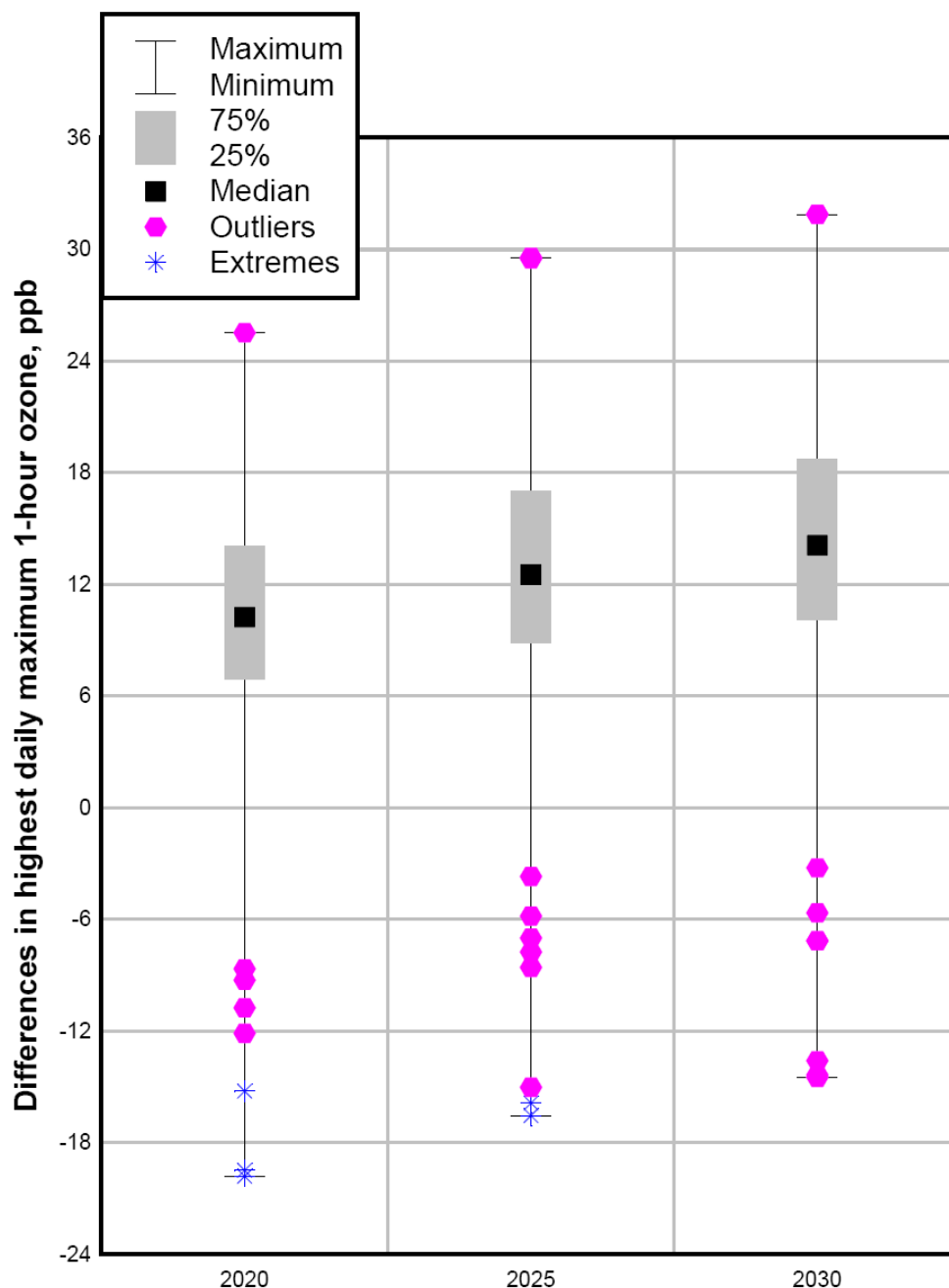
2008 to 39.6 ppb in 2020, to 39.1 ppb in 2025 and to 38.8 ppb in 2030. As a result, SUMO35 for the 122-day period declined from 1005 ppb days to 713 ppb days in 2020, representing a 29% reduction, down to 649 ppb days in 2025 and to 616 ppb days in 2030.

7.2.3 Impact of the Emission Projections to 2020 on Secondary Inorganic Aerosol

The 122-day average secondary inorganic aerosol mass concentrations decreased from 4.68 µg m^{-3} in the 2008 base case to 3.76 µg m^{-3} in the 2020 scenario case. This represents a decrease of 0.86 µg m^{-3}, that is, about a 20% reduction. SIA mass declined to 3.65 µg m^{-3} in 2025 and to 3.56 µg m^{-3} by 2030.

7.3 Impact of chemical mechanism choice on air quality policy development

7.3.1 Introduction

The PTM model has been used to evaluate the impact of chemical mechanism choice on air quality policy development. The Defra Model Intercomparison Exercise has been completed by a number of modelling groups each using their own models and input data. These models have used a range of different chemical mechanisms as well as meteorological and other input data. Within the AQMEII model intercomparison initiative, no attempt has been made to harmonise chemical mechanism choice whilst the emissions and meteorological input data have been carefully harmonised. If Defra is to choose between any of these models and modelling groups, it will need some understanding of the relative merits of the different chemical mechanisms.

The aim of this work programme item is therefore to evaluate the impact of chemical mechanism choice against the 'gold standard' of the Master Chemical Mechanism for a number of issues of relevance to air quality policy development.

Policy makers expect that any model used to underpin O_3 policy formulation should be able to reproduce satisfactorily real world behaviour in terms of observed O_3 levels. An evaluation of atmospheric chemical mechanisms must therefore look more deeply than a model's ability to reproduce history. Hence, in this study, we largely take for granted comparison with observation and move on to other diagnostic issues that are of greater policy relevance. We have attempted to answer questions, such as, how does the choice of chemical mechanism influence:

- the responses to VOC and NO_x controls?
- the amount of ozone formed on one day compared to the next, for a given VOC species?
- the relationship between VOC and NO_x emissions in one country and O_3 levels in another?

7.3.2 Approach

Six chemical mechanisms have been employed in this study, see Table 7.1, spanning over two orders of magnitude in chemical complexity. The most complex chemical mechanism employed is the Master Chemical Mechanism (MCM), a near-explicit chemical mechanism describing the detailed degradation of a large number of emitted organic compounds. This has been employed and further developed in this project (Objective 9) to describe formation of ozone and other secondary pollutants under conditions appropriate to the atmospheric boundary layer. The MCM chemical mechanism can be accessed via the University of Leeds website (http://mcm.leeds.ac.uk/MCM). The degradation chemistry used in the MCM chemical mechanism has been developed using published protocols (Saunders et al., 2003; Jenkin et al., 2003; Bloss et al., 2005). The MCMv3.1 version used addressed 173 emitted VOC species and employed 4,355 reactive compounds taking part in 12,723 chemical reactions.

We have also employed the Common Representative Intermediates mechanism version 2 (CRI v2), a reduced mechanism of intermediate complexity which is directly traceable to the

Table 7.1. Details of the chemical mechanisms compared and evaluated in this study.

Chemical mechanism	Number of emitted VOCs	Number of chemical reactions	Number of chemical species
MCMv3.1	173	12,733	4,355
CRIv2	99	1,168	455
CBM4	10	88	42
CB05	14	145	56
SAPRC-99	31	216	77
SAPRC-07	18	140	52

MCM (Jenkin et al., 2008). This mechanism has also been further developed and tested in this project under Objective 9. The CRI mechanism addresses 99 emitted VOC species and employs 455 reactive compounds taking part in 1,168 chemical reactions. The emissions of all the emitted CRI VOCs were scaled up by a factor of 1/0.9079 to account for the additional O_3 formed from the VOCs species that were not in the CRIv2 mechanism but were in the NAEI VOC speciation.

We have employed two versions of the Carbon Bond Mechanism: CBM4 and CB-05 and two versions of the SAPRC chemical mechanism: SAPRC-99 and SAPRC-07. The CBM4 is the most highly condensed chemical mechanism employed in this study and the version used here addressed CH_4 and 10 emitted VOC species (PAR, ETH, OLE, ALD2, FORM, TOL, XYL, CH_3OH, C_2H_5OH and ISOP), 42 reactive compounds and 88 chemical reactions including the inorganic reactions. The CB05 chemical mechanism addressed CH_4 and 14 emitted VOC species (ETHA, PAR, ETH, OLE, IOLE, ALD2, ALDX, FORM, TOL, XYL, CH_3OH, C_2H_5OH, ISOP and TERP), 56 reactive compounds and 145 chemical reactions.

The version of the SAPRC-99 chemical mechanism employed here addressed 31 emitted VOC species in addition to CH_4, and employed 77 chemical species taking part in 216 chemical reactions, including the inorganic reactions. The SAPRC-07 is an update of the SAPRC-99 chemical mechanism and treated 18 emitted VOC species and 52 reactive species taking part in 140 chemical reactions.

The assignments of the 173 emitted species in the NAEI VOC emission inventory to the SAPRC and Carbon Bond surrogate species were taken from Carter (2010).

The six chemical mechanisms have been harmonised in such a way as to facilitate comparison and evaluation. This means that our evaluation does not deal necessarily with the actual chemical mechanism produced by the mechanism developers. Our study addresses a harmonised version of each chemical mechanism produced by the implementation of the four steps detailed below. For simplicity, each chemical mechanism is still referred to by its original name and it is implicitly understood that reference is being made to the harmonised version. The following steps were taken to harmonise each chemical mechanism:

Step 1: the fast photochemical reactions involving O^3P, O^1D, OH, H, HO_2, NO_3 with N_2, O_2, H_2O, CO, O_3, NO, NO_2, HNO_3, HO_2NO_2, N_2O_5, SO_2, sulphate and nitrate aerosol, (the so-called inorganic reactions), were replaced by a common set of 47 reactions, of which 35 were thermal reactions, 8 were photochemical and 4 were aerosol formation reactions.

Step 2: all complex temperature, pressure and humidity dependent rate coefficients were replaced by a common set of 17 rate coefficients.

Step 3: the formation and thermal decomposition of all PAN-type molecules were replaced by a common pair of temperature and pressure-dependent reaction rate coefficients.

Step 4: all photolysis rate coefficients were replaced by a common set based on the J-values provided on the MCM website.

These harmonisation steps leave unchanged the simplifications and approximations made by the developers in addressing the organic reactions that degrade the emitted VOC species to produce ozone. Whereas the MCMv3.1 contains over 15,000 chemical reactions, the other mechanisms condense down this atmospheric chemistry by over two orders of magnitude, see Table 7.1. It is this condensation that is being evaluated in this study, using the MCMv3.1 as the 'gold standard'. This evaluation is not affected by the harmonisation steps detailed above.

The PTM model was set up as described above. One thousand equal probability 96-hour back track trajectories were generated by the NAME model for 15:00z to 15:15z for each day of the PUMA campaign held during June and July 1999. The PTM model was run for each of these trajectories using the CBM4 chemical mechanism. Both the model and the observations exhibited periods of background O_3 with levels in the 20 – 50 ppb from 20th to 25th June and from 27th June to 1st July with an O_3 episode on 26th June in between (Derwent et al. 2010b). On the 26th June 1999, the PTM predicted a 15:00 z O_3 mixing ratio of 77.1 ± 4 ppb for the University of Birmingham, Pritchatts Road field site based on the highest 4 out of the 1000 equal-probability trajectories. When the chemical mechanism was switched to the CRI and MCMv3.1 chemical mechanisms from the CBM4 mechanism, the model O_3 mixing ratio changed to 84.1 ± 6 ppb and 78.6 ± 5 ppb, respectively. Within the stated 1 – σ confidence limits, these model calculated peak O_3 mixing ratios are indistinguishable between the different mechanisms.

These model predicted peak O_3 mixing ratios compare closely with the observed maximum mid-afternoon hourly levels of 92 ppb observed at the Stoke-on-Trent and Leamington Spa urban monitoring sites and the range 76 – 92 ppb observed across all 8 AURN monitoring sites in Central England. On this basis, the PTM model performance was considered acceptable and it was concluded that model performance was independent of these chosen mechanisms.

7.3.3 Evaluation of Selected Chemical Mechanisms

In this study to evaluate the policy impacts of chemical mechanism choice, the PTM model was set up as described above for the PUMA campaign held in Central England during 1999. The emissions data were taken for 1999 and one of the 1000 equal probability trajectories was selected for 26th June. Figure 7.2 shows the path taken for this 96-hour trajectory. It began over the coast of the Netherlands, having travelled across the North Atlantic Ocean and the British Isles during the previous few days. It then travelled close to the Belgium – Netherlands border and then the Belgium – Germany border before entering France. The air parcel travelled in a south-westerly direction and then westerly before turning northerly and exiting France through Normandy. It then travelled in a northerly direction across southern England before arriving in central England at 18:00 z on 26th June 1999. Exchange with the free troposphere was switched off as was dry deposition of hydroperoxides and peroxy acids.

7.3.3.1 *Responses to NO$_x$ and VOC emission controls*

An important policy output of photochemical O_3 models is the response to O_3 precursor emission reductions. Here the PTM model responses to 30% reductions in emissions of NO_x and VOCs were estimated using the 6 chemical mechanisms with all other model input parameters held constant. The emission reductions were applied across-the-board, that is to say, they were applied to all UK and European emission source categories equally. No changes in VOC speciation are made and biogenic emissions of isoprene and terpenes are left unchanged.

Figure 7.2. 96-hour back-track air mass trajectory for 26th June 1999 that gave the highest model ozone level at Pritchatt's Road, Birmingham
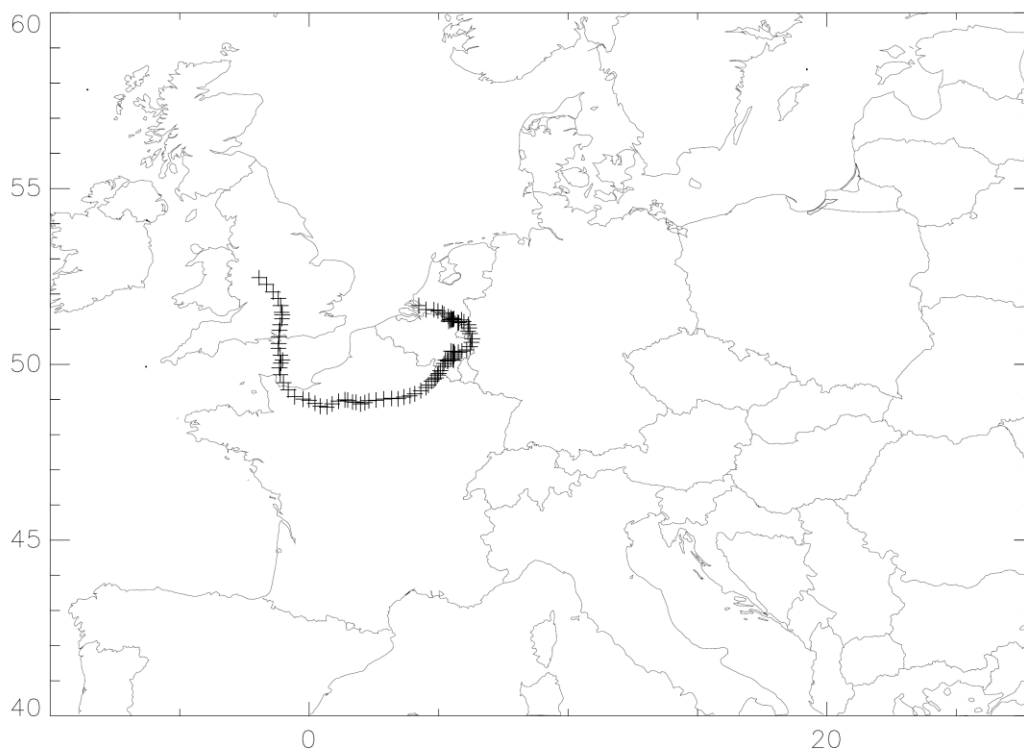
With all chemical mechanisms and for both the NO_x and VOC emission reduction cases, O_3 levels at the arrival point at Pritchatts Road, Birmingham fell relative to the base case. The O_3 responses (calculated as base case – emission reduction case) achieved are presented in Table 7.2 for the two emission cases and the six chemical mechanisms. The PTM model responses to the 30% reductions in NO_x emissions were more varied across the six chemical mechanisms compared with the responses to the reductions in VOC emissions, as shown by the relative standard deviations. The SAPRC-99 mechanism gave the greatest response in the NO_x scenario case whereas the CRI mechanism gave the least, with a range of about a factor of 3 – 4 between them. The CRI mechanism gave the greatest response in the VOC scenario case whereas the CBM4 mechanism gave the least, with a range of about a factor of 2 between them.

There is an indication that those chemical mechanisms that give greater responses in the NO_x scenario case give smaller responses in the VOC scenario case, as indicated by the approximately inverse relationship between the two responses, see Figure 7.3. However, all chemical mechanisms gave greater O_3 responses in the VOC scenario case compared with the NO_x scenario case, despite the apparent inverse relationship. That the VOC scenario responses were greater than the NO_x scenario responses, points to the PTM being VOC-limited for the 15:00z 26th June 1999 trajectory. The SAPRC-07 and SAPRC-99 chemical mechanisms were the least VOC-limited and the MCMv3.1, CRI and CB05 chemical mechanism were the strongest VOC-limited.

Table 7.2: The O$_3$ responses achieved at Pritchatts Road, Birmingham with 30% across-the-board reductions in NO$_x$ and VOCs emissions with each chemical mechanism.

Chemical mechanism	O$_3$ response to 30% NO$_x$ emission reductions, ppb	O$_3$ response to 30% VOC emission reductions, ppb
MCMv3.1	2.4	12.1
CRI	2.2	14.0
SAPRC-99	7.7	9.4
SAPRC-07	6.8	11.7
CBM4	5.2	6.5
CB05	2.4	13.8
Average	4.5 ± 2.5	11.3 ± 2.9

Notes:

a. O$_3$ responses are shown as (base case) – (scenario case) and are in ppb.

b. emission reductions were applied equally to all man-made emission source categories independent of location.

c. no changes were made to biogenic emission of isoprene and terpenes.

Figure 7.3: Scatter plot of the PTM model responses in the NO$_x$ and VOC scenarios with the six chemical mechanisms. O$_3$ responses are shown as base case – scenario case in ppb
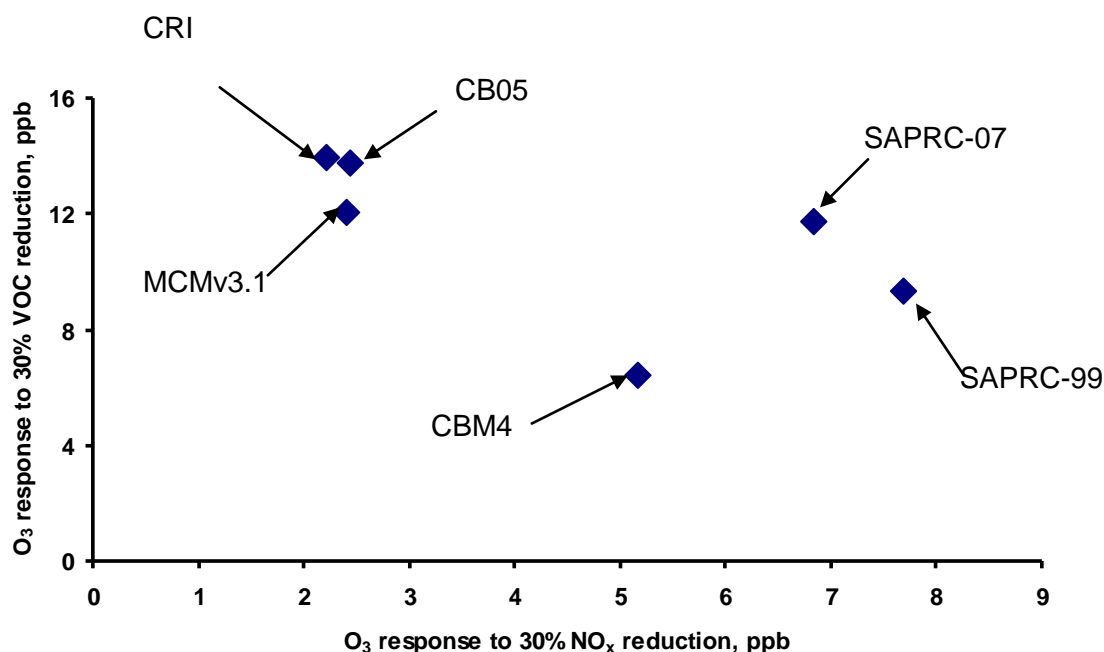
7.3.3.2 NO_y speciation

The atmospheric chemical processes that produce the elevated photochemical O_3 levels are peroxy radical-driven NO to NO_2 conversion processes, such as:

$RO_2 + NO = RO + NO_2$
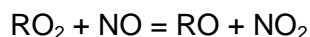
The processes that produce the peroxy radicals are the OH radical driven oxidation processes such as :

$RH + OH = RO_2 + products$

So an essential prerequisite for the production of elevated O_3 levels is a sufficient steady state concentration of OH radicals. A direct consequence of this OH steady state is the efficient oxidation of NO_x to oxidised nitrogen compounds (NO_y). It is therefore impossible to produce O_3 photochemically without oxidising NO_x to NO_y. Indeed, the capacity of the atmosphere to produce O_3 is limited by the availability of NO_x. There are two main types of NO_y oxidation products: nitric acid (HNO_3) and peroxyacetylnitrates (PANs):

$OH + NO_2 = HNO_3$

$RCO(O_2) + NO_2 = PAN$

As a result of the photochemical processes, elevated levels of both O_3 and NO_z (= NO_y – NO_x) are produced and there is a relationship between the elevation in these two quantities, O_3 and NO_z. Here, we show how these elevations in O_3 and NO_z are chemical mechanism dependent.

Table 7.3 presents the final O_3 and NO_z mixing ratios for the PTM model run for 15:00z 26th June 1999 at Pritchatts Road, Birmingham with the six chemical mechanisms. Despite fixing the fast photochemistry, the initial NO_x boundary conditions and the NO_x emissions to be identical with each of the chemical mechanisms, the final NO_z mixing ratios span a range of 2.2 ppb in a mean of 24.7 ppb. The O_3 productivities span the range from 3.95 to 4.63 molecules per molecule of NO_x oxidised. The CB05 chemical mechanism was the least productive and SAPRC-07 was the most productive, according to this index, see Table 7.3.

Table 7.3: The elevations in O_3 and NO_z along the base case trajectory arriving at Pritchatts Road, Birmingham at 15:00z on 26th June 1999 with the 6 chemical mechanisms.

Chemical mechanism	Final [O_3], ppb	Final [NO_z], ppb	[O_3] / [NO_z]
MCMv3.1	112.9	25.6	4.40
CRI	104.1	25.6	4.07
CBM4	101.6	25.5	3.99
CB05	92.5	23.4	3.95
SAPRC-99	102.5	24.1	4.26
SAPRC-07	111.0	24.0	4.63
Average	104.1 ± 7.3	24.7 ± 1.0	4.21 ± 0.26

There were also systematic differences in the speciation of the oxidised nitrogen species that made up the NO_z. The CB05 and CBM4 chemical mechanisms gave roughly similar fractions of the final NO_z as HNO_3 and PANs, with both about 0.2, the remainder being nitrate aerosol.

In contrast, the MCMv3.1 and SAPRC-07 chemical mechanisms gave widely different fractions with values above 0.3 for PAN and much less than 0.2 for HNO_3. There appears to be clear relationships between the O_3 productivities expressed as O_3 molecules produced per molecule of NO_x oxidised and the fractions of the final NO_z found as PAN and HNO_3, see Figure 7.4. O_3 productivities increase with increasing fractions of final NO_z as PAN and decrease with increasing fractions found as HNO_3. The MCMv3.1 and SAPRC-07 chemical mechanisms show the greatest O_3 productivities and favour PAN formation over HNO_3 formation.

Figure 7.4: Scatter plots of the fraction of NO_z present as PAN (filled diamonds) and as HNO_3 (filled squares) at the arrival point of the trajectory at 15:00z 26th June 1999 versus the ratio of the final O_3 to NO_z mixing ratios for the six chemical mechanisms.
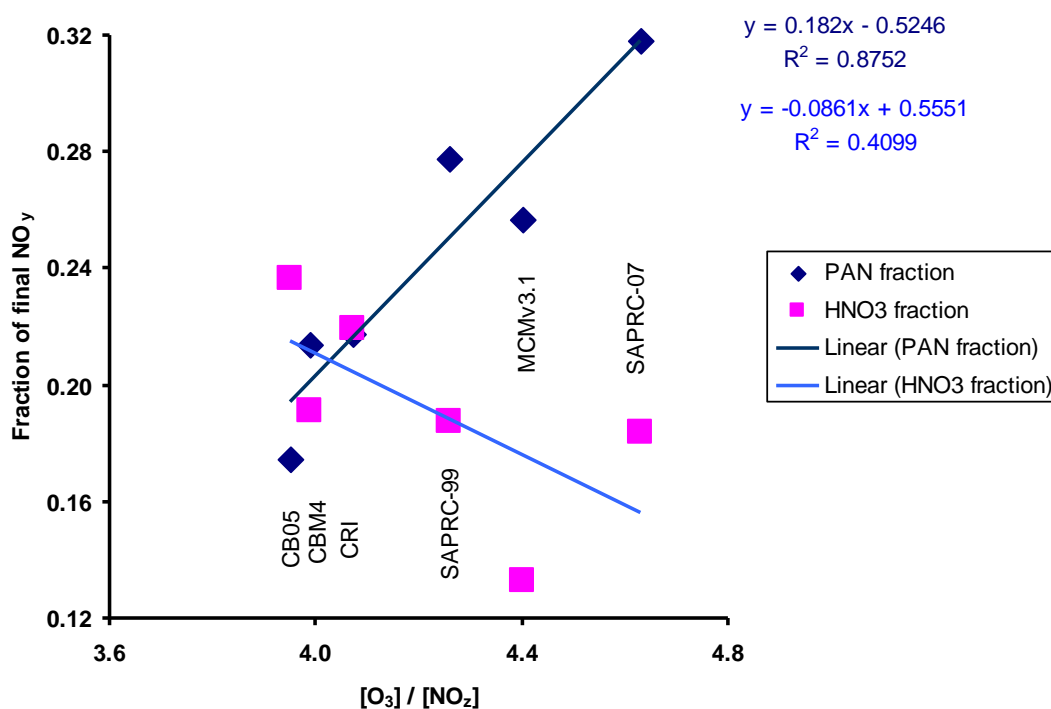
7.3.3.3 *Estimation of VOC reactivities*

An important application for photochemical models has been the estimation of VOC reactivities and the design of reactivity-based policies for reducing O_3 levels. The PTM model O_3 responses to hour long pulses of VOC emissions have been investigated using the different chemical mechanisms. The base case involved the PTM model being run as described above. The sensitivity case involved adding an extra emission of ethylene during the hour starting at 09:00z on the 3rd day of travel. By subtracting the O_3 mixing ratios calculated in the sensitivity case from the base case, the PTM model response to the additional emission pulse of ethylene could be estimated. To get an appreciable O_3 excess over the base case (calculated as emission pulse case – base case), the instantaneous ethylene emission during the hour starting at 09:00z in the base case had to be scaled by a factor of 100. The scaling factor was entirely arbitrary and was set so that the O_3 excesses were large enough to be discernible yet not too large to be beyond the linear range.

Figure 7.5 shows how the excess O_3 levels produced by the ethylene pulse varied between the different chemical mechanisms. The excess O_3 levels rose from zero and then flattened out by 18:00z on the 3rd day, (travel time 48 – 71 hours). The excesses with the MCMv3.1, CB05 and SAPRC-99 chemical mechanisms were closely similar at about 0.56 – 0.59 ppb,

Figure 7.5: Excess O$_3$ levels produced by the injection of an hour long pulse of ethylene at 09:00z on the third day of travel calculated by the PTM model with the different chemical mechanisms. Excess O$_3$ levels are shown as emission pulse case – base case in ppb.

Reactivity calculation for ethylene
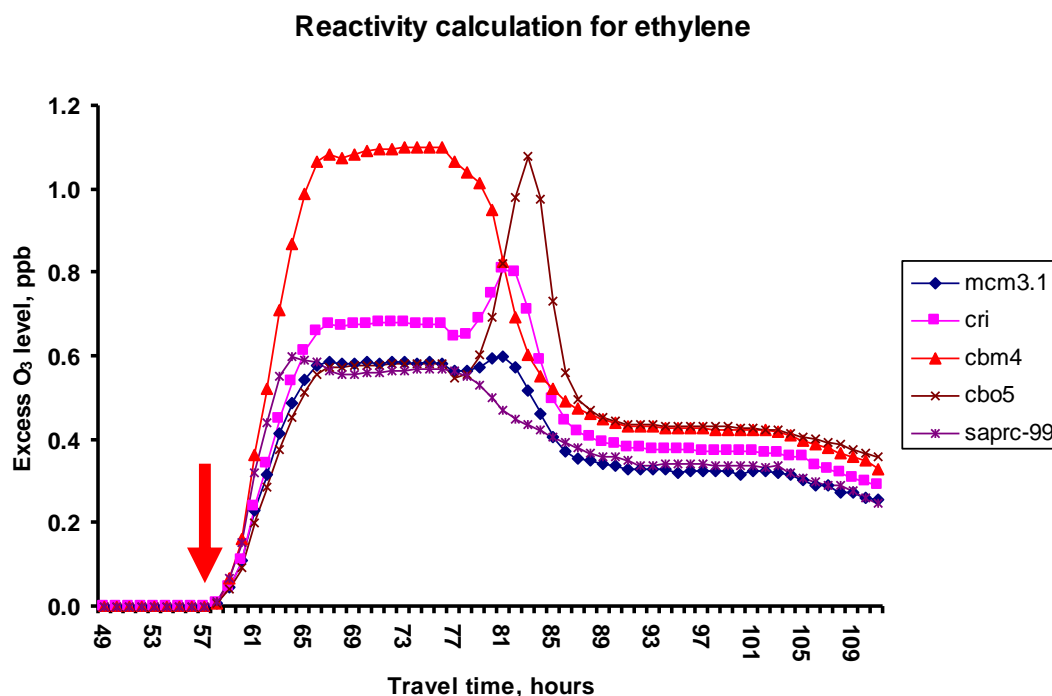
whereas those with the CRI and CBM4 chemical mechanisms were significantly higher at 0.68 and 1.09 ppb, respectively.

The excess O$_3$ levels rose again after 09:00z on the 4th day, (travel time 72 – 95 hours), reflecting further stimulated O$_3$ production from the carry-over of unreacted ethylene and from secondary oxidation products. The excess O$_3$ levels on the 4th day were much more varied and covered the range from zero with the CBM4 and SAPRC-99 chemical mechanisms and up to 0.53 ppb with the CB05 chemical mechanism. The MCMv3.1 chemical mechanism gave a small 4th day production of 0.03 ppb and the CRI, 0.16 ppb.

Figure 7.6 presents the corresponding plots for hour long emission pulses of n-butane. For this organic compound, the MCMv3.1, CRI and CB05 chemical mechanisms gave similar 3rd day excess O$_3$ levels with the SAPRC-99 and CBM4 giving significantly greater levels.

The corresponding plots for toluene, see Figure 7.7, show much more diversity because of the lack of general understanding of the detailed mechanism of toluene degradation in the atmosphere. With toluene, the CB05 chemical mechanism gave the least 3rd day excess O$_3$ levels. The MCMv3.1, CRI and SAPRC-99 chemical mechanisms gave roughly similar excess O$_3$ levels, with the CBM4 mechanism giving a significantly greater level. On the 4th day, the excess O$_3$ levels turned negative with the CBM4, CB05 and SAPRC-99 chemical mechanisms but remained positive with the MCMv3.1 and CRI chemical mechanisms.

There was little diversity between the excess O$_3$ levels produced by pulses of isoprene, with the MCMv3.1, CRI, CBM4 and CB05 chemical mechanisms showing closely similar behaviour, see Figure 7.8. The SAPRC-99 chemical mechanism showed a different time development during the late afternoon and night-time of the 3rd day. Only the CRI and CB05 chemical mechanisms showed evidence of 4th day production from the carry-over of secondary reaction products.

Figure 7.6: Excess O₃ levels produced by the injection of an hour long pulse of n-butane at 09:00z on the third day of travel calculated by the PTM model with the different chemical mechanisms. Excess O₃ levels are shown as emission pulse case – base case in ppb.

Reactivity calculation for n-butane

Figure 7.7: Excess O₃ levels produced by the injection of an hour long pulse of toluene at 09:00z on the third day of travel calculated by the PTM model with the different chemical mechanisms. Excess O₃ levels are shown as emission pulse case –base case in ppb.

Reactivity calculation for toluene

Figure 7.8: Excess O$_3$ levels produced by the injection of an hour long pulse of isoprene at 09:00z on the third day of travel calculated by the PTM model with the different chemical mechanisms. Excess O$_3$ levels are shown as emission pulse case – base case in ppb.
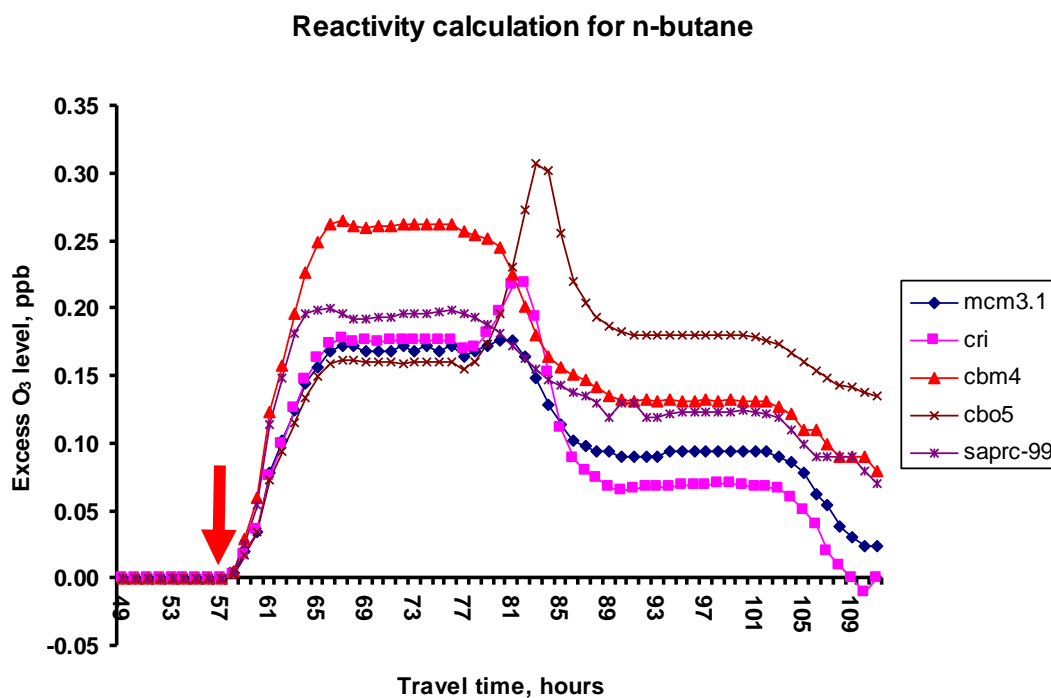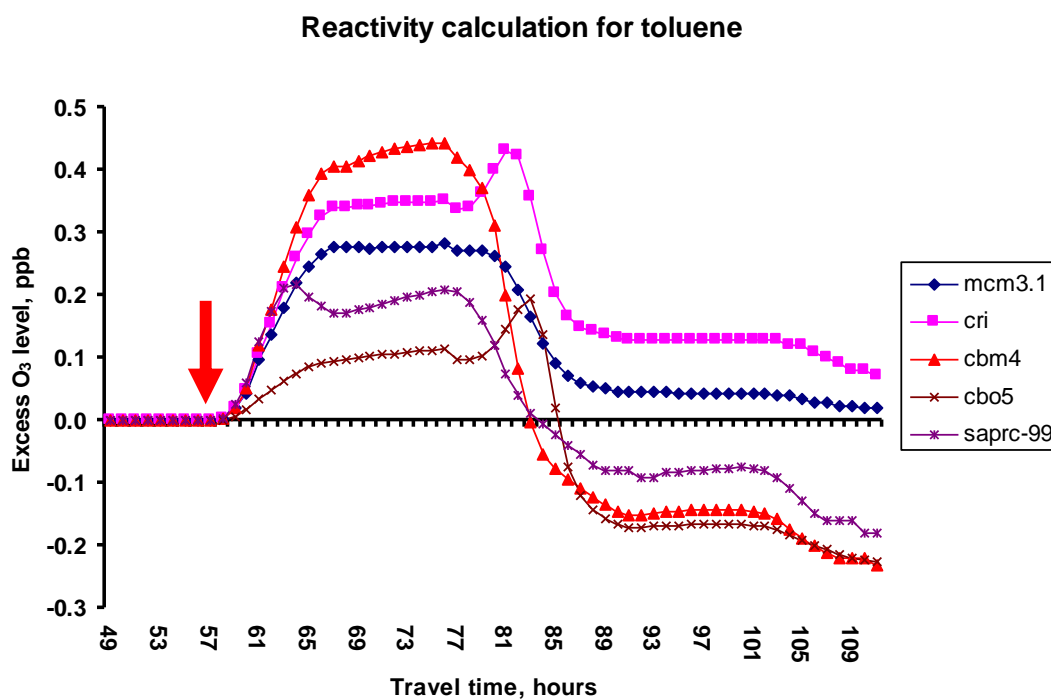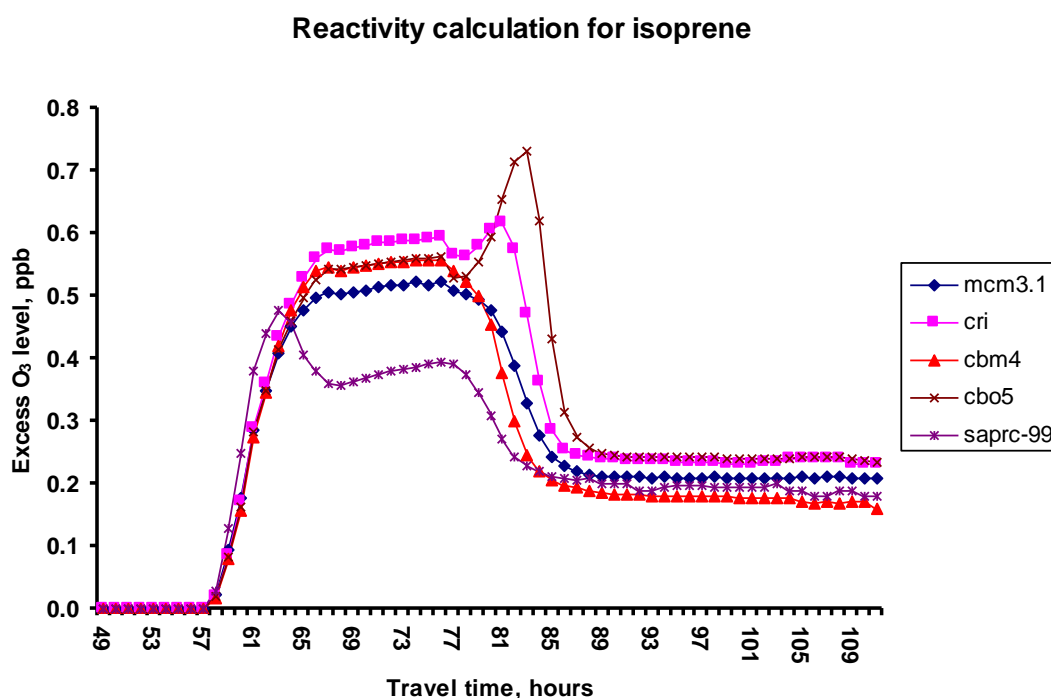

Reactivity calculation for isoprene

7.3.3.4 Source – receptor relationships between VOC emissions and downwind O$_3$

A further important application for photochemical models is the determination of source – receptor relationships. Here, the VOC emissions from the Netherlands are switched off and the impact determined on the O$_3$ mixing ratios downwind and at the arrival point

A further important application for photochemical models is the determination of source – receptor relationships. Here, the VOC emissions from the Netherlands are switched off and the impact determined on the O$_3$ mixing ratios downwind and at the arrival point in central England, relative to those in the base case with Netherlands VOC emissions switched on. The PTM model responses (calculated as base case – zero emissions case) are plotted out in Figure 7.9 for the different chemical mechanisms. O$_3$ mixing ratios were lower with Netherlands VOC emissions switched off compared with the base case, with the differences being greatest on the 3rd day compared to the 2nd and 4th days. Peak O$_3$ differences were found to be in the range between 3.45 for the MCMv3.1 chemical mechanism and 5.06 ppb for CBM4. The shape of the O$_3$ differences were similar for most of the chemical mechanisms, with the exception of that for the CB05 chemical mechanism which showed its maximum on the 4th day instead of the 3rd day.

At the arrival point at Pritchatts Road, Birmingham, after 96 hours, the Netherlands VOC emissions appeared account for between 0.84 and 1.41 ppb of the O$_3$ modelled in the base case, with a mean value of 1.13 ± 0.2 ppb. The Netherlands contributions were closely similar with the CB05, MCMv3.1 and CRI chemical mechanisms but smallest with CBM4 and greatest with SAPRC-99.

Figure 7.9: Differences in O$_3$ levels caused by switching off of the VOC emissions from the Netherlands with the different chemical mechanisms. Differences are shown as base case – zero emissions case in ppb.
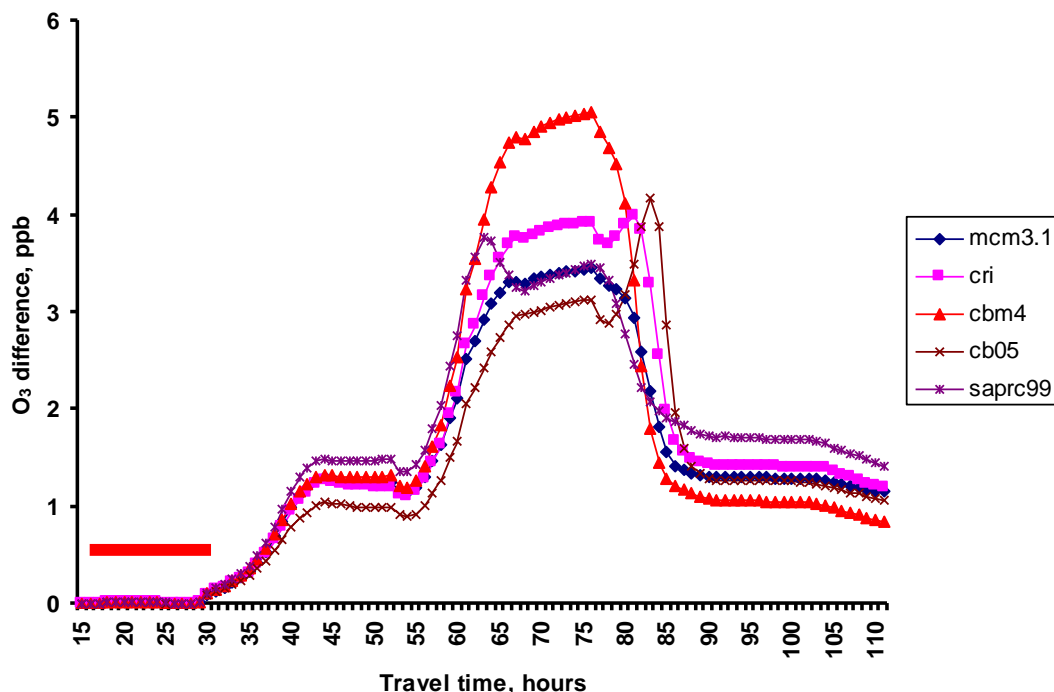
7.4 Monte Carlo parametric uncertainty analysis of the impact of scenarios for the negotiations of the revision of the Gothenburg Protocol on ozone levels at Harwell

The Convention on Long-range Transboundary Air Pollution has embarked on the revision of its Gothenburg multi-pollutant/multi-effect protocol. To inform negotiations about the scope for further cost-effective measures, a series of 7 emission control scenarios have been developed that illustrate options for cost-effective improvements in air quality in Europe. These emission control scenarios address country-by-country emissions for 2020 of SO$_2$, NO$_x$, PM, VOCs, NH$_3$ and CO (Amann et al., 2011). Here we assess the impact of these scenarios on ozone levels modelled at Harwell, Oxfordshire, in the UK using the PTM model (Derwent et al., 2009). The 7 emission control scenarios for 2020 are introduced in Table 7.4. The emissions refer to the rest of Europe in the PTM model domain outside of the UK including Germany (former Federal Republic of Germany), France, Netherlands, Belgium, Luxembourg, Ireland and Denmark.

The LOW, MID and HIGH scenarios refer to three basic levels of ambition in emission reductions. LOW[*] and HIGH[*] are variants or sensitivity cases. LOW* increases the ambition level in the LOW case for eutrophication to 50% while HIGH* reduces the ambition level in the HIGH case for ground-level ozone to 50%. MFR refer to a Maximum Feasible Reduction scenario.

Table 7.4: Pollutant emissions in thousand tonnes per year for 1990 and for 2020 in the seven emission control scenarios for the rest of Europe domain proposed for the CLRTAP negotiations (Amann et al., 2011).

Year	Scenario	NMVOC	NH$_3$	NO$_x$	SO$_2$	CO
1990		6327	1630	5410	6625	24343
2020	Baseline	1826	1461	1641	624	4915
2020	LOW	1716	1327	1583	610	4814
2020	LOW*	1718	1166	1580	622	4876
2020	MID	1666	1121	1524	601	4798
2020	HIGH*	1617	1040	1482	542	4563
2020	HIGH	1485	1073	1431	543	4477
2020	MFR	1257	957	1387	503	4056

7.4.1 PTM model predictions for 2008 and 2020

The PTM model (Derwent et al., 2009a) was set up using 'best estimate' BE input for a 122 day base case covering the period from 1st April to 31st July 2008 for the rural Harwell location in Oxfordshire, UK. The model predicted daily maximum ozone levels which should be directly comparable with the mid-afternoon hourly maxima reported by the AURN. Ozone observations demonstrated the occurrence of photochemical episodes producing ozone levels in excess of 50 ppb on 24th – 26th April, 5th – 12th May, 21st – 24th May, 8th – 9th June, 1st July and 24th – 28th July. The peak hourly ozone level of 76 ppb was recorded on 11th May 2008.

The PTM model results for this study period are compared with the observations in Figure 7.10, showing how it is able to account accurately for all the observed day-by-day variability in the observed ozone levels. Model results are presented from 4 versions of the model using different chemical mechanisms: CBM4, CB05, SAPRC-99 and SAPRC-07. The PTM model showed mean biases of -0.45 to -1.6 ppb, mean fractional biases of -0.004 to -0.026 and root mean square errors of 2.3 to 3.8 ppb, using the 4 chemical mechanisms. PTM model performance was considered entirely satisfactory using the benchmarks presented by Derwent et al., (2010c) and model performance was found to be independent of chemical mechanism choice.

The PTM model was then rerun for each of the 2020 emission scenario variants and with each chemical mechanism. The impacts of the emission scenarios depended on which metric was used to describe the ozone levels. Here, we have chosen three metrics:

- the average of the daily maximum ozone levels predicted over the 122 day period,
- the highest daily maximum ozone level found in the 122 day period,
- the number of days in which the maximum ozone level exceeded 50 ppb.

Considering the average of the 122 daily maximum ozone levels, the model predictions are summarised in Figure 7.11. Compared with the differences between the 2008 and 2020 base case which were 1.9 – 3.8 ppb, the declines across the 2020 emission scenario variants were somewhat smaller, 1.0 – 1.4 ppb. SAPRC-07 gave the largest difference between the 2008 and 2020 base cases and the largest difference between the 2020 base case and 2020 MFR scenario variants. CBM4 gave the smallest difference between the 2008 and 2020 base cases and the smallest difference between the 2020 variants. Much of the air quality improvement between 2008 and 2020 was achieved with the lowest level of ambition in the

Figure 7.10: Comparison of observed and PTM model daily maximum ozone levels for 1st April to 31st July at Harwell, Oxfordshire.

Figure 7.11: The impact of the 2020 emission scenarios relative to the 2008 base case on the average daily maximum ozone predicted with the PTM model using different chemical mechanisms.

2020 base case. The 2020 variants with increasing levels of ambition appeared to offer little further improvement in air quality.

The highest daily maximum ozone in the 2020 base case increased above the 2008 base case with the SAPRC-07 mechanism but decreased below the 2008 base case with the CBM4, CB05 and SAPRC-99 mechanisms, see Figure 7.12. The differences between the
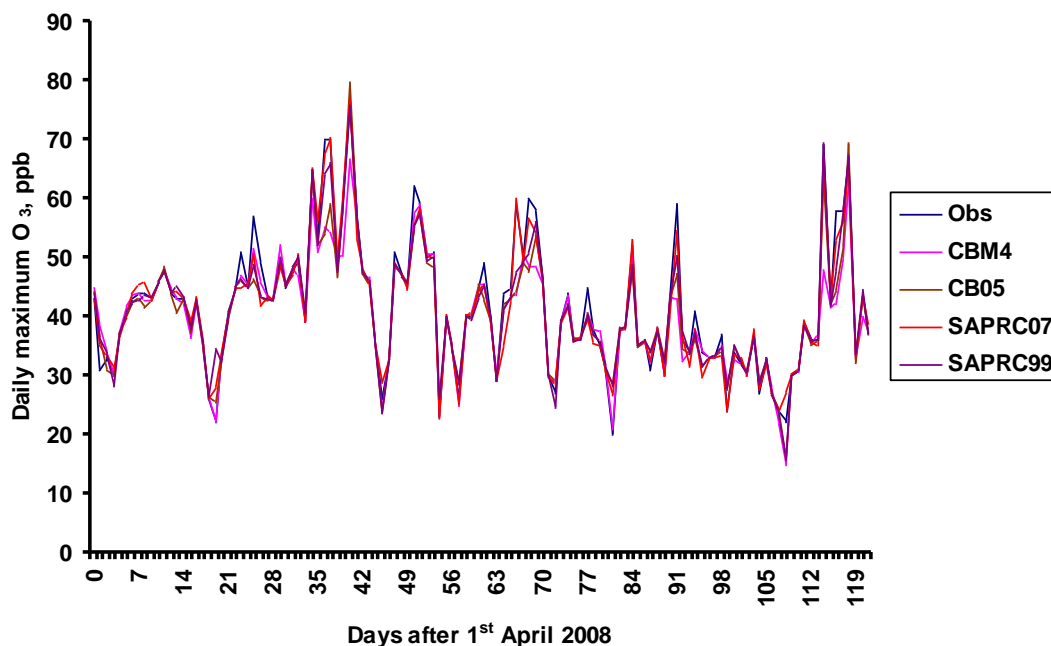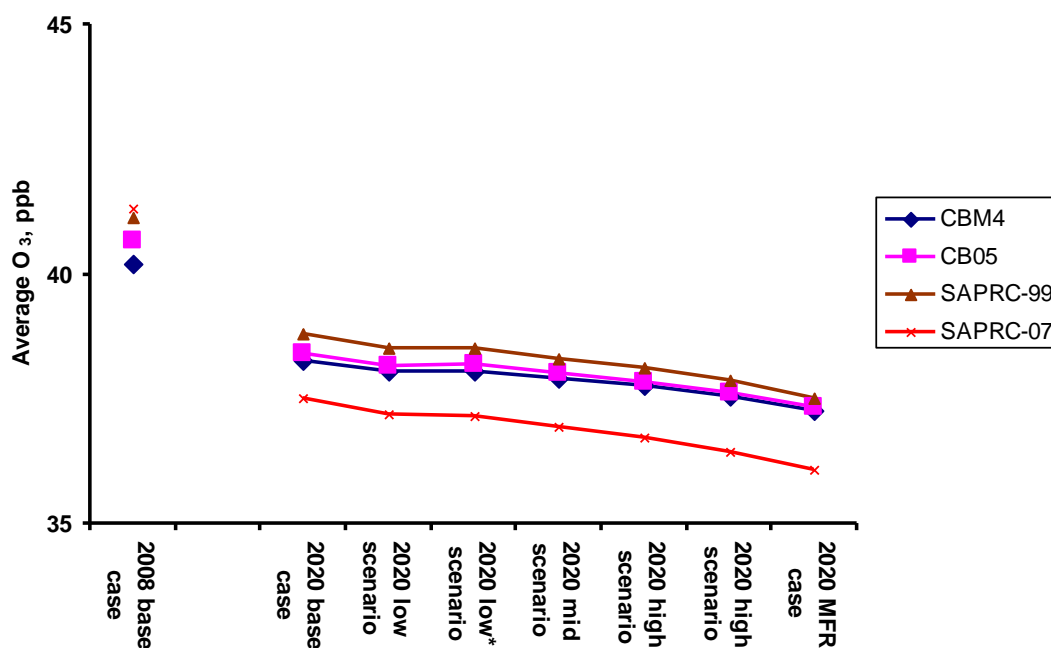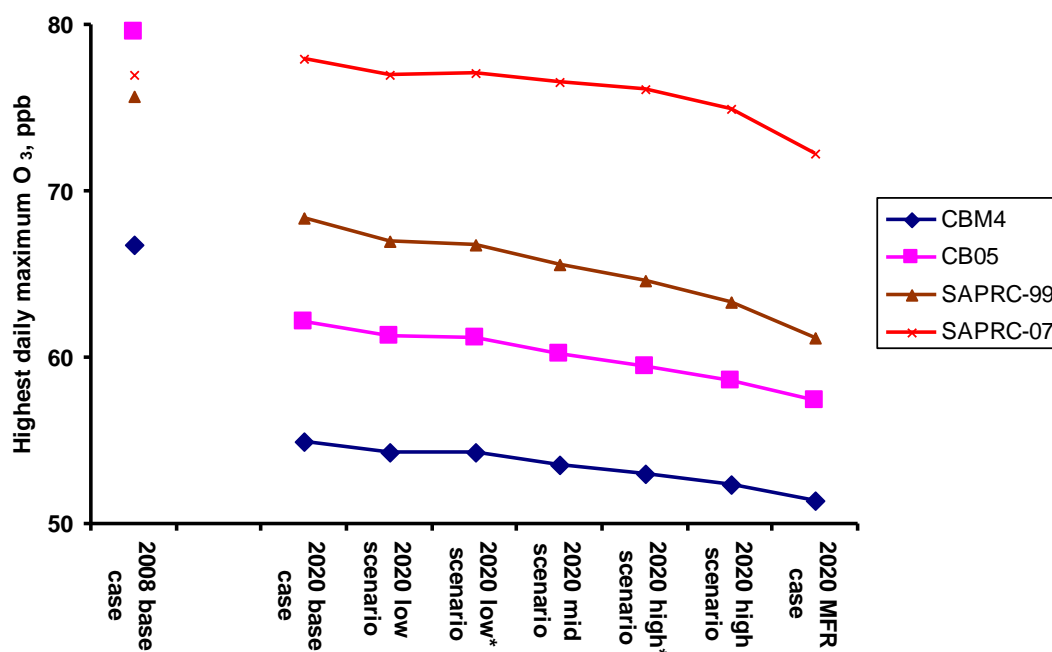
Figure 7.12: The impact of the 2020 emission scenarios relative to the 2008 base case on the highest daily maximum ozone predicted with the PTM model using different chemical mechanisms.


2008 and 2020 base cases with the CBM4, CB05 and SAPRC-99 mechanisms were 7.3 – 18.6 ppb and were significantly larger than the declines across the 2020 scenario variants which were 3.6 – 7.2 ppb. CBM05 gave the largest difference between the 2008 and 2020 base cases whereas SAPRC-99 gave the largest difference between the 2020 base case and MFR scenario variants. SAPRC-07 gave the smallest difference between the 2008 and 2020 base cases, whereas CBM4 gave the smallest difference between the 2020 scenario variants. However, the level of ambition achieved in any of the 2020 scenario variants was not sufficient to reduce the highest daily maximum ozone level to below 50 ppb. Overall, the model predictions showed little robustness to chemical mechanism choice. Despite this lack of apparent robustness, some improvement in air quality was predicted to occur with increasing level of ambition across the 2020 scenario variants by all the chemical mechanisms.

Overall, there is a dramatic reduction in the number of 50 ppb exceedance days between 2008 and 2020, see Figure 7.13, and this is robust to chemical mechanism choice. The largest reductions in exceedance days between the 2008 and 2020 base cases were found with the CBM4 and SAPRC-7 mechanisms, the smallest with the CB05 and SAPRC-99 mechanisms. The largest declines across the 2020 scenario variants were seen with the SAPRC-99 and SAPRC-07 mechanisms and the least with the CBM4 and CB05 mechanisms. However, the level of ambition achieved in any of the 2020 scenario variants was not enough to reduce the number of exceedance days to zero.

7.4.1.1 Summary

Looking across the three ozone metrics and the four chemical mechanisms, there are some features that look robust and other features where there are conflicting responses. Dramatic differences were seen between the 2008 and 2020 base cases with generally smaller differences between the 2020 scenario variants. It was a recurring theme that the air quality improvements predicted to arise in the 2020 scenarios were largely achieved with the lowest level of ambition. Increasing levels of ambition offered some air quality improvement but this was not always dramatic. The 2020 Maximum Feasible Reduction scenario variant did not

Figure 7.13: The impact of the 2020 emission scenarios relative to the 2008 base case on the number of 50 ppb exceedance days predicted with the PTM model using different chemical mechanisms.
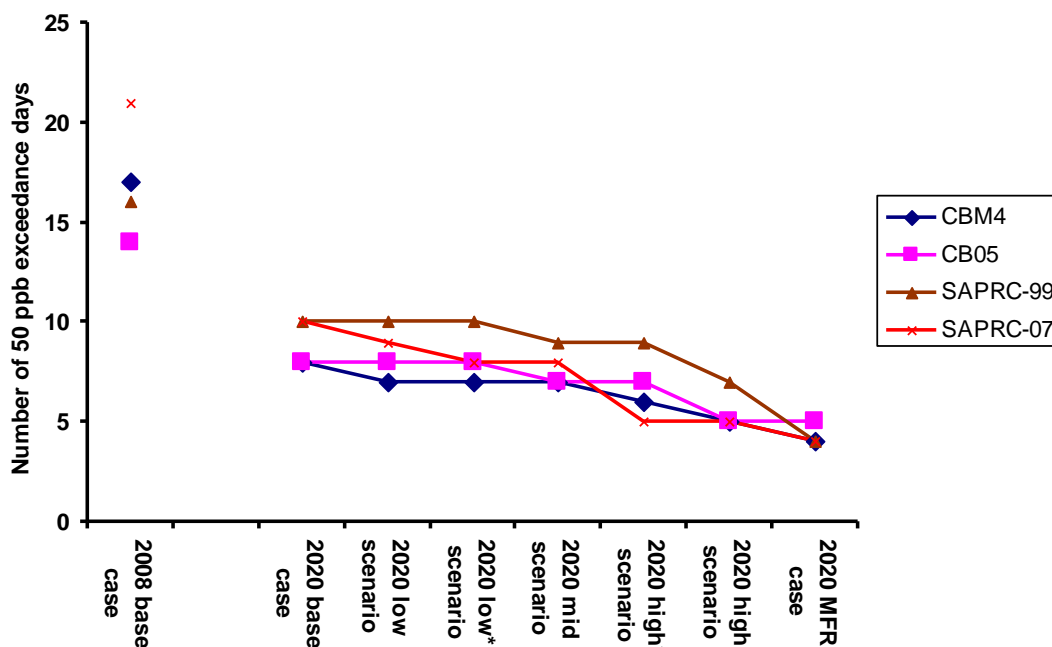
achieve a sufficient level of ambition to reduce the number of 50 ppb exceedance days to zero.

All of the results presented in this section above have used 'best estimate' input data. It remains to be seen whether any of these statements about air quality improvements between 2008 and 2020 are robust because of the uncertainties in the model predictions that arise from the uncertainties in the 'best estimate' input data. This issue is addressed in the following section.

7.4.2   Monte Carlo Parametric Uncertainty Analysis

The comparison of model predictions with observations shown in Figure 7.10 has been carried out with the 'best estimate' model input data. However, there may be many other different sets of input parameters that would give equally acceptable model performance against the AURN observations. To reject the concept of an optimal model represented by the 'best estimate' parameter set in favour of multiple possible or plausible parameter sets is called equifinality (Beven and Freer, 2001). One implication of equifinality is that the uncertainty with the use of models as predictive tools in the policy context might be wider than hitherto thought. If there are many different acceptable parameter sets, all of which are consistent with the AURN observations, then the range of model results in a policy context is likely to be greater than might be suggested by the 'best estimate' input alone. Acceptable model performance with 'best estimate' input may lull the policy-maker into a false sense of security about the adequacy and robustness of policy model predictions. In this section, a Monte Carlo approach is employed to address the limitations of model runs employing 'best estimate' model input.

The Monte Carlo analysis of model input uncertainties has three stages. In the first stage, the uncertainties are described in each model input parameter. In the second stage, the uncertainty range in each model input parameter is sampled randomly and input values are

assigned for all model input parameters for a particular model run. In the third stage, the PTM model is run repeatedly a large number of times with each run having a different and randomly selected set of input parameters. In our implementation, the number of PTM model runs is at least 1000 and may approach 50,000 in some cases. These numbers of model runs would be unthinkable with a large Eulerian grid-based air quality policy model but are possible with a photochemical trajectory model.

Table 7.5 presents the uncertainty ranges assigned to each model input parameter at the initialisation of each model run. Each uncertainty range describes the 1 – 99% (3 – σ) confidence range for that parameter. The probability distribution within that range is generally taken to be equally distributed with parameter value, that is to say it has a 'top hat' shape. For some input parameters, the probability distribution has been assumed to be 'Gaussian' in shape, see Table 7.5. In all cases, the 3 – σ confidence ranges and shapes have been assigned subjectively.

Table 7.5: Representation of the uncertainties in the PTM model input parameters in the Monte Carlo study of parametric uncertainties.

Input parameter	Representation	Range
CO emissions	multiplicative scaling	x 0.5 – 2.0
CH_4 emissions	multiplicative scaling	x 0.5 – 2.0
C_5H_8 emissions	multiplicative scaling	x 0.25 – 4.0
NH_3 emissions	multiplicative scaling	x 0.5 – 2.0
NO_x emissions	multiplicative scaling	x 0.5 – 2.0
SO_2 emissions	multiplicative scaling	x 0.5 – 2.0
VOC emissions	multiplicative scaling	x 0.5 – 2.0
VOC speciation	multiplicative scaling	x 0.5 – 2.0
Air parcel longitude	additive	± 0 – 0.45 ^{o}
Air parcel latitude	additive	± 0 – 0.28 ^{o}
Boundary conditions	multiplicative scaling	
Boundary layer depth	multiplicative scaling	x 0.5 – 2.0
Choice of mechanism	Random	
Choice of trajectory	Random	
Dry deposition velocity	multiplicative scaling	x 0 – 1.0
Photolysis rate coefficient	multiplicative scaling	x 0.7 – 1.3
Rate coefficient	multiplicative scaling	x 0.7 – 1.3
Relative humidity	multiplicative scaling	x 0.5 – 2.0
Temperature	additive	± 0 – 3 ^{o}C

Notes:

a. all assignments in this table are subjective.

b. a scaling factor of unity represents 'best estimate' model input.

Chemical mechanism uncertainty is handled in two steps. In the first step, chemical mechanism choice is addressed by randomly choosing one of the chemical mechanisms. Because of the size and complexity of the MCMv3.1, this mechanism choice has been excluded from the Monte Carlo analysis and choice is restricted to the 4 simpler and more condensed mechanisms: CBM4, CB05, SAPRC-99 and SAPRC-07. In the second step, each rate coefficient and photolysis rate is assigned an uncertain scaling factor in both the 'inorganic' and 'organic' parts of each mechanism. These scaling factors are taken to be independent of each other and no attempt has been made to address any interactions between the uncertainties in particular rate coefficients that may arise through their laboratory determination or evaluation. We have chosen to assume that each rate coefficient and photolysis rate has an uncertainty of ± 30% about their 'best estimate' value and not followed the uncertainty recommendations in the literature. We have also chosen to represent the uncertainty in the rate coefficients at 298 K and 1 atmosphere pressure and not separately treated uncertainties in temperature and pressure dependences. We have also not chosen to treat separately any dependence of uncertainty on solar zenith angle or stratospheric ozone column. Each model run therefore has a different random choice of chemical mechanism and a different random choice of rate coefficients and photolysis rates which address uncertainty about the 'best estimate' input values.

After chemical mechanism uncertainty, the next most important area of model uncertainty lies in the treatment of emissions. A scaling factor was applied to the instantaneous emissions of NH_3, VOC, isoprene, NO_x, SO_2, CO and CH_4 at each point along the air mass trajectory. These scaling factors were assigned at the initialisation of each model run and were held constant throughout the model run. In this way, uncertainties were assumed to be constant throughout the model domain and independent of time of day and season. The scaling factors were assigned a 3 – σ range of ± a factor of 2 for all emissions other than isoprene which was assigned a 3 – σ range of ± a factor of 4. In addition, uncertainties were assigned to the VOC speciation used to split the total VOC emission into emissions for each individual VOC species by adopting an additional scaling factor of ± 2.

Uncertainties in meteorological input were handled in two stages. In the first stage, a random choice was made between 30 independently determined 96-hour back track air mass trajectories provided by the NAME atmospheric dispersion model for 15:00z to 15:15z on each day of the 122 day study period for Harwell, Oxfordshire. In the second stage, scaling parameters were assigned to particular meteorological input parameters when each run was initialised. These scaling parameters were held constant throughout that run on the basis that they were independent of location throughout the model domain. Uncertainties in air parcel location along the selected trajectory path were handled by adding a fixed offset or error term to the 'best estimate' latitude and longitude. Uncertainties in air parcel temperature were handled in the same manner using fixed offsets. Uncertainties in boundary layer depths and relative humidity were handled with multiplicative scaling factors of ± a factor of 2 about the 'best estimate' values.

Other areas of model uncertainty were addressed as described in Table 7.5. Uncertainty in the model boundary conditions for O_3, NO_x, CO, CH_4 and HCHO were addressed by multiplicative scaling factors applied to the 'best estimate' literature values. Uncertainties in deposition velocities for O_3, NO_2, H_2O_2, HNO_3 and SO_2 were similarly treated using scaling factors. However, in this case, the scaling factors covered a 3 – σ of 0 – 1 so that the uncertainty range was not central about the 'best estimate'. This addressed the situation where in some photochemical pollution episodes the effect of drought has been to reduce the uptake of O_3 and other pollutants because of stomatal closure. The uncertainty range is thus not equally distributed about the 'best estimate' value which is set for typical long range transport conditions across Europe.

The PTM model was then run repeatedly with each run having a randomly selected set of initial model parameters as detailed in Table 7.5. In our study of the summer of 2008 at Harwell, Oxfordshire, 4000 model runs were performed covering the 122 day period. The O_3 mixing ratios at the arrival point were compared with the AURN observations for each day of

the 122 day study period. If the model O_3 mixing ratio was found to be acceptably within the range of the observations, within a range of ± 2.5 ppb, that is typically about 5%, then that particular input parameter set was classified as 'acceptable' and was stored for later use. If not, the run and its particular set of input parameters was rejected and no further use was made of it. Of the 4,000 parameter sets selected by Monte Carlo sampling, only 19% were found to be 'acceptable'.

The PTM model was then run with each set of 'acceptable' parameters for each of the 2020 emission scenario variants. The runs were then paired up so that there were consistent 2008 base case and 2020 scenario variants for each 'acceptable' parameter set.

### 7.4.2.1 Probabilistic PTM model predictions for 2008 and 2020

Using Monte Carlo sampling, we have generated many thousands of parameter sets which span the uncertainty ranges in all the significant PTM model input parameters. We have adopted a stringent test for a parameter set to be acceptable and applied this test on each day of the 122 day study period. By this means, we have converted the model output from a time series of 122 single 'best estimate' predictions to a time series of 122 daily probability distributions. The probability distributions for each day were obtained by ranking the 'acceptable' results for each day and estimating the 16-, 50- and 84-percentiles and extreme ranges. These daily probability distributions differed markedly from day-to-day because of the different balance between the major ozone production and destruction processes operating on that day and because of their different inherent uncertainties. The average daily maximum ozone level over the study period was estimated as the average of the 50-percentile values and its 16- and 84-percentiles by averaging over the respective percentiles.

Exactly the same 'acceptable' parameter sets were then used again for each of the 2020 emission scenarios and the results were stored together so that there was a consistent set of daily probability distributions for 2008 and the 2020 variants. In this way, an uncertain set of daily model responses was generated for the 2020 emission scenario variants.

The uncertain model responses to the 2020 emission scenarios are summarised in Figures 7.14 and 7.15. In these figures, solid bars are used to represent the 50-percentile values of the ozone metric, together with their 1-σ error bars estimated from the 16- and 84-percentiles. There was a statistically significant difference between the average daily maximum ozone levels predicted for the 2008 and 2020 base cases as shown by the relative sizes of the 1-σ confidence limits in the 2008 base case and that of the decrease between the 50-percentile values in the 2008 and 2020 base cases, see Figure 7.14. There was a high probability that the difference between the 2008 and 2020 base cases was more than 0.4 ppb but less than 3.5 ppb. However, the decline in the 50-percentiles across the 2020 scenario variants from the 2020 base case to the 2020 MFR scenario variant was small compared to the uncertainties in the ozone levels as shown by the 1-σ error bars.

The position appears much the same with the highest daily maximum ozone levels in Figure 7.15. Again, the difference between the 2008 and 2020 base cases was statistically significant at the 1-σ level of confidence. By examining the frequency distribution of the difference between the 2008 and 2020 base cases, it could be seen that there was a high probability (at the 5 – 95% confidence level) that this difference was greater than 2 ppb but less than 20 ppb. The 1-σ confidence range for the 2020 MFR scenario did not reach 50 ppb at its lowest limit and so the 50 ppb level was not reached at the 1-σ level of confidence.

Figure 7.14: Probabilistic predictions of the impact of the 2020 scenario variants relative to 2008 on average daily maximum ozone from the Monte Carlo uncertainty analysis, with the 50-percentiles shown as a solid bars and the 1-σ confidence ranges shown with error bars.


Average O_3, ppb
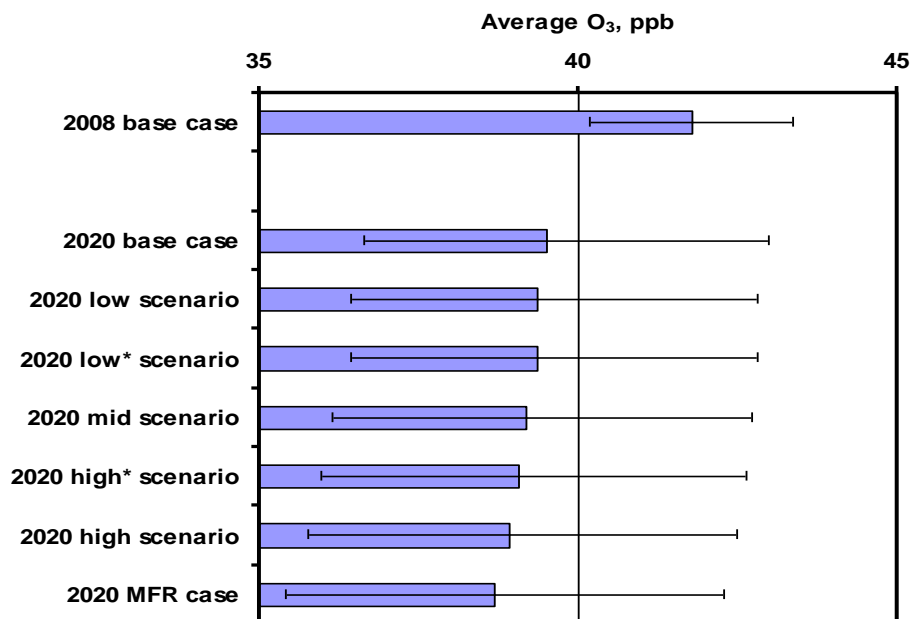
Figure 7.15: Probabilistic predictions of the impact of the 2020 scenario variants relative to 2008 on the highest daily maximum ozone from the uncertainty analysis, with the 50-percentiles shown as a solid bars and the 1-σ confidence ranges shown with error bars.

Highest daily maximum O_3, ppb
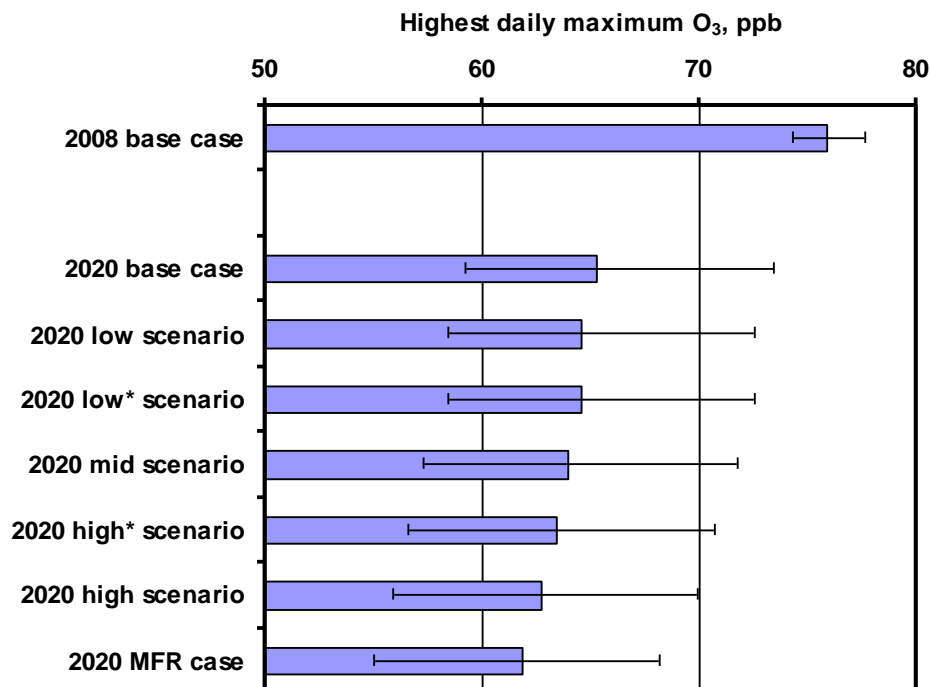
The frequency distributions of the highest daily maximum ozone in each of the emission scenario cases are shown in Figure 7.16. This diagram also shows the 50 ppb level and that it was only reached in the tails of the frequency distributions. In the 2020 base case, there was less than 1 chance in 100 that the 50 ppb level would be reached and this only rose to 4 chances in 100 with the 2020 MFR scenario variant. The likelihood that the 50 ppb level would be reached with the 2020 MFR scenario variant was therefore small.

Figure 7.16: Probability distributions of the impact of the 2020 scenario variants relative to 2008 on the highest daily maximum ozone, showing the 50 ppb target level in the tail of the probability distributions.
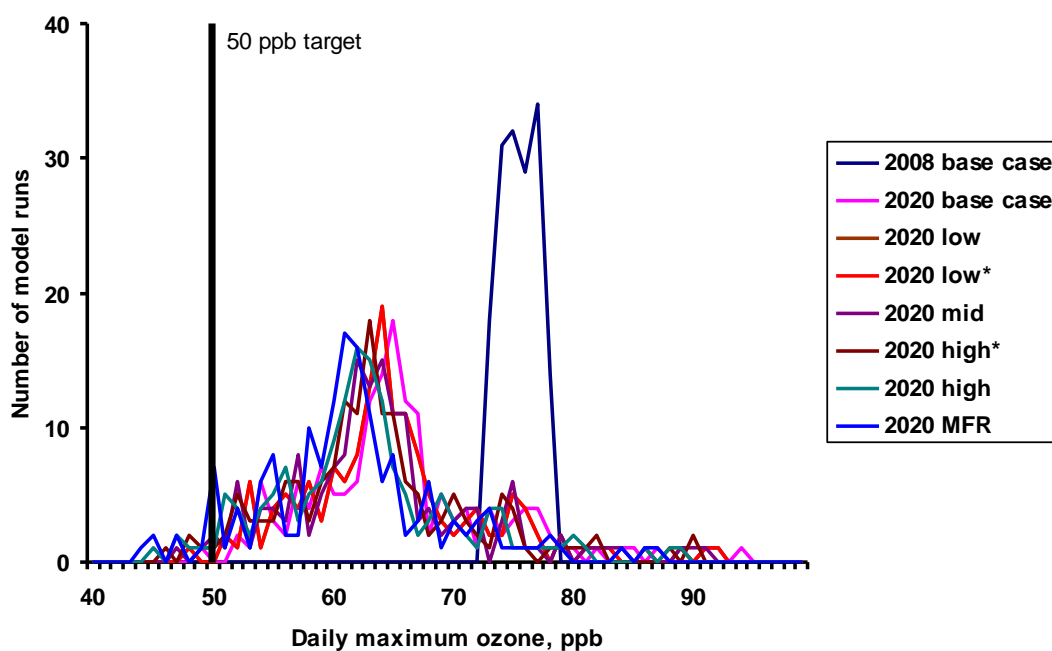
Looking at the influence of the 2020 emission scenarios on the highest daily maximum ozone, the issue is whether the air quality improvement across the 2020 scenario variants is statistically significant. To this end, the frequency distribution of the differences in highest daily maximum ozone between the 2020 base case and 2020 MFR scenario variants was determined for the 'acceptable' parameter sets. This distribution showed that there was a high probability that the difference in highest daily maximum ozone was at least 2 ppb but a low probability that it was more than 10 ppb. On this basis, it can be concluded that it was highly probable that the decline across the 2020 scenario variants was small but statistically significant.

7.4.2.2   Influence of chemical mechanism choice under uncertainty

In this section, the influence of chemical mechanism choice is examined in the runs with both 'best estimate' and 'acceptable' parameter sets. The influence of chemical mechanism choice has already been summarised in Section 7.4.1 above. Each of the Monte Carlo runs used a randomly selected chemical mechanism and so the 'acceptable' runs could be straightforwardly divided up by chemical mechanism. There were approximately the same number of 'acceptable' runs with each of the four chemical mechanisms: 4.6% with CBM4, 4.9% with CB05, 4.8% with SAPRC-99 and 4.5% with SAPRC-07.

Both the 'best estimate' and acceptable' runs demonstrated the same overall influence of emission scenario on average daily maximum ozone. There was generally a large difference between the 2008 and 2020 base cases, followed by a relatively smaller decline across the 2020 scenario variants. These features are clearly shown in both sets of runs with all chemical mechanisms. The only point of departure was in the decline across the 2020 scenario variants between the 2020 base case and MFR cases. With the CB05 mechanism, the difference across the 2020 cases was 1.1 ppb in both sets of runs, taking the 50-percentile values of the 'acceptable' runs. For the CBM4, SAPRC-07 and SAPRC-99 mechanisms, the 'best estimate' runs overestimated the declines across the scenarios by about 50%, compared with the 'acceptable' runs.

Generally the 'best estimate' and 'acceptable' runs showed the same overall influence of emission scenario on the highest daily maximum ozone. The CBM4, CB05 and SAPRC-99 mechanisms demonstrated this general behaviour in both sets of runs. However, the 'best estimate' runs with the SAPRC-07 mechanism failed to show the large difference between the 2008 and 2020 bas cases, whereas the 'acceptable' runs did. In fact there was no apparent difference in the 'acceptable' runs between any of the chemical mechanisms in this regard. There is therefore a clear point of departure here from the behaviour of the 'acceptable' runs as shown by the 'best estimate' runs.

There was a generally small decline in highest daily maximum ozone across the 2020 scenario variants in both the 'best estimate' and 'acceptable' runs with all four chemical mechanisms. The declines across the scenarios were significantly overestimated with the 'best estimate' runs with the CB05 and SAPRC-07 chemical mechanisms but were grossly so with the CBM4 and SAPRC-99 mechanisms. Again, there were no apparent differences between the 'acceptable' runs between any of the chemical mechanisms in the declines across the 2020 scenarios.

7.4.3 Summary

- Monte Carlo parametric uncertainty analysis has been applied to the assessment of the likely impact of scenarios for the renegotiation of the Gothenburg Protocol promulgated by IIASA/GAINS on ozone levels at Harwell, Oxfordshire using the PTM model.

- There is a high probability that the emission scenarios for 2020 will reduce the average daily maximum ozone levels over a 122-day period by at least 0.4 ppb but not more than 3.5 ppb from about 42 ppb currently, between the 2008 and 2020 base cases.

- The decline in the 50-percentile average daily maximum ozone levels across the 2020 scenario variants from the 2020 base case to the 2020 MFR scenario case was small compared to the uncertainties in the ozone levels as shown by the 1-σ error bars.

- There is a high probability that the highest daily maximum ozone level during the 122-day period of 76 ppb will be reduced by at least 2 ppb but not more than 20 ppb between the 2008 and 2020 base cases.

- There was a high probability that the difference in highest daily maximum ozone between the 2020 base case and 2020 Maximum Feasible Reduction case was at least 2 ppb but a low probability that it was more than 10 ppb. On this basis, it can be concluded that it was highly probable that the decline across the 2020 scenario variants was small but statistically significant.

- In the 2020 base case, there was less than 1 chance in 100 that the highest daily maximum ozone would be reduced to below the 50 ppb level and this only rose to 4 chances in 100 with the 2020 MFR scenario variant. The likelihood that the 50 ppb level would be reached with the 2020 MFR scenario variant was therefore small.

7.5 Secondary pollutant air quality and climate change

This task addresses the impact of climate change on secondary pollutant air quality, specifically ozone. Attention was focussed on the sensitivity of secondary pollutant air quality to increasing emissions of isoprene using global and regional air quality models.

7.5.1 Background

There is much current interest from policy makers in the issue of air quality and climate change. This stems from a concern that all the efforts made to improve regional air quality might be undone by the influence of global climate change. There are a number of mechanisms by which global climate change may adversely impact on regional air quality. However, the study of these mechanisms is in its infancy. Equally well, other mechanisms may come into focus as our understanding of global biogeochemical cycles improves in the future. Here we focus on one of the mechanisms by which air quality and climate change may be coupled together involving isoprene and ozone. The thesis is that as surface temperatures rise through global climate change, biogenic isoprene emissions will increase in intensity, stimulating ozone production and leading to a deterioration in regional air quality.

There is observational evidence to support the isoprene-ozone air quality-global climate change linkage. Global climate change will undoubtedly lead to increased surface temperatures. Increased vegetation temperatures lead to increased biogenic emissions. Smog chamber studies demonstrate that isoprene is a potent source of photochemical ozone. However, to perform a quantitative assessment of the importance of the isoprene-ozone air quality-global climate change linkage, policy makers will need access to coupled biogeochemical-climate change models. These models are at an early stage of development in terms of the process descriptions included and the spatial scales with which they are implemented.

One of the many compromises currently adopted in coupled climate change-biogeochemistry models involves simplification of the atmospheric chemistry processes. Laboratory, smog chamber and chemical mechanism studies have shown that there are upwards of 500 or so individual chemical reactions involved in the atmospheric oxidation of isoprene to form ozone. It is difficult to represent more than one tenth of these in current global climate models that have any degree of coupling with biogeochemical processes. The question addressed by this current study is whether the simplifications made to the representation of the atmospheric chemistry of isoprene in coupled climate change biogeochemistry models in any way compromises their ability of address the isoprene-ozone air quality-climate change linkage.

7.5.2 Modelling results

To address the isoprene-ozone air quality linkage, a hierarchy of models has been assembled, as follows:

Model A: a global 3-D Lagrangian STOCHEM model running a comprehensive chemical mechanism, the CRI chemical mechanism,

Model B: a 0-D box model based on the PTM running a variety of condensed chemical mechanisms, including the CRI mechanism.

A series of model experiments was performed using the STOCHEM – CRI global 3-D model to study the global scale impact of isoprene on the chemistry of ozone and OH. Each experiment was 15-months in length and began on 1st October. There was a 6 month spin-up period up until 31st March. Then, two model runs were initiated, one was a base case experiment which continued without change. The second model run had an extra emission of isoprene but in all other aspects was exactly the same as the base case experiment. Isoprene emissions were perturbed over a 10° latitude x 10° longitude region of Europe covering 45 – 55 ^{o}N and 0 – 10° E. The additional isoprene emissions amounted to between 1 and 10 Tg/yr over the 10° x 10° region.

Increasing isoprene levels increased ozone levels and depleted OH levels locally over north west Europe. Similar behaviour to that seen for north west Europe was found when the extra isoprene emissions were injected over North America although the results were quantitatively different. When extra isoprene emissions were injected over Amazonia, both ozone and OH levels were depleted, showing the importance of the different NO$_x$ environments on the perturbed isoprene chemistry.

A version of the 0-D photochemical box model was set up with the CRI chemical mechanism. The box model concentrations for 30 long-lived chemical species were set to the monthly values for the 10° x 10° grid box over north west Europe from the base case run of the STOCHEM-CRI 3-D model. The 0-D box model was integrated for 5 days with the mixing ratios of the 30 long-lived chemical species reset to the 3-D STOCHEM values after every time step. The flux of material required to maintain the 3-D model values was integrated over the 5 day model experiment and together with the mixing ratios of the unconstrained reactive species, provided the 0-D box model output. The 0-D box model was then rerun with the output from the STOCHEM-CRI 3-D model with the addition of extra isoprene and NO$_x$. By taking the differences between the box model runs with the base case and additional isoprene and NO$_x$, estimates could be made of the impact of increased isoprene on the fluxes of the 30 selected constrained species and the time-averaged hydroxyl radical concentrations. Differences were estimated using pairs of box model experiments covering the month of July.

The chemical mechanism in the 0-D box model was then replaced with a variety of different chemical mechanisms with a view to understanding how isoprene chemistry is described in the different chemical mechanisms. The additional chemical mechanisms examined included: MCMv3.1, CB05, SAPRC-99 and UKCA. The 0-D box model was thus set up with five chemical mechanisms, representing two orders of magnitude differing in chemical complexity from the 'gold standard' MCMv3.1 to the highly condensed CB05.

The five chemical mechanisms have been harmonised in such a way as to facilitate comparison and evaluation. This means that our evaluation does not deal necessarily with the actual chemical mechanism produced by the mechanism developers. Our study addresses a harmonised version of each chemical mechanism produced by the implementation of the four steps detailed below. For simplicity, each chemical mechanism is still referred to by its original name and it is implicitly understood that reference is being made to the harmonised version. To distinguish our harmonised mechanisms from the published mechanisms, we refer henceforward to the mechanism names using quotation marks, ''. The following steps were taken to harmonise each chemical mechanism:

Step 1: the fast photochemical reactions involving O^{3}P, O^{1}D, OH, H, HO$_2$, NO$_3$ with N$_2$, O$_2$, H$_2$O, CO, O$_3$, NO, NO$_2$, HNO$_3$, HO$_2$NO$_2$, N$_2$O$_5$, SO$_2$, sulphate and nitrate aerosol, (the so-called inorganic reactions), were replaced by a common set of 47 reactions, of which 35 were thermal reactions, 8 were photochemical and 4 were aerosol formation reactions.

Step 2: all complex temperature, pressure and humidity dependent rate coefficients were replaced by a common set of 17 rate coefficients.

Step 3: the formation and thermal decomposition of all PAN-type molecules were replaced by a common pair of temperature and pressure-dependent reaction rate coefficients.

Step 4: all photolysis rate coefficients were replaced by a common set based on the J-values provided on the MCM website.

These harmonisation steps left unchanged the simplifications and approximations made by the developers in addressing the organic reactions that degrade the emitted VOC species to produce ozone. It is the same harmonisation procedure utilised in the modelling described in Section 7.3. Whereas the MCMv3.1 contains over 15,000 chemical reactions, the other mechanisms condense down this atmospheric chemistry by over two orders of magnitude. It is this condensation that is being evaluated in this study, using the MCMv3.1 as the 'gold standard' and this evaluation is not affected by the harmonisation steps detailed above. The MCMv3.1 and CRIv2 mechanisms are already harmonised and so no further changes to these mechanisms were required. All other model input data were unchanged between the different 0-D box model versions. No wet nor dry deposition processes nor exchange processes with the free troposphere were modelled for any species.

Figures 7.17 and 7.18 show scatter plots of the impact of extra 1 and 5 ppb isoprene, respectively, on the differences between the ozone fluxes in the perturbed and base cases that were required to constrain ozone levels, for different levels of NO_x. The impacts of the extra isoprene in each figure have been the same, that is, to increase the net rate of photochemical ozone production. This increase in the net rate of ozone production apparently increased with increasing NO_x levels. There was a tendency for the increase in net rate to level off at high NO_x with the 1 ppb extra isoprene but this tendency was less marked with 5 ppb extra.

Figure 7.17: Scatter plots of changes in the net rate of photochemical ozone production vs base case NO_x for the 0-D box model running five chemical mechanisms for 1 ppb extra isoprene over north west Europe.
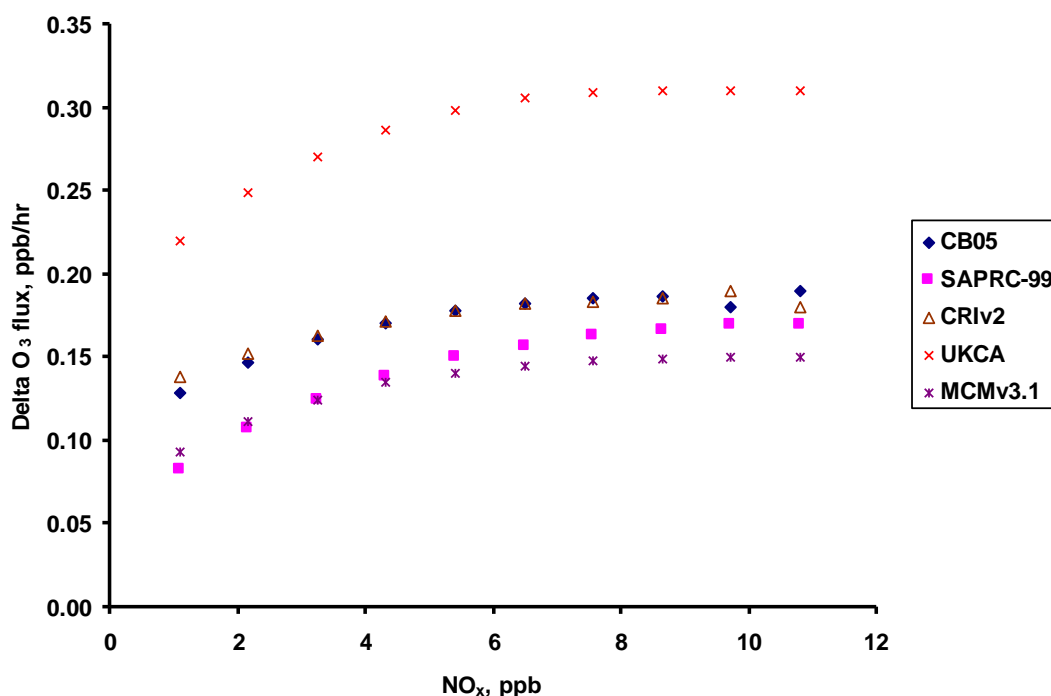
Figure 7.18: Scatter plots of changes in the net rate of photochemical ozone production vs base case NO$_x$ for the 0-D box model running five chemical mechanisms for 5 ppb extra isoprene over north west Europe.
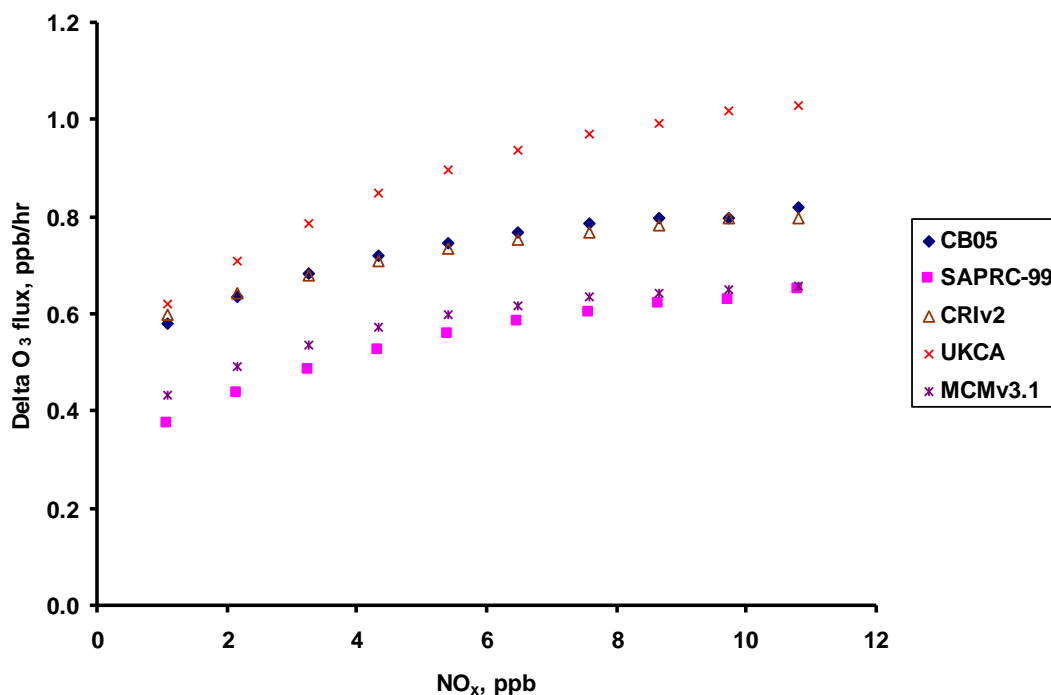
Whilst all the five mechanisms give qualitatively the same results in Figures 7.17 and 7.18, there were quantitative differences. Accepting, the MCMv3.1 as the gold standard, then for 1 ppb extra isoprene, the other mechanisms indicated heightened changes in the net photochemical ozone production relative to the MCMv3.1. The 'SAPRC-99' mechanism gave results that were closest to the MCMv3.1 and the 'UKCA' gave results that were furthest away, by about a factor of two. For 5 ppb extra isoprene, the MCMv3.1 and 'SAPRC-99' mechanisms gave similar responses, with the other mechanisms giving heightened changes in the net rate of photochemical ozone production. Again, the 'UKCA' mechanism gave close to double the reponse of the MCMv3.1.

All mechanisms showed OH radical depletions on addition of extra isoprene with these depletions increasing then decreasing with increasing NO$_x$ levels. Figures 7.19 and 7.20 show scatter plots of the impact of 1 and 5 ppb extra isoprene, respectively, on the differences between the 5-day average hydroxyl radical concentrations in the perturbed and base case runs, for different levels of NO$_x$.

For 1 ppb extra isoprene, see Figure 7.19, the MCMv3.1 and CRIv2 mechanisms gave closely similar results whilst the other mechanisms overestimated them. At high NO$_x$, the results obtained with the MCMv3.1, CRIv2 and 'SAPRC-99' mechanisms agreed closely whilst the 'CB05' mechanism underestimated the OH depletions and the 'UKCA' mechanism overestimated them. For 5 ppb extra isoprene, see Figure 7.20, the MCMv3.1 mechanism showed the smallest OH depletions, with closely similar results from the CRIv2 mechanism. The other mechanisms showed significantly greater OH depletions compared with the MCMv3.1, particularly under low-NO$_x$ conditions.

Figure 7.19: Scatter plot of the change in the 5-day averaged OH radical concentrations vs base case NO$_x$ for 1 ppb extra isoprene over north west Europe.
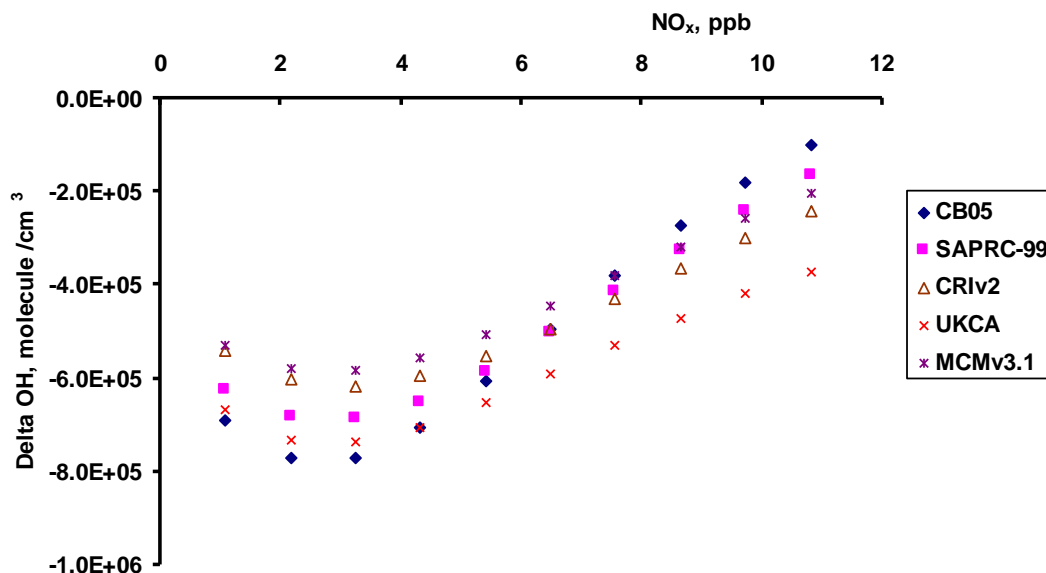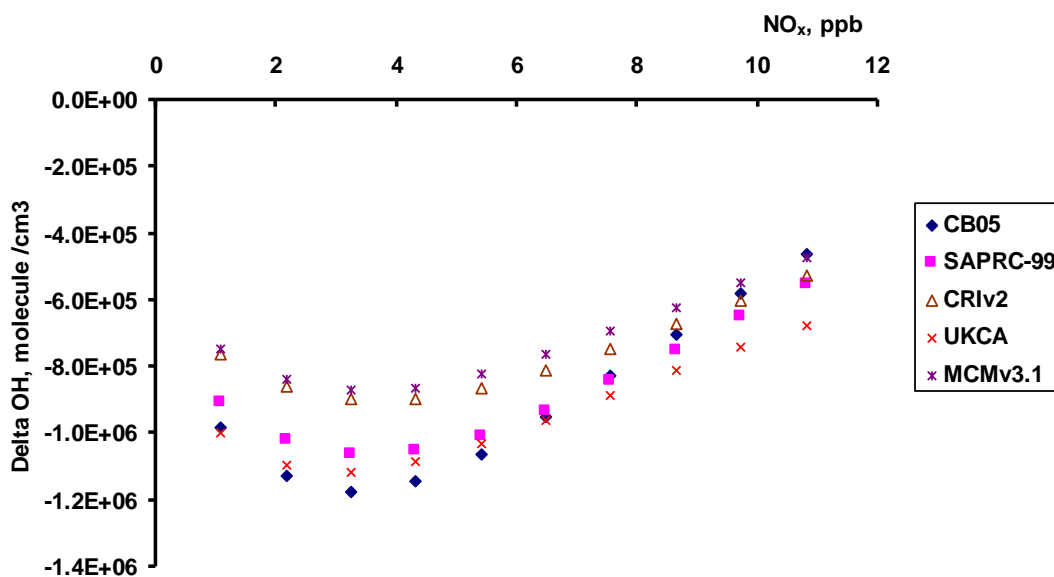

Figure 7.20: Scatter plot of the change in the 5-day averaged OH radical concentrations vs base case NO$_x$ for 5 ppb extra isoprene over north west Europe.

7.5.3 Conclusions

For the global climate models to predict correctly the response of ground-level ozone to increased isoprene emissions driven by increasing surface temperatures, they will need access to chemical mechanisms that deal accurately with the atmospheric chemistry of isoprene. It is often the case, though, that these models are only able to incorporate highly simplified and condensed chemical mechanisms, particularly of isoprene chemistry. Increasing isoprene emissions has impacts on the local rate of ozone production and loss and on the recycling of HO_x radicals. The former leads to increased ozone levels in high-NO_x regions and decreased ozone in low-NO_x regions. The latter leads to decreased OH levels and hence increased global methane levels, irrespective of the levels of NO_x.

In this study, we have examined the impact of increased local isoprene emissions on ozone and methane using a global 3-D chemistry-transport model STOCHEM running with the CRIv2 chemistry. We have built a 0-D box model which is constrained by the output from the global model for north west Europe as a test-bed to examine a variety of chemical mechanisms that cover a range of a factor of 100 in chemical complexity. We have found different ozone and OH responses to increased levels of isoprene in these box model experiments that differed only with respect to chemical mechanism.

Generally speaking the CRIv2 and 'SAPRC-99' give results that were closely similar to that of the MCMv3.1 which was our 'gold-standard'. The results from the 'UKCA' mechanism, developed specially for the Met Office climate change models, and the 'CB05' mechanism gave changes in the rates of net photochemical ozone production and depletions in time-averaged OH levels that were significantly different from those obtained with the MCMv3.1. These latter two mechanisms were therefore not recommended for assessment of the isoprene – ozone climate change linkage without further adjustment.

7.6 Summary and main conclusions

The main conclusions of the PTM ozone modelling work for Objectives 10.2 and 10.3 can be summarised as follows:

> **Summary:**
>
> - **The impact of chemical mechanism choice on ozone air quality policy development has been studied in detail. The response of ozone concentrations to changes in NO_x and VOC emissions predicted by versions of the PTM using 6 different chemical schemes of varying degrees of complexity was assessed and found to be quite varied. Other diagnostic evaluations of the different mechanisms were carried out showing the degree of variability in VOC reactivities and source-receptor relationships inferred by each mechanism**
>
> - **Monte Carlo parametric uncertainty analysis was applied to the assessment of the likely impact of 7 different emission reduction scenarios for the renegotiation of the Gothenburg Protocol promulgated by IIASA/GAINS on ozone levels at Harwell, Oxfordshire**
>
> - **The analysis showed that there is a high probability that the European emission scenarios for 2020 will reduce the average daily maximum ozone levels over a 122-day summer period by at least 0.4 ppb but not more than 3.5 ppb from current levels of 42 ppb**
>
> - **There is a high probability that the emission scenarios for 2020 will reduce the highest daily maximum ozone level over a 122-day summer period by at least 2 ppb but not more than 20 ppb from the 2008 level of 76 ppb**
>
> - **There was a high probability that the difference in highest daily maximum ozone between the 2020 base case and the most ambitious 2020 Maximum**

Feasible Reduction case was at least 2 ppb but a low probability that it would be more than 10 ppb. On this basis, it can be concluded that it was highly probable that the decline across the 2020 scenario variants was small but statistically significant.

- In the 2020 base case, there was less than 1 chance in 100 that the highest daily maximum ozone would be reduced to below the 50 ppb level and this only rose to 4 chances in 100 with the 2020 MFR scenario variant. The likelihood that the 50 ppb level would be reached with the 2020 MFR scenario variant was therefore small

- Further probabilistic uncertainty analysis was done on the influence of different UK precursor emission reductions on daily maximum ozone concentrations in 2020, 2025 and 2030 based on the latest UEP43 energy projections.

- This analysis showed that there was an 88% chance that the 2020 baseline emission projections would lead to an improvement in peak ozone modelled at the Harwell site, but less than 1% chance that peak ozone would be reduced to below 50 ppb in any of the model years

- The impact of climate change on ozone has been assessed, focusing on the response of predicted ozone concentrations to increasing isoprene emissions from natural sources occurring as a result of rising surface temperatures.

- The work has specifically focused on how predicted ozone responses vary according to what chemical reaction schemes are used in models. Four different chemical schemes were assessed and compared against the benchmark Master Chemical Mechanism. The work has indicated how the representation of atmospheric chemistry processes in global and regional air quality models is important in determining how changes in biogenic emissions caused by climate change will affect predicted changes in ground-level ozone formation.

8 Assessments of Background and Urban-Scale Oxidant

8.1 Background oxidant mapping

8.1.1 Introduction

It is well-established that the behaviour of ozone (O_3), NO and NO_2 in the atmosphere is coupled by the following reactions,

$$NO + O_3 \rightarrow NO_2 + O_2 \qquad\qquad (1)$$

$$NO_2 + \text{sunlight} (+ O_2) \rightarrow NO + O_3 \qquad\qquad (2)$$

and it is because of this strong chemical coupling that the term "oxidant" is sometimes used as a collective term for NO_2 and O_3. This reaction cycle partitions NO_x between its component forms of NO and NO_2, and oxidant between its component forms of O_3 and NO_2, but conserves both NO_X and oxidant. As a result, oxidant derived from background O_3 is partitioned between the forms of NO_2 and O_3, with a progressively greater proportion in the form of NO_2 as NO_x increases as a result of received emissions. In urban areas, oxidant can also be derived significantly from directly emitted NO_2, and this is also partitioned between the forms of NO_2 and O_3, with a progressively greater proportion in the form of O_3 as NO_x decreases with dilution.

Consistent with this, previous analyses of ambient data have shown that the level of oxidant, [OX], at a given location in the UK is made up of a combination of a background (NO_x-independent) source and a local (NO_x-dependent) source, denoted here as $[OX]_B$ and $[OX]_L$, respectively:

$$[OX] = [OX]_B + [OX]_L \qquad\qquad (i)$$

$[OX]_L$ is derived from primary emissions of NO_2, and is usually represented by the term $f_{NO2}[NO_x]$, where f_{NO2} is the fraction of NO_x emitted as NO_2. $[OX]_B$ provides a quantification of the ozone concentration which would exist at the given location in the notional absence of NO_x, i.e. when the local-scale chemical coupling described above cannot occur.

During the reporting period, work for **Objective 11** has focused on characterising the geographical variation of annual mean $[OX]_B$ over the UK, and applying the higher resolution mapping methodology developed within the present contract to produce a 10 km x 10 km map for 2010. This activity provides input data to help improve and inform NO_2 and ozone modelling activities using the Pollution Climate Model (PCM) in the UKAAQA programme.

8.1.2 Generation of an optimised annual mean $[OX]_B$ map for 2010

The mapping methodology developed within the present contract allows the geographical variation of annual mean $[OX]_B$ over the UK to be described in terms of the variation of a hemispheric baseline component, $[OX]_H$, and a regional-scale modification, $[OX]_R$, such that:

$$[OX]_B = [OX]_H + [OX]_R \qquad\qquad (ii)$$

As fully described previously, the variation of these components is described relative to three geographical co-ordinates (denoted d_1, d_2 and d_3) by the following equations,

$$[OX]_H = [OX]_H^{\circ} \exp(-3.30 \times 10^{-4} d_{1^{\circ}}) \qquad\qquad (ii)$$

$$[OX]_R = F.[OX]_{R\ chem} + [OX]_{R\ dep} \qquad\qquad (iii)$$

where $d_{1^\circ} = d_1 \exp(-1.57 \times 10^{-3} d_2)$, $[OX]_{R\ chem} = (1.563 - (1.68 \times 10^{-3} d_2))$ and $[OX]_{R\ dep} = (-3.02 \times 10^{-3} d_3)$. The method was optimized on the basis of archived data for the oxidant components over the period 2001-2006, and full details are given in the 2010 annual report.

The oxidant components described above show year-to-year variability, by virtue of variations in the magnitude of regional and global scale influences on emissions and chemical processing. Modelling of annual mean data for individual years therefore requires year-specific values of the oxidant components. As described in detail previously, this is achieved by scaling the $[OX]_H$ and $[OX]_R$ 2001-2006 reference maps, by applying optimised values of $[OX]_H^\circ$ (a reference hemispheric baseline value) and F (a photochemical pollution scaling factor) for a given year.

This was done through comparison of $[OX]_B$ data from up to 40 sites throughout the UK, with the values calculated for the 1 km x 1 km grid squares containing those sites. The sites were selected to be comparatively unpolluted (annual mean $[NO_x] < 25$ ppb) so that the initial correction for $[OX]_L$ (derived from primary NO_2) was small. The value of F was independently determined on the basis of maximum hourly-mean ozone data from long-running rural sites, leading to a value of 0.4. This indicates that the level of photochemical pollution in 2010 is estimated to be 40 % of the average of the years 2001-2006. The wider $[OX]_B$ dataset from up to 40 sites was then used to optimize values of $[OX]_H^\circ$, leading to a value of 32.44 ppb for 2010, by minimising the square deviation. This is the lowest value of all considered years to date. For comparison, values of $[OX]_H^\circ$ and F are shown in Table 8.1 for all the years in the period 2001-2010.

A comparison of the observed and parameterised annual mean $[OX]_B$ values is shown in Figure 8.1 for 2010, for the averages of the zones throughout the UK. This shows a reasonably good correlation, although the observed values for the sites within the south-west and north-west zones tended to be consistently greater than those simulated. It is also noted that observed data in some zones displayed an unusually large amount of scatter in the 2010 data, owing to the existence of outliers. For example, Lullington Heath has an exceptionally low value of $[OX]_B$, 25.7 ppb in 2010, being nearly 6 ppb lower than the average of the other considered sites in the zone. The reason for localised wide variability in the data within the same geographical region is unclear, and of course cannot be captured by the methodology described here.

The associated parameterisation of $[OX]_B$ over the UK for 2010 is shown, along with those for 2001-2009, in Figure 8.2. The values calculated for each 1km x 1km OS grid square are based on the co-ordinates of the grid square centre. These values have been supplied to AEA for application in annual mean NO_2 and ozone modelling activities using the Pollution Climate Model (PCM).

Table 8.1: Year-specific annual mean values of $[OX]_H^\circ$ and F for use in empirical modelling.

Year	2001	2002	2003	2004	2005	2006	2007	2008	2009	2010
$[OX]_H^\circ$ (ppb)	34.82	34.53	36.27	34.97	33.97	34.67	33.73	34.81	33.10	32.44
F	0.859	0.816	1.334	0.988	0.581	1.422	0.25	0.5	0.5	0.4

Figure 8.1: Comparison of observed and parameterised [OX]$_B$ for UK zones in 2010.
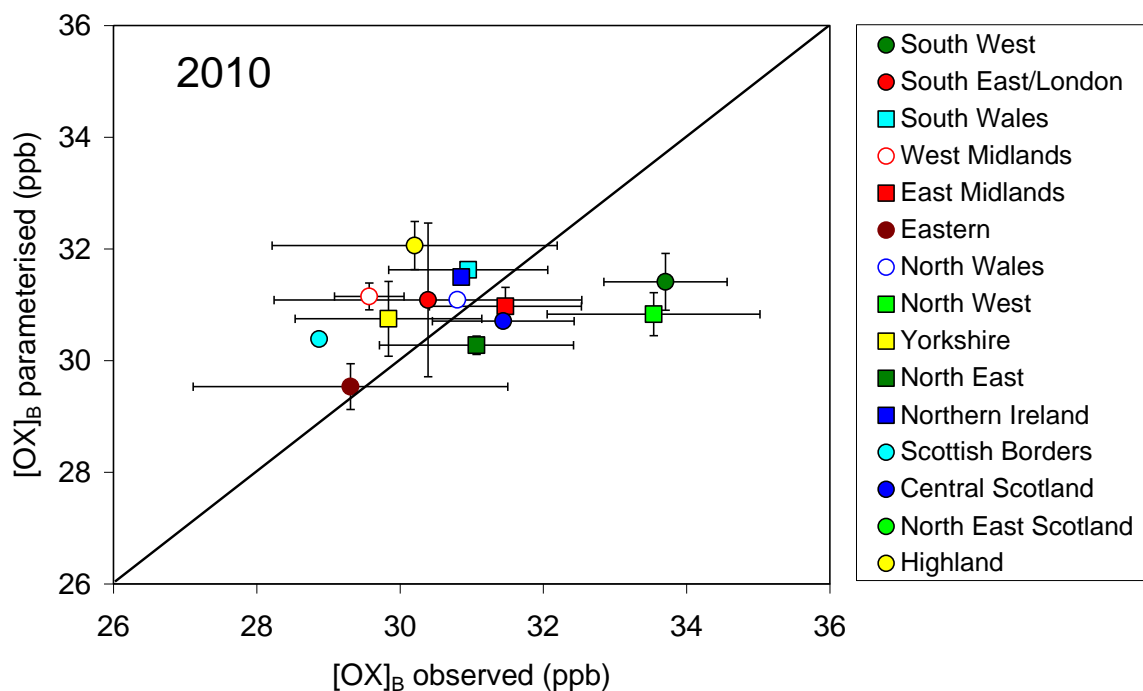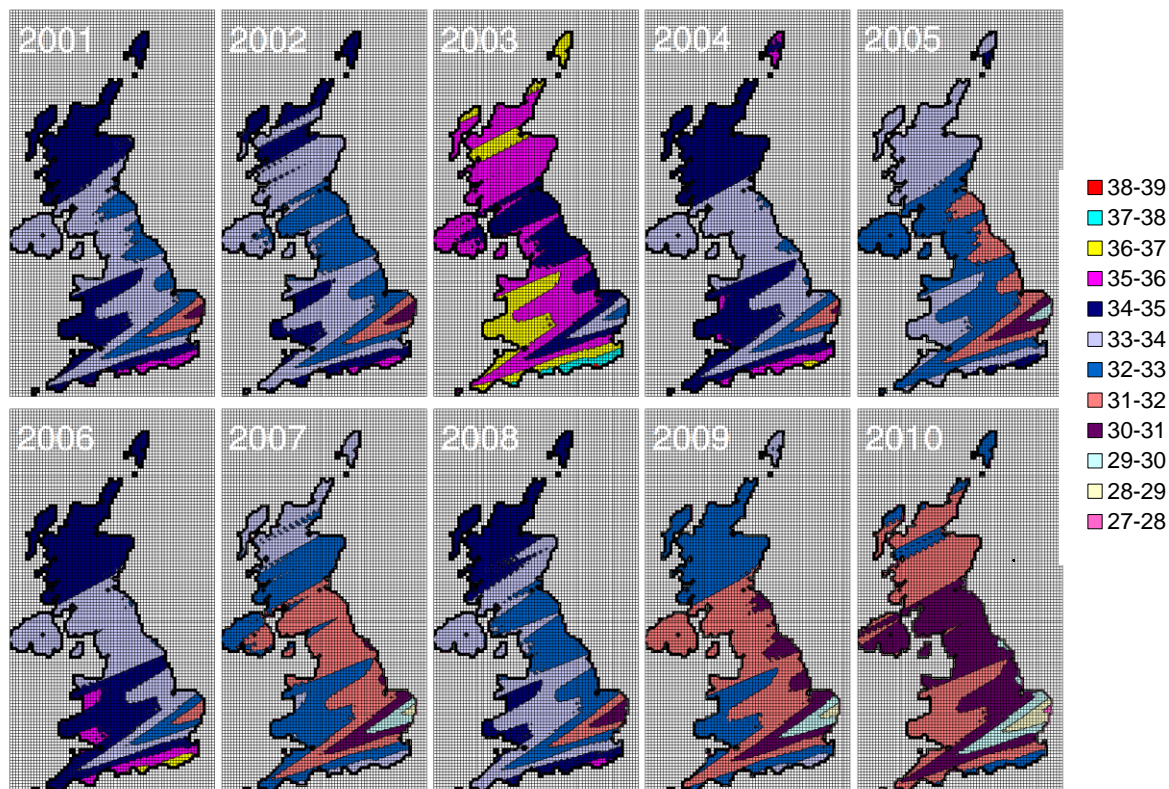

Figure 8.2: Parameterised spatial variation of [OX]$_B$ (= [OX]$_H$ + [OX]$_R$) over the UK (in ppb) for each year in the time period 2001-2010.

8.2 Assessment of urban-scale oxidant formation over the London conurbation

8.2.1 Introduction

An analysis of hourly-mean ozone and NO_X data from a series of five photochemical episodes in the UK over the period 1999-2006, reported previously, provided evidence for urban-scale oxidant production along a transect of sites across the London conurbation. Although the results were scattered, three of the five events (30th July 1999, 15th July 2003 and 17th July 2006) yielded statistically significant oxidant production rates, with the inferred background oxidant production rate averaged over all five events being 5.8 ppb h^{-1}. No evidence for a significant temporal trend in the background oxidant production rate was apparent.

These data have been used to evaluate current understanding of VOC oxidation chemistry occurring over the Greater London conurbation. This has been carried out using a boundary layer box model to simulate chemical processing under photochemical episode conditions. This has mainly focused on the conditions of the earliest event in the time series (30th July 1999), because more extensive data are available for hydrocarbons at London sites to assist evaluation. However, the impact of implementing a trend in emissions inputs, derived from the LAEI, over the period up to 2008 has also been investigated, and the sensitivities of the results to prevailing temperature and relative humidity have been considered.

8.2.2 MCM v3.2 single-layer model description

The box model inputs are summarised in Table 8.2. The model aims to represent a well-mixed boundary layer over London, which receives emissions of NOx, CO, SO_2 and speciated anthropogenic non-methane VOCs, at spatially-averaged rates based on the totals reported for 1999 by the LAEI and the area covered by the inventory. The non-methane VOC speciation was based on Passant (2002), for the distribution of component sources, as reported by the LAEI, and the processing of the emissions was initially represented using the recently updated MCM v3.2. Emissions of biogenic VOCs were also considered, as described further below. The simulations were run for a 4 hour period (13:00-17:00h), and thus represent the relatively slow east-to-west passage of air across London which occurred during the episode on the afternoon of 30th July 1999. The model was initialised using mixing ratios of O_3, NOx, CO and SO_2 measured at Bexley (i.e, towards the eastern edge of Greater London) at 13:00h. Mixing ratios of a large number of non-methane VOCs (including hydrocarbons and emitted and product oxygenates) were also initialised, using those simulated for the 6th August 2003 episode at Writtle (Essex) by Utembe et al. (2005) using the Photochemical Trajectory Model (PTM) with MCM v3.1. Those data are thus representative of the organic composition of aged air arriving in the UK following several days chemical processing over Europe under anticyclonic conditions.

8.2.3 Sensitivity of $[OX]_B$ production rates to emissions inputs, temperature and humidity

Several scenarios were considered, in which impact and sensitivity of the system to the various model inputs were investigated. These scenarios are described in the following paragraphs, with the associated simulated $[OX]_B$ production rates shown in Figure 8.3:

(i) <u>Initialisation run</u>: The model was initially run with the emissions switched off, to examine the impact of the continued processing of the species at their initialised concentrations, representative of the aged air entering the London conurbation (Run 1). This resulted in an average production rate of background oxidant, $[OX]_B$, of 3.24 ppb h^{-1} over the four hour period (as indicated above, $[OX]_B$ represents a NO_x-independent background level that can be influenced by the chemical processing of VOCs and NO_x prior to arrival at a given location, but which has been corrected for the local NO_x-dependent contribution derived from primary

Table 8.2: Summary of input conditions in the London box model.

		Comment
Boundary layer depth	1300 m	Based on typical afternoon boundary layer depth under summertime anticyclonic conditions, as used in the PTM.
Temperature	301 K	Based on measurements made at Silwood Park, Ascot, Berkshire on the afternoon of 30th July 1999, during the EU PRIME campaign.
Relative humidity	36%	
Base emission rates		
CO	268.9 kg km^{-2} day^{-1}	Average daily emission rate, based on the LAEI total for 1999. The applied rate was adjusted for diurnal and seasonal variations, based on the temporal factors reported by Jenkin et al. (2000). VOC speciation based on Passant (2002), for the source category contributions reported by the LAEI (dominated by 39.3% road transport and 40.5% solvent usage). NOx was emitted as 90% NO, 9.5% NO_2 and 0.5% HONO.
SO_2	6.9 kg km^{-2} day^{-1}	
NOx	113.3 kg km^{-2} day^{-1}	
Anthropogenic VOCs	107.7 kg km^{-2} day^{-1}	
Biogenic VOCs	3.0 kg km^{-2} day^{-1}	Average daily emission rate, based on an annual UK total of 267 ktonne, derived from information from the EU NATAIR project (Steinbrecher et al., 2009). The applied rate was adjusted for diurnal and seasonal variations, based on the temporal factors reported by Jenkin et al. (2000). The rate was further scaled by a factor of 10, based on the observed isoprene mixing ratio (see text). The applied speciation, also based on NATAIR for the UK, was 7.5% isoprene and 54.1% monoterpenes (24.1% α-pinene; 19.6% β-pinene; 12.0% limonene), with the remainder unrepresented in the present calculations.
Initial mixing ratios		
O_3	84 ppb	Based on measurements at Bexley AURN site at 13:00 h on 30th July 1999.
NO	0 ppb	
NO_2	10 ppb	
CO	170 ppb	
CH_4	2007 ppb	Fixed throughout simulation. Value inferred approximately from that of CO at Bloomsbury AURN site, using the expression $[CH_4]$ = 1860 + 0.3[CO], based on data recorded at Royal Holloway in 1999 by the group of Dr David Lowry (http://www.gl.rhul.ac.uk/METH/).
non-methane VOCs	various	Based on PTM output for hydrocarbons and oxygenates at Writtle, Essex, for the 6th August 2003 ozone episode, as tabulated by Utembe et al. (2005).

emissions of NO_2). This demonstrates that the continued processing of the initial composition still retains a substantial propensity to generate oxidant in the absence of continued emissions inputs, but that this is about a factor of two lower than the production rate inferred from the London transect observations on the 30th July 1999, (7.8 ± 4.3) ppb h^{-1}. The simulation also showed that NO_x decayed from its initial mixing ratio of 10 ppb with a time constant of about 2 hours, which is consistent with its removal mainly via the reaction of NO_2 with OH, the simulated average OH radical concentration being 6.0×10^6 molecule cm^{-3}.

(ii) <u>Addition of anthropogenic emissions</u>: The inclusion of the emissions from anthropogenic sources was examined (Run 2), at the rates given in Table 8.2, which resulted in the mixing ratio of NO_x being maintained at about 10 ppb throughout the four hour period. The addition of anthropogenic emissions was found to have only a marginal impact on the production rate of $[OX]_B$, which decreased slightly to 3.10 ppb h^{-1}. The lack of a net effect results from almost identical compensating effects of VOC and NOx inputs under the prevailing VOC-limited conditions. This was confirmed by adding the NO_x emissions alone (Run 3), which decreased $[OX]_B$ production rate to 1.92 ppb h^{-1}.

Figure 8.3: Production rates of background oxidant, [OX]$_B$, simulated with the single-layer box model for 30th July 1999 conditions. The scenarios, which are fully described in the text, are also summarised. Results are shown for both MCM v3.2 and CRI v2.1 versions of the model.
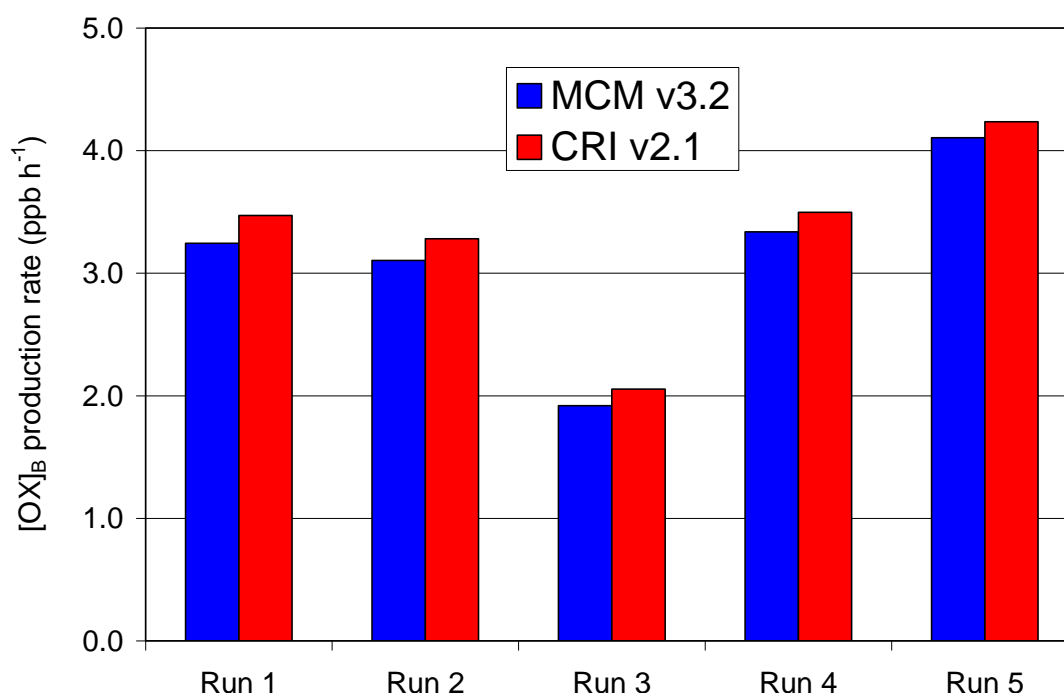
Run number	Description
1	Continued processing of the species at their initialised concentrations, representative of the aged air prior to entering the London conurbation.
2	Run 1 + addition of anthropogenic emissions of NO$_x$, CO, SO$_2$ and non-methane VOCs.
3	Run 1 + addition of anthropogenic NO$_x$ emissions only.
4	Run 2 + addition of biogenic emissions of isoprene.
5	Run 2 + addition of biogenic emissions of isoprene and monoterpenes.

The simulated [OX]$_B$ production rate of about 3 ppb h^{-1} is somewhat lower than the oxidant observations suggest, and also lower than that inferred previously from the analysis of the observations of hydrocarbons and their likely processing rates. Examination of the simulated hydrocarbon distribution indicates that, although the less reactive VOCs were simulated to be present at comparable mixing ratios to those observed at Bloomsbury UCL, the mixing ratios of the more reactive VOCs are systematically lower than those observed (see Figure 8.3). This is probably indicative of comparing near ground level observations with a simulated boundary layer average, as the more reactive VOCs will likely display vertical gradients in their mixing ratios.

(iii) Addition of biogenic emissions: A representation of biogenic VOC emissions was implemented, as summarised in Table 8.2. Because there are no emissions data specifically for the London conurbation, emission rates were based on average UK emissions densities, using annual totals reported in the EU NATAIR project (Steinbrecher et al., 2009), with temporal factors to describe average diurnal and seasonal variations. Initially, the emissions of isoprene only were considered (Run 4), which are estimated to account for only 7.5 % of the total. Even allowing for the systematic under-simulation of reactive hydrocarbons comment on above, the simulated mixing ratio of biogenic isoprene was substantially underestimated, and it was necessary to further increase the emissions rate by a factor of 10 to provide a consistent input.

This can be rationalised, at least in part, by the temperature on the afternoon of July 30th 1999 being substantially greater than represented by the seasonal average. This input of isoprene resulted in an increase in the [OX]$_B$ production rate to 3.34 ppb h^{-1}.

As indicated above, isoprene represents only quite a small fraction (7.5 %) of the UK biogenic VOC total, according to available estimates. Monoterpenes are estimated to account for a much larger fraction of 54.1 %, although it emphasised that the relative contributions potentially vary widely depending on the types of vegetation at a given location. As an illustration, emissions of monoterpenes were included at this relative level (Run 5), divided between α–pinene, β–pinene and limonene (see Table 8.2). This resulted in a further elevation of the [OX]$_B$ production rate to 4.11 ppb h^{-1}, a value which falls just within the quoted 2σ uncertainty bounds of the observed production rate, (7.8 ± 4.3) ppb h^{-1}. Under these illustrative conditions, sensitivity tests showed that 54 % of this was due to anthropogenic VOC emissions, with 10 % and 36 % being due to isoprene and monoterpenes respectively. As indicated above, this substantial contribution from monoterpenes may or may not be applicable to London, but it does indicate that characterisation of emissions of species other than isoprene from biogenic sources would be informative. Note also that isoprene and monoterpenes are reported to account for about 62 % of the total UK biogenic emissions. The remainder is reported to be emitted as "other VOCs", which may include both unreactive species (e.g., acetone; methanol) and reactive species (e.g., sesquiterpenes).

(iv) Consideration of the temporal trend in emissions from the LAEI: Using the conditions of Run 5 as a base case model version, the anthropogenic emissions inputs were varied on the basis of annual totals reported by the LAEI, for which data are available for selected years in the period 1999-2008, as shown in Figure 8.4. These figures represent those originally reported for the given year, such that earlier data do not reflect more recent changes which may have been implemented into inventory procedures or assumptions. It is noted that the data therefore show some discontinuities, with a notable realignment apparent in the 2008 data, particularly for non-methane VOCs and CO.

The resultant simulated [OX]$_B$ production rates, shown in Figure 8.5, all lie in the approximate range 4.0–4.3 ppb h^{-1}. As also shown in the figure, the trend in [OX]$_B$ production rates closely follows the trend in the ratio of the non-methane VOC and NOx emissions inputs. This indicates that chemical processing is occurring under VOC-limited conditions, and is consistent with the results of the sensitivity tests reported above. These results suggest that there is unlikely to have been a significant trend in urban-scale [OX]$_B$ production rates over the London conurbation during photochemical episodes, in agreement with those inferred from observations.

(v) Consideration of the influence of temperature and relative humidity: In all the above simulations, the temperature and relative humidity have been set at values of 300.7 K (27.5 ˚C) and 35.7 %; these values being based on measurements made at Silwood Park, Ascot on the afternoon of 30th July 1999, during the EU PRIME campaign (see Table 8.2). Recognising that higher temperatures have been recorded during some photochemical episodes, and that temperatures over the London conurbation are typically higher than in surrounding rural areas, additional calculations were carried out with the temperature increased by 5 ˚C and 10 ˚C. These were initially carried out with the relative humidity maintained at 35.7 %, such that the absolute water vapour concentration increases by factors of 1.30 and 1.66. As shown in Figure 8.6, this had a notable increasing impact on the simulated [OX]$_B$ production rates, with respective values of 5.81 ppb h^{-1} and 7.79 ppb h^{-1} resulting from the 5 ˚C and 10 ˚C temperature increases.

Figure 8.4: Trend in annual emission totals reported by the LAEI for selected years over the period 1999-2008.

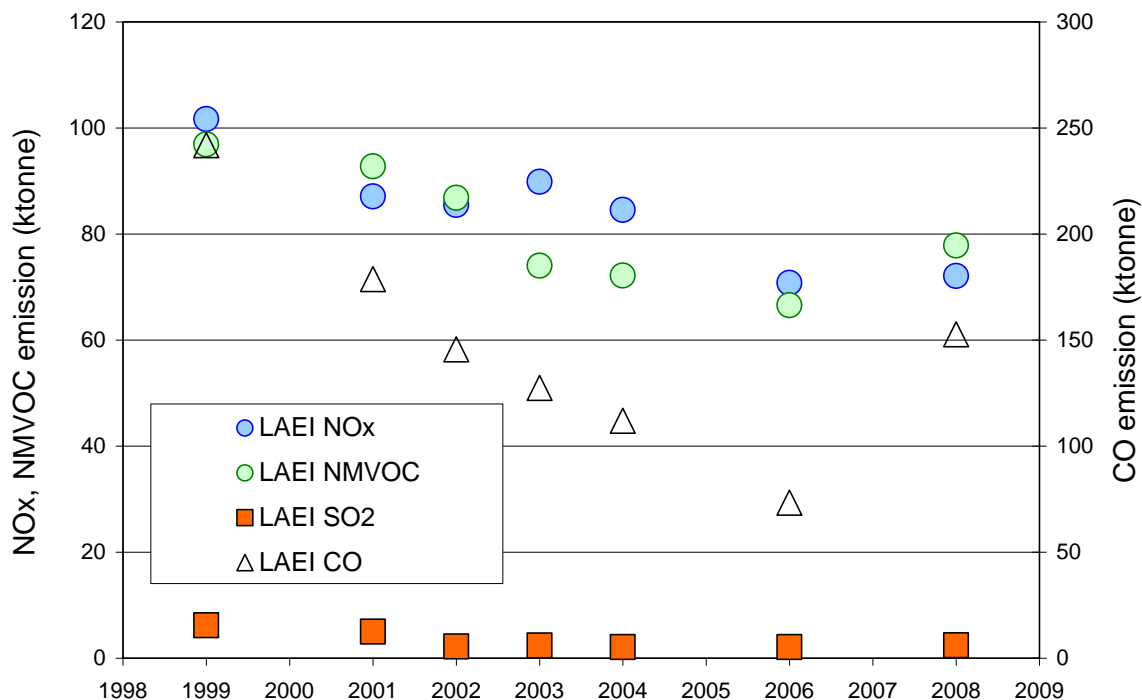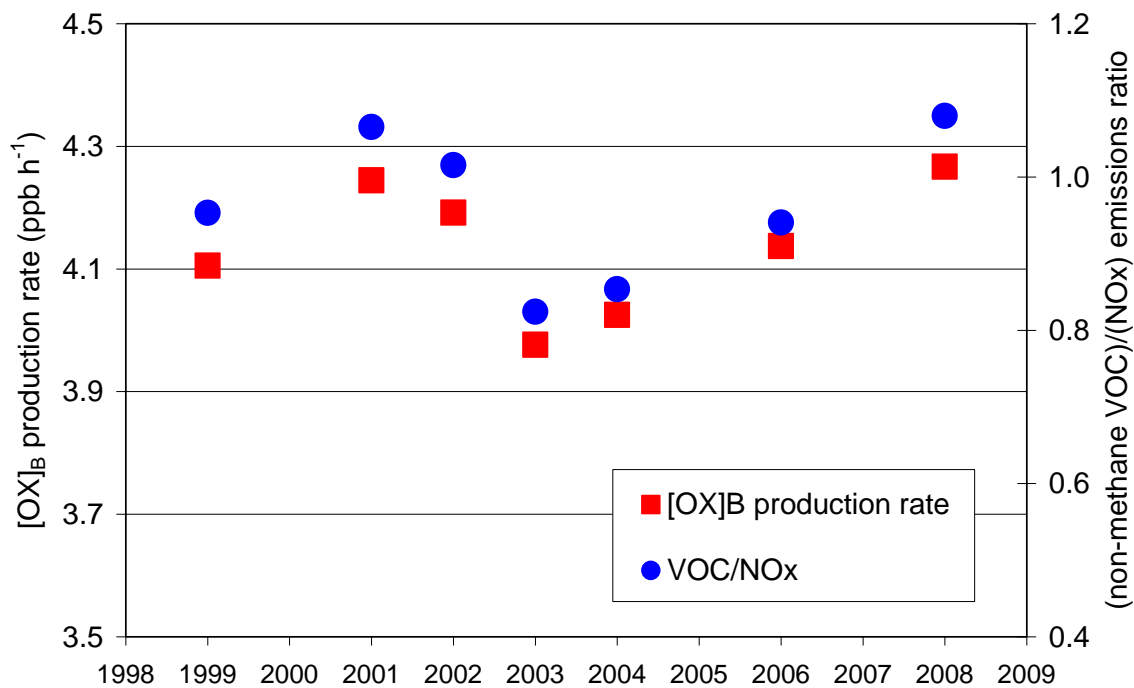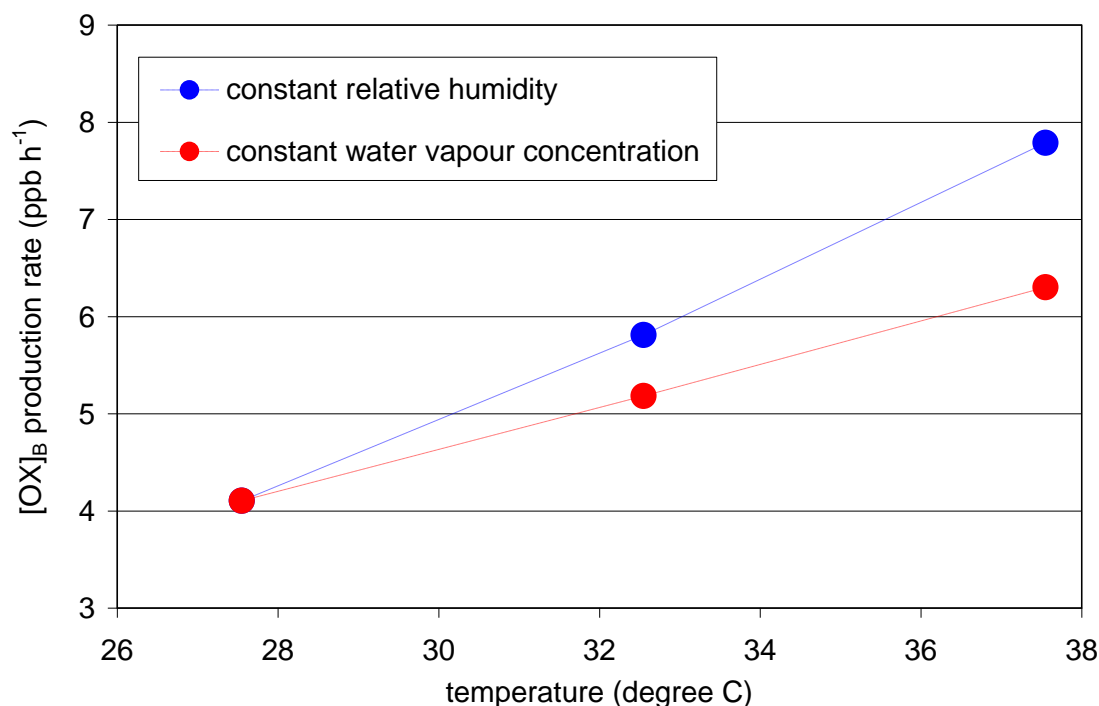**Figure 8.5: Trend in the simulated production rate of background oxidant, $[OX]_B$, and in the relative emissions of anthropogenic non-methane VOCs and NOx.**

Figure 8.6: Influence of temperature on the simulated production rate of background oxidant, $[OX]_B$, relative to the 30th July 1999 base case scenario for which T = 27.5 °C and relative humidity = 35.7 %.

There are broadly two contributory factors to these increases: (a) the increasing temperature tends to increase the efficiency of radical-propagated VOC oxidation cycles which drive oxidant formation. This is because the rates of propagating reactions tend to increase relative to those of terminating reactions, and also because the stability of temporary radical reservoirs (especially PANs) is reduced; and (b) the increasing water vapour concentration increases the efficiency of radical formation following the photolysis of ozone, thereby promoting further VOC oxidation.

To separate out these two influences, additional calculations were carried out in which the temperature was increased whilst maintaining the water vapour concentration at a fixed value, corresponding to reductions in relative humidity to about 28 % and 21 % with the temperature increases. As also shown in Figure 8.6, the increases in simulated $[OX]_B$ production rates were still notable, with respective values of 5.18 ppb h^{-1} and 6.30 ppb h^{-1} resulting from the 5 °C and 10 °C temperature increases. These are effectively due to the temperature dependence of the chemistry (i.e., factor "(a)") alone, and suggest that each of the factors described above have broadly comparable influences in the first set of calculations.

It should also be noted that temperature increases also directly influence the emission rates of biogenic VOCs, and potentially result in increases of emissions from some anthropogenic source sectors (e.g., road transport evaporative emissions). These effects have not been considered here.

8.2.4 Development and application of a multi-level CRI v2.1 box model

(i) <u>Application of CRI v2.1 in the single layer box model</u>: In order to limit the run time of a multi-level version of the model, it was intended to use the traceable reduced mechanism CRI v2.1 instead of the much more detailed MCM v3.2. To validate the use of CRI v2.1, the initial series of five simulations was repeated with the MCM v3.2 chemistry replaced by that of CRI v2.1. The results, shown in Figures 8.3 and 8.7, confirm that CRI v2.1 is able to recreate the general features of both the oxidant production rates and hydrocarbon distribution/reactivity simulated with MCM v3.2, establishing that CRI v2.1 is suitable for purpose.

Figure 8.7: Comparison of the distribution of 24 hydrocarbon mixing ratios (upper panel) and their reactivities towards OH radicals (lower panel), simulated with the MCM v3.2 and CRI v2.1 versions of the single layer box model for 30th July 1999 conditions, using the "Run 5" reference scenario. The displayed hydrocarbons are those for which ambient measurements are typically reported from the hydrocarbon network sites. Note that isoprene is divided into anthropogenic and biogenic contributions. The total simulated OH reactivity of the displayed hydrocarbons is 1.49 s^{-1} and 1.52 s^{-1}for the MCM v3.2 and CRI v2.1 simulations, respectively.
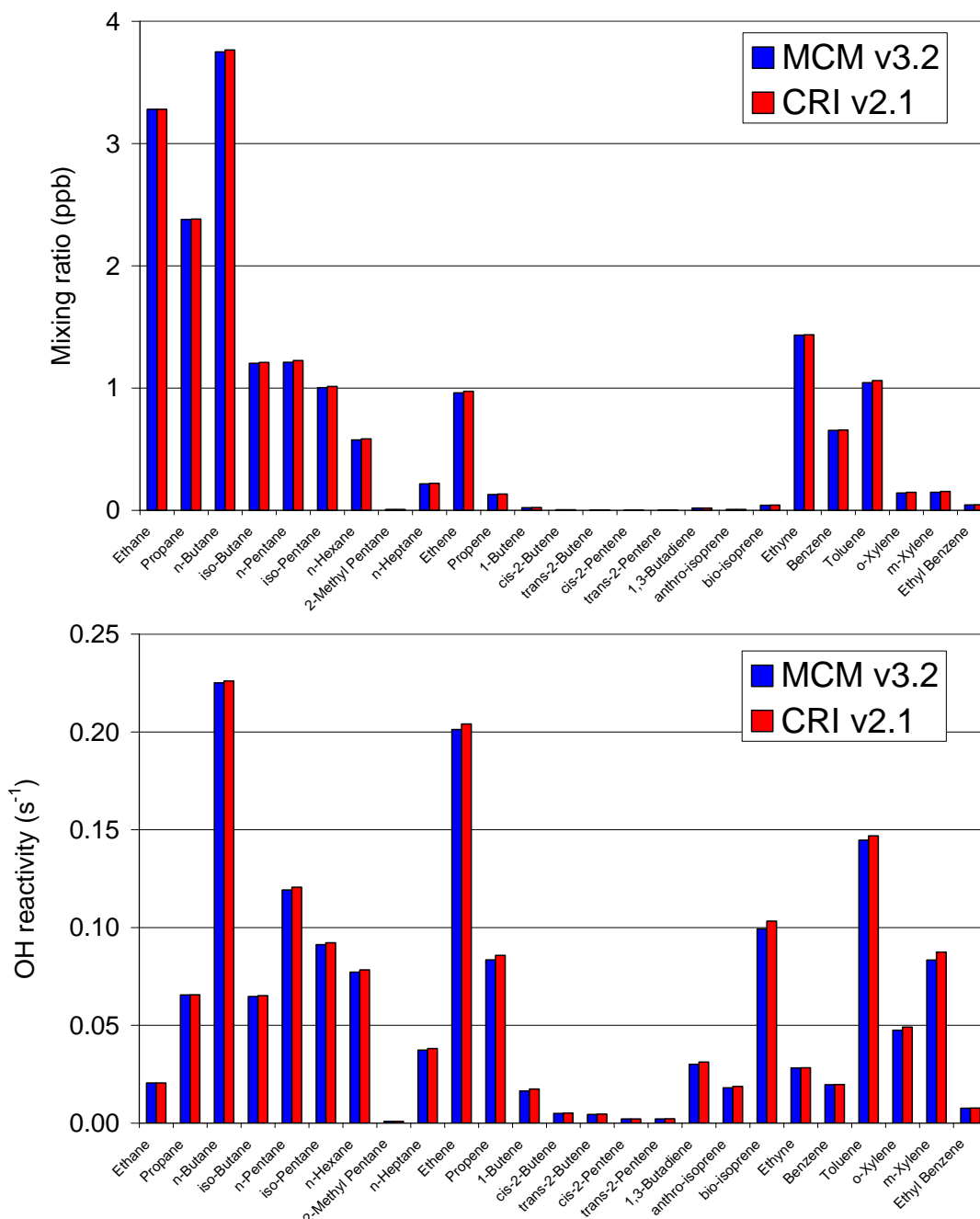
(ii) <u>Multi-level model set-up and application</u>: In the multi-level model, the boundary layer was divided into 13 instantaneously-mixed levels, each 100 m in depth. The resultant total boundary layer depth (1300 m) is thus identical to that in the single layer model and also to the maximum daytime boundary layer depth usually applied with the PTM for simulating photochemical episode conditions. The air exchanges vertically between adjacent levels with a single characteristic time constant. There are no losses from the top of the boundary layer (i.e., it is assumed that

exchange with the free troposphere is negligible on the 4 hour simulation timescale), and losses through deposition occur only from the lowest level. Similarly, the emissions inputs feed only into the lowest level. The initialised species mixing ratios applied in the single layer model are applied to each of the 13 levels of the multi-level model. As indicated above, those data are designed to be representative of the composition of aged air arriving in the UK following several days chemical processing over Europe under anticyclonic conditions, and for which complete mixing throughout the boundary layer would be expected. For simplicity, the horizontal transport in each level is assumed to occur at the same rate. Although the horizontal velocity might be expected to show a vertical gradient, the simplistic assumption applied here reflects that the high temperatures associated with photochemical episode conditions are characterised by relatively rapid vertical convective mixing.

The effect of varying the exchange time constant between the levels was investigated, with particular attention paid to the impact on the simulated vertical profiles of reactive hydrocarbons. It was found that a time constant of 5 minutes resulted in a strong vertical profile for isoprene (the most reactive hydrocarbon considered) with the 4-hour average mixing ratio decreasing by about a factor of two for every 200 m increase in altitude. This is similar to that reported by Vieno et al. (2010) for isoprene in the August 2003 heatwave, as simulated with the more sophisticated boundary layer representation in the EMEP4UK model. All the simulations reported here were therefore performed with a 5 minute vertical exchange time constant.

The set of 30th July 1999 simulations described above, and presented in Figure 8.3 (Runs 1−5), were once again repeated with the multi-level model. Figure 8.8 shows the resultant simulated $[OX]_B$ production rates in the lowest model level and averaged over the whole boundary layer depth. Logically, the boundary layer average values are almost identical to those simulated with the CRI v2.1 version of the single layer box model, as shown in Figure 8.6. Owing to the influence of deposition, the net $[OX]_B$ production rates show a distinct vertical gradient such that the lowest level values are typically 1−1.5 ppb h^{-1} lower than the average.

Figure 8.8: Production rates of background oxidant, $[OX]_B$, simulated with the CRI v2.1 multi-level box model for 30th July 1999 conditions. The results are shown for the lowest model level (corresponding to the first 100 m) and averaged over the entire boundary layer depth.
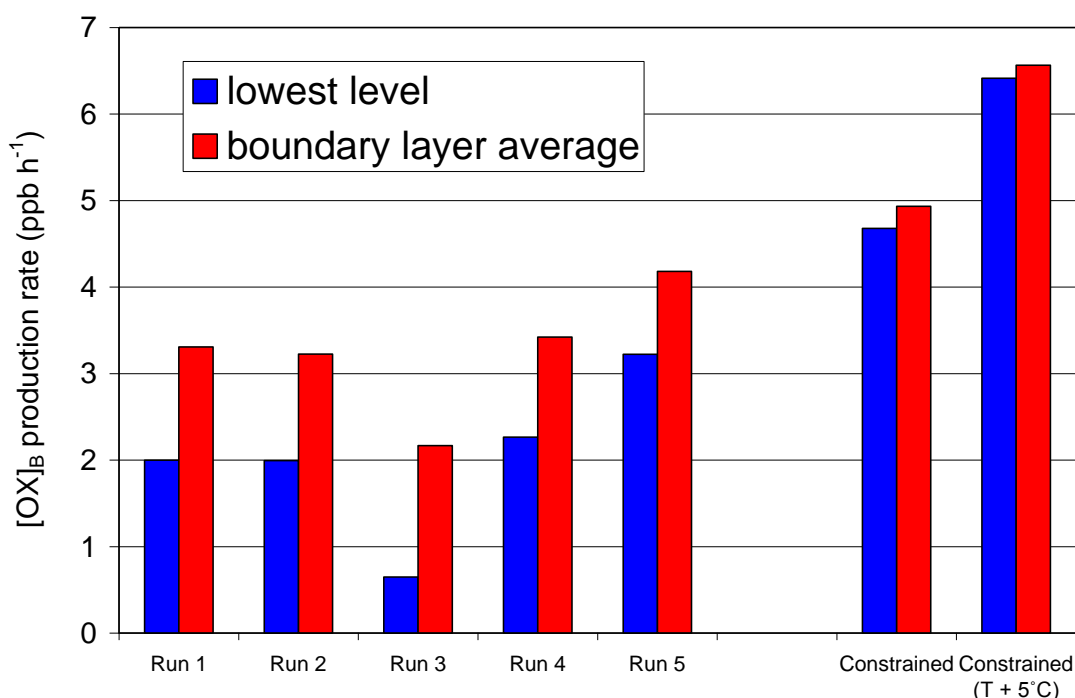
This leads to a lowest level $[OX]_B$ production rate of 3.22 ppb h^{-1} in the Run 5 reference simulation. Compared with the results of the single layer box model calculations discussed above, this is inevitably in poorer agreement with the observed average figure of 5.8 ppb h^{-1}, and also just outside the quoted 2σ uncertainty bounds of the value of (7.8 ± 4.3) ppb h^{-1} observed specifically for the 30th July 1999 event. However, the vertical structure of the model allows a more direct comparison of the simulated level and distribution of emitted hydrocarbons, and a judgement on whether the quantities injected into the model are reasonable.

(iii) <u>Comparison of hydrocarbon data and observationally-constrained simulations</u>: Observational data for speciated hydrocarbons are available for three London sites on 30th July 1999, namely Marylebone Rd., Bloomsbury (UCL) and Eltham. The data for the afternoon of that day are summarised in Figure 8.9, showing both the measured mixing ratios of the 24 monitored hydrocarbons, and their associated reactivities towards OH radicals.

Figure 8.9: Observational data for 24 hydrocarbons at London sites on the afternoon of 30th July 1999, based on the average of data over the period 12:00h-18:00h. Note that isoprene is divided into anthropogenic and biogenic contributions (biogenic in green)
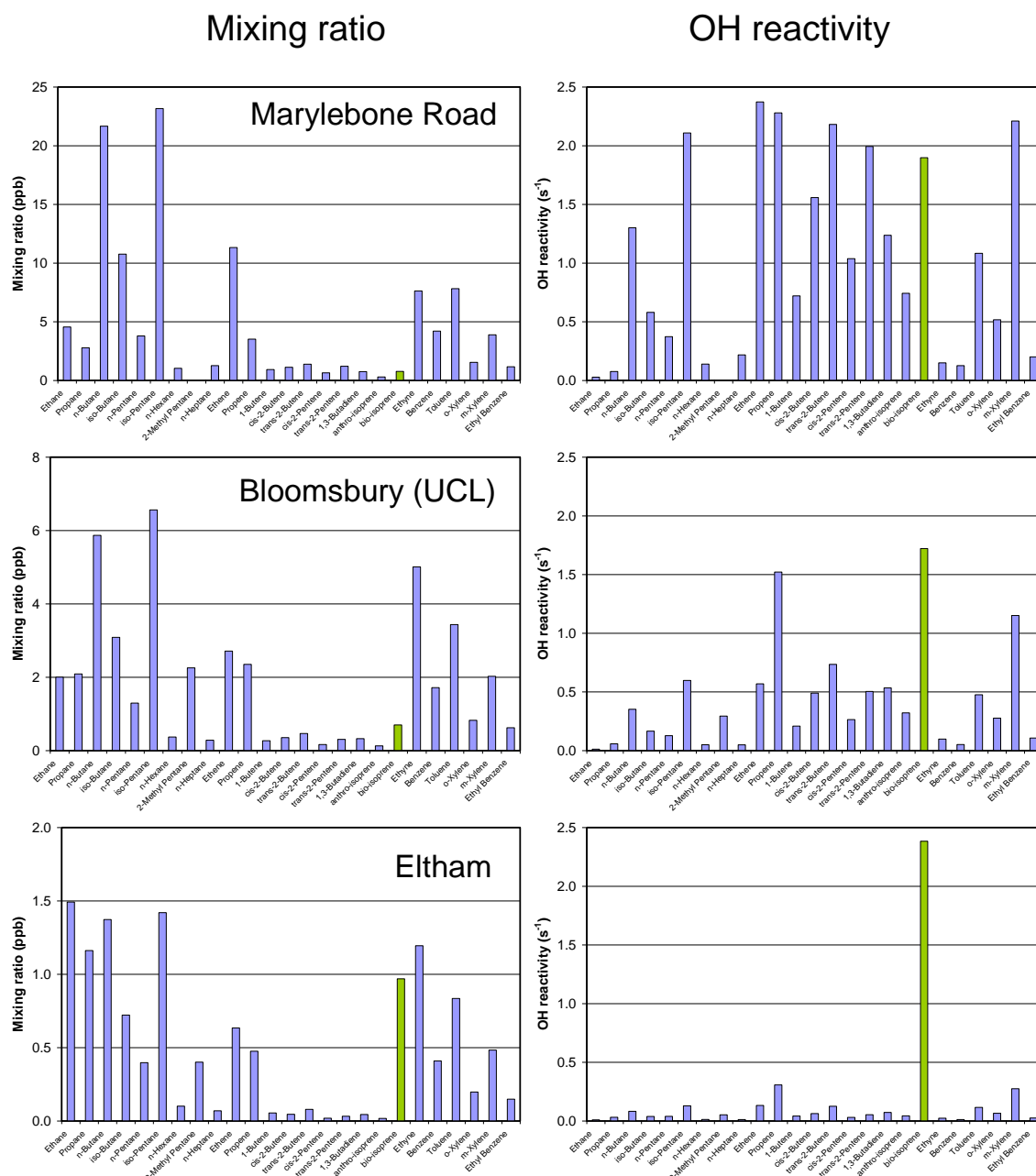
In each case, the isoprene data are separated into anthropogenic and biogenic contributions, using 1,3-butadiene as a marker for the anthropogenic contribution (see AQEG, 2009). The data clearly demonstrate a wide range of conditions, with the collective OH reactivity of the measured anthropogenic hydrocarbon set falling from 23.2 s^{-1} at Marylebone Rd (a central London kerbside site) to 9.0 s^{-1} at Bloomsbury UCL (a central London background location) to 1.8 s^{-1} at Eltham (a suburban background site towards the east of the Greater London conurbation). The simulated reactivity of the anthropogenic hydrocarbons in the lowest model level is almost identical to that measured at Eltham, and this should be broadly indicative of the average reactivity of that hydrocarbon set in Greater London under photochemical conditions in 1999. However, a comparison of the speciation suggests that the model tends to overestimate the mixing ratios of several un-reactive or relatively un-reactive species (e.g., several alkanes, ethyne, benzene and toluene) whilst underestimating the mixing ratios of propene and all higher alkenes by factors of up to five. It therefore appears that the applied emissions speciation does not recreate that observed. This may be partially because the measurements tend to reflect the road transport contribution, whereas the model emissions input has about equal (and together dominant) contributions from solvent usage (40.5 %) and road transport (39.3 %). The mixing ratios of the un-reactive species are also strongly influenced by the model initialisation, which was based on independent measurements outside London (see Table 8.2).

Figure 8.9 also shows that the mixing ratio of biogenic isoprene is comparable at the three London sites (approaching 1 ppb), consistent with a diffuse background vegetation source. This results in an associated OH reactivity of about 2 s^{-1}, which should be broadly indicative of the average reactivity of biogenic isoprene in Greater London. This leads to the, possibly unexpected, conclusion that the average OH reactivities of the measured anthropogenic and biogenic hydrocarbons were about the same under photochemical episode conditions in 1999. The preliminary representation of biogenic emissions used in the model results in a lowest level mixing ratio (and OH reactivity) of isoprene which is about a factor of five lower than that observed, suggesting a strongly under-represented biogenic source.

In view of these discrepancies, the model set-up was adjusted so that the mixing ratios of the measured hydrocarbons were constrained on the basis of the Eltham observations. The observed data were assumed to correspond to an altitude of 2 m, and the relative vertical profiles throughout the boundary layer were assigned on the basis of those simulated above with the unconstrained model. Figure 8.10 summarises the impact of the input data in terms of the OH reactivities associated with the constrained mixing ratios. Relative to the unconstrained model, these show a reduction in the reactivity associated with anthropogenic alkanes and aromatics, and an increase in the reactivity of anthropogenic alkenes and biogenic isoprene. The data also show that these latter reactive hydrocarbon categories display stronger vertical profiles, such that the average boundary layer OH reactivity of biogenic isoprene is reduced to about 40 % of that of the measured anthropogenic hydrocarbon total.

The observationally-constrained version of the model was run with the emissions of the unmeasured VOCs, NOx, CO and SO$_2$, and the unmeasured species initialisations, unchanged from the unconstrained model. To ensure that that the relative levels of NOx and VOCs were consistent with the Eltham observations, the model was run iteratively with the constrained mixing ratios of the anthropogenic hydrocarbons being slightly scaled (reduced) until the relative total simulated reactivities of the hydrocarbons and NOx matched those observed. This ensured that systematic errors associated with artificially changing the VOC/NOx ratio were avoided, and reflects that the simulated average London conditions are similar to (rather than identical to) those measured at Eltham.

Figure 8.10: OH radical reactivities associated with the observationally-constrained mixing ratios of the measured hydrocarbons used in the multi-level model. The observed values are based on the measurements at Eltham. The model values were defined by applying the relative vertical profiles derived from the unconstrained model simulations.
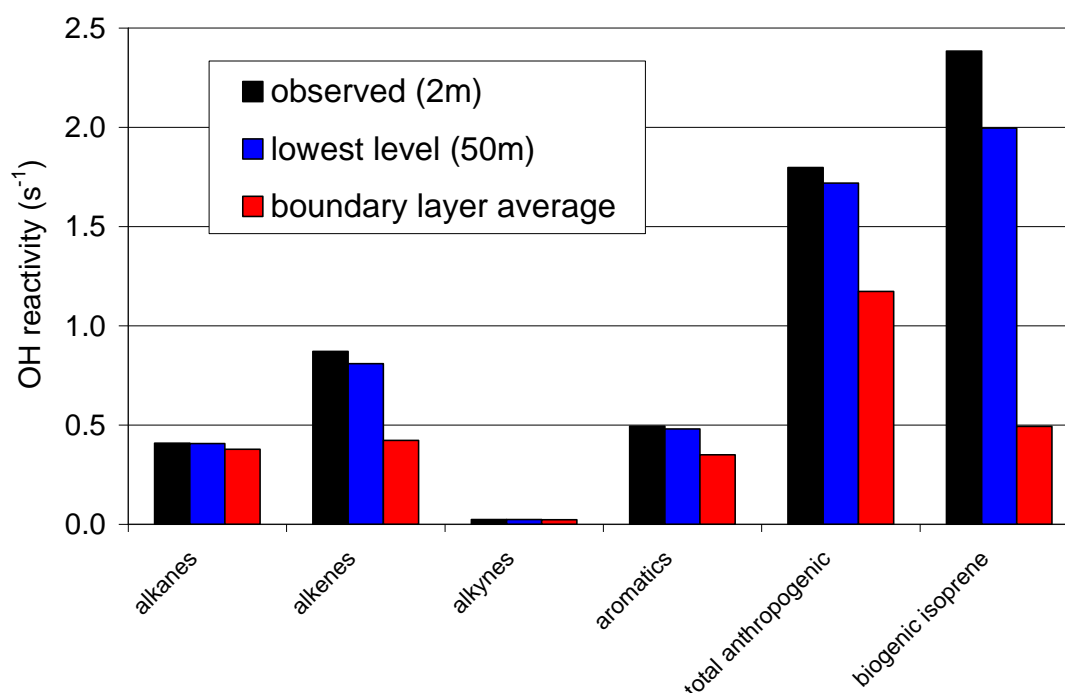
The simulated $[OX]_B$ production rates in the lowest model level and averaged over the whole boundary layer depth are shown in Figure 8.8, along with the results of the unconstrained model discussed above. The observationally constrained version of the model simulates a lowest level net $[OX]_B$ production rate of 4.68 ppb h^{-1}, which is notably greater than the value of 3.22 ppb h^{-1} obtained in the reference Run 5 with the unconstrained model. This value is also in much closer agreement with the observed average $[OX]_B$ production rate of 5.8 ppb h^{-1}, and the value of (7.8 ± 4.3) ppb h^{-1} observed specifically for the 30th July 1999 event. The $[OX]_B$ production rates simulated with the constrained model also show a much weaker dependence on altitude, such that the boundary layer average value, 4.93 ppb h^{-1}, is only marginally greater than the lowest level value (see Figure 8.8). This is because the impact of deposition on the lower level production rates are largely offset by the impact of a higher abundance of reactive anthropogenic alkenes and biogenic isoprene in the constrained model, with these species displaying strong vertical profiles. This results in not only a more pronounced vertical profile for the OH reactivity of the VOCs, but also an important altitude-dependent radical source resulting from the partial removal of the alkenes by reaction with ozone, which is more important nearer the surface. Also shown in Figure 8.8 is the effect of increasing the constrained model temperature by 5 °C (constant relative humidity). Similarly to the results discussed above for the MCM v3.2 single layer model (shown in Figure 8.5), this has a notable impact on the lowest level $[OX]_B$ production rate, which is increased to 6.41 ppb h^{-1}. Both of these increasing effects thus have contributions from increasing the primary radical production rate.

8.2.5 Conclusions and recommendations

The calculations presented above show that urban oxidant production rates inferred from observational data under photochemical episode conditions can broadly be explained by current understanding of the chemical processing of the urban atmosphere under such conditions, provided a number of model inputs are represented correctly. In particular, the results were found to be sensitive to the relative (and absolute) inputs of VOCs and NOx into the model, the applied VOC speciation and the prevailing temperature and relative humidity. The representation of the

chemistry of the VOC speciation also needs to be adequately represented, including coverage of highly reactive species.

The work has allowed a limited assessment of the model emissions inputs in relation to observational data. This provided some support for the reported data, but also demonstrated some discrepancies which generally appear to relate to the application of inventory-based average quantities to the simulation of specific (i.e., not average) conditions and locations. In particular, the input of reactive VOCs of both anthropogenic and biogenic origin appeared to be under-represented, such that constraining ambient mixing ratios on the basis of observations resulted in improved model performance. **The results suggest that it would be valuable to use archived and emerging monitoring data to carry out a much more extensive evaluation of emissions inventory data and methods, and of how that information is then applied in ozone models.** Such evaluation activities should ideally include consideration of the temporal and temperature dependences of emissions sources, the use of VOC speciation to evaluate contributions from different source sectors under different conditions, consideration of vertical profiles (where available), and further assessment of the role and contribution of VOCs from biogenic sources.

Finally, the analysis presented here is concerned with accounting for urban-scale oxidant production rates measured under photochemical episode conditions. It would be instructive to use such data to evaluate the performance of Eulerian models such as CMAQ under such conditions.

8.3 Summary and main conclusions

The main conclusions of the work of Objective 11 on the assessment of background and urban-scale oxidant can be summarised as follows:

> **Summary:**
>
> - **The geographical variation of annual mean oxidant over the UK has been characterised and the higher resolution mapping methodology developed to produce a 1km x 1km map for 2010. This activity extends earlier work and provides parameterised spatial variation in oxidant concentrations over the UK for each year between 2001 and 2010 which will improve and inform NO_2 and ozone modelling activities using the Pollution Climate Model (PCM) in the Defra UKAAQA programme**
>
> - **The potential impact of urban-scale photochemistry on oxidant production over the London conurbation has been assessed using a boundary layer box model to simulate chemical processing.**
>
> - **Urban oxidant production rates inferred from observational data under photochemical episode conditions can broadly be explained by current understanding of the chemical processing of the urban atmosphere under such conditions, provided a number of model inputs are represented correctly.**
>
> - **In particular, the results were found to be sensitive to the relative (and absolute) inputs of VOCs and NO_x into the model, the applied VOC speciation and the prevailing temperature and relative humidity.**
>
> - **The work has allowed a limited assessment of the emissions inputs to the model in relation to observational data. This provided some support for the reported data, but also demonstrated some discrepancies. In particular, the input of reactive VOCs of both anthropogenic and biogenic origin appeared to be under-represented by the emissions data.**
>
> - **The work suggests that it would be valuable to use monitoring data to carry out a much more extensive evaluation of emissions inventory data and of how**

that information is then applied in ozone models including consideration of the temporal and temperature dependences of emissions sources and the use of VOC speciation profiles.

9 Other Project Activities

Other project activities have been carried out in 2011 involving the project consortium members.

9.1 Model review activities

Aside from the main project objectives, the project consortium has participated in a range of activities relating to Defra's Model Intercomparison Exercise (MIE) which continued during 2011.

In January, Tim Murrells and Sally Cooke (AEA) and Dick Derwent (rdscientific) attended the meeting for Group 2 (Regional and Transboundary pollution including ozone) to answer questions by the Air Quality Modelling Review Steering Group on the performance of the OSRM and PTM following the submission of model results and background information on each model in Phase I of the MIE during 2010. A further meeting was attended in June at which the second phase of the modelling intercomparison exercise was discussed.

In September, comments were provided on the report "*Review of Air Quality Modelling in Defra*" prepared by the Steering Group. The responses focused on the factual/technical content of the report, including the section on the OSRM. In the latter part of 2011, detailed results from 2006 ozone simulations under different NO_x and VOC emission scenarios were provided to the Steering group for statistical analysis and diagnostic evaluation under Phase 2 of the MIE (see Section 6.3).

9.2 Ad-hoc queries

In February, the project responded to an ad-hoc query passed on from Defra's helpdesk on the role played by hydrocarbon emissions from vehicle exhausts in the formation of smog and the benefit of reducing HC emissions from all petrol emissions by 40%. Following an initial response, information was also provided to Defra on the share of benzene and 1,3-butadiene emissions from petrol vehicles and from petrol distribution.

Following Defra's appearance in front of the Environment Audit Committee in July, the EAC asked some further questions including one on quantification of the significance of trans-boundary air pollutants on meeting air pollution targets. The project team helped Defra formulate a response to the EAC on the contribution of emissions from outside the UK to ozone in the UK.

In July, results were provided to Defra from the OSRM for simulations of ozone concentrations in 2020 close to the Harwell site taking into account emission reductions corresponding to one of the Gothenburg scenarios previously modelled. Results were provided for the AOT40 and Days Greater than 120 μgm^{-3} Air Quality Directive metrics

In September, we provided a response to a Defra query on the emission sectors contributing most to ozone formation in the UK. This was to help Defra respond to a report on the damage that ozone causes crops.

9.3 Project meetings and reports

An annual progress meeting on the project was held at Defra on 8th November. Progress made on the core objectives was presented by the consortium members as well as activities in the MIE.

Three quarterly progress reports were prepared for Defra providing a summary of the progress made on each of the various project objectives and project management related issues.

9.4 Technical reports and publications

A paper was submitted to the Journal of the Air & Waste Management Association based on work undertaken in the project entitled "*Are Photochemical Oxidant Control Strategies Robust to the Choice of Chemical Mechanism*?", RG Derwent and TP Murrells.

Dick Derwent gave a presentation "*Impact of Chemical Mechanism Choice on Air Quality Policy Development*" at the 12th TFMM Meeting in Zurich on 11 – 13th May 2011, based on work done under this contract.

10 Conclusions and Policy Relevance

The work carried out during 2011 in the second phase of the project has involved the further research and application of models describing the formation and removal of tropospheric ozone and secondary organic aerosol for use in Defra policy. The main focus has been on the application of models to understand the current ground-level ozone climate in the UK and predict its future response to changes in precursor emissions.

This has been supported by further analysis of monitoring data to understand the coupling between ozone and NO_2 concentrations and the contributions of hemispheric and regional components to background concentrations and the effects of locally emitted NO_x. Air quality monitoring data in London have also been analysed to provide evidence for urban-scale photochemical production of oxidant (O_3 and NO_2) under pollution episode conditions.

Work has been completed on developing a chemical mechanism for ozone models that describes the atmospheric degradation of chlorinated solvents. This will allow models to be used for assessing ozone formation in future solvent assessment activities covering a wider range of solvent types

Current modelling tools have been used to support Defra policy on ozone and secondary PM air quality. The OSRM has been used to model the UK ozone climate in 2009 and 2010 and has been used to forecast ozone concentrations in 2020-2030 for a range of UK and European emission scenarios. The OSRM has also been used to develop maps of secondary organic aerosols for the first time.

The PTM has been used for a probabilistic uncertainty analysis of modelled ozone episodes and the likely impact of different emission reduction scenarios. The work has specifically focused on how predicted ozone responses vary according to what chemical reaction schemes are used in models.

To achieve the main aims of the project, the work was divided into three main objectives. The main conclusions reached for each objective are summarised below, taken from Sections 3-8.

Objective 9: **Improvement to Photochemical Reaction Schemes for Treatment of Biogenic Emissions and Emissions of Chlorinated VOCs from Solvents (Section 3)**

Summary:

- **The Master Chemical Mechanism (MCM) schemes for the atmospheric oxidation of chlorinated solvents have been revised and a reduced representation of the schemes in the CRI mechanism has been developed.**

- **The new schemes have been tested for a range of chlorinated VOCs and shown to perform well.**

- **This therefore provides the possibility of using models containing the new reduced schemes in future solvent assessment activities covering a wider range of solvent types.**

Objective 10.1: Modelling the UK Ozone Climate in 2009 and 2010 (Section 4)

Summary:

- **Both 2009 and 2010 were predominantly low ozone, but showed some characteristics of being moderate ozone years.**

- **When comparing the OSRM results for 2009 and 2010 with measured data for the two EU Air Quality Directive metrics the OSRM generally overestimated concentrations in both years. The OSRM overestimates ozone concentrations more in 2010 than in 2009.**

- **This is consistent with the way the OSRM has overestimated these ozone metrics in previous low ozone years (2004, 2005 and 2007)**

- **The model code for the original version of the OSRM and the CRI-SOA version have been restructured to bring them to the same level of development, and provide a format to keep the versions in line in the future. The difference between the two versions is in terms of the chemical schemes used.**

- **The original version was used for the 2009 simulation, but the new version was used for the 2010 simulation. Performance evaluations showed that the original and new versions of the OSRM performed the same within acceptable limits.**

Objective 10.3: Modelling Secondary Organic Aerosol Formation with the OSRM (Section 5)

Summary:

- **The SOA code from the CRIv2-R5 reduced chemical scheme has been successfully incorporated into the OSRM allowing this model to simulate organic aerosol formation for the first time. The new version has been optimised by upgrading biogenic emissions to account for the role of $\alpha-$ and $\beta-$pinene in SOA formation**

- **The results from the OSRM show that when averaged over a year, total organic aerosol mass concentrations are similar at different sites and show little inter-year variability, with annual mean concentrations falling within a range of 1-3 μgm^{-3} OA.**

- **However this masks a large range in spatial and temporal variation as can be seen by the range of maximum concentrations at different sites, months and years which vary over a range of 10-80 μgm^{-3} OA**

- **Seasonal trends in SOA in 2008 modelled by the OSRM are similar to those reported for the PTM, although the OSRM estimates lower concentrations.**

- **Maps have been developed at 10x10km resolution showing the spatial distribution of different components of SOA. Biogenic SOA components show a different distribution to the anthropogenic components**

- **The OSRM has potential for assessing the impact of UK and European precursor emissions on the spatial distribution of SOA concentrations in the UK**

Objective 10.2: Modelling Support for Ozone Policy Using the OSRM (Section 6)

Summary:

- **The OSRM has been used to model the future UK ground-level ozone climate for a number of different UK and European emission scenarios assuming meteorological conditions representative of 2006 and 2007**

- **Some of these referred to changes in UK emissions according to the latest DECC energy scenarios up to 2030. All scenarios led to increases in the AOT40 and Days Greater than 120 µgm^{-3} ozone metrics for 2020-2030 relative to values calculated for 2006. The differences in the values of the metrics between different model years (2020-2030) were greater than they were between different emission scenarios**

- **Maps of annual mean organic aerosol concentrations were calculated for 2020 showing different spatial patterns using 2006 and 2007 meteorology**

- **Further simulations were carried out for different UK and European emission scenarios with different levels of ambition for 2020. The analysis indicated that it will be important for comparable reductions in emissions to be achieved across Europe as well as in the UK to prevent ozone concentrations in the UK rising.**

- **It also shows the benefits to be achieved by reducing VOC emissions across Europe. These results will help inform Defra's policy relating to potential future national emission ceilings**

Objective 10.2 and 10.3: Modelling Support for Ozone Policy Using the PTM (Section 7)

Summary:

- **The impact of chemical mechanism choice on ozone air quality policy development has been studied in detail. The response of ozone concentrations to changes in NO$_x$ and VOC emissions predicted by versions of the PTM using 6 different chemical schemes of varying degrees of complexity was assessed and found to be quite varied. Other diagnostic evaluations of the different mechanisms were carried out showing the degree of variability in VOC reactivities and source-receptor relationships inferred by each mechanism**

- **Monte Carlo parametric uncertainty analysis was applied to the assessment of the likely impact of 7 different emission reduction scenarios for the renegotiation of the Gothenburg Protocol promulgated by IIASA/GAINS on ozone levels at Harwell, Oxfordshire**

- **The analysis showed that there is a high probability that the European emission scenarios for 2020 will reduce the average daily maximum ozone levels over a 122-day summer period by at least 0.4 ppb but not more than 3.5 ppb from current levels of 42 ppb**

- **There is a high probability that the emission scenarios for 2020 will reduce the highest daily maximum ozone level over a 122-day summer period by at least 2 ppb but not more than 20 ppb from the 2008 level of 76 ppb**

- **There was a high probability that the difference in highest daily maximum ozone between the 2020 base case and the most ambitious 2020 Maximum Feasible Reduction case was at least 2 ppb but a low probability that it would be more than 10 ppb. On this basis, it can be concluded that it was highly probable that the decline across the 2020 scenario variants was small but**

statistically significant.

- In the 2020 base case, there was less than 1 chance in 100 that the highest daily maximum ozone would be reduced to below the 50 ppb level and this only rose to 4 chances in 100 with the 2020 MFR scenario variant. The likelihood that the 50 ppb level would be reached with the 2020 MFR scenario variant was therefore small

- Further probabilistic uncertainty analysis was done on the influence of different UK precursor emission reductions on daily maximum ozone concentrations in 2020, 2025 and 2030 based on the latest UEP43 energy projections.

- This analysis showed that there was an 88% chance that the 2020 baseline emission projections would lead to an improvement in peak ozone modelled at the Harwell site, but less than 1% chance that peak ozone would be reduced to below 50 ppb in any of the model years

- The impact of climate change on ozone has been assessed, focusing on the response of predicted ozone concentrations to increasing isoprene emissions from natural sources occurring as a result of rising surface temperatures.

- The work has specifically focused on how predicted ozone responses vary according to what chemical reaction schemes are used in models. Four different chemical schemes were assessed and compared against the benchmark Master Chemical Mechanism. The work has indicated how the representation of atmospheric chemistry processes in global and regional air quality models is important in determining how changes in biogenic emissions caused by climate change will affect predicted changes in ground-level ozone formation.

Objective 11: Assessments of Background and Urban-Scale Oxidant (Section 8)

Summary:

- The geographical variation of annual mean oxidant over the UK has been characterised and the higher resolution mapping methodology developed to produce a 1km x 1km map for 2010. This activity extends earlier work and provides parameterised spatial variation in oxidant concentrations over the UK for each year between 2001 and 2010 which will improve and inform NO_2 and ozone modelling activities using the Pollution Climate Model (PCM) in the Defra UKAAQA programme

- The potential impact of urban-scale photochemistry on oxidant production over the London conurbation has been assessed using a boundary layer box model to simulate chemical processing.

- Urban oxidant production rates inferred from observational data under photochemical episode conditions can broadly be explained by current understanding of the chemical processing of the urban atmosphere under such conditions, provided a number of model inputs are represented correctly.

- In particular, the results were found to be sensitive to the relative (and absolute) inputs of VOCs and NO_x into the model, the applied VOC speciation and the prevailing temperature and relative humidity.

- The work has allowed a limited assessment of the emissions inputs to the model in relation to observational data. This provided some support for the reported data, but also demonstrated some discrepancies. In particular, the

input of reactive VOCs of both anthropogenic and biogenic origin appeared to be under-represented by the emissions data.

- **The work suggests that it would be valuable to use monitoring data to carry out a much more extensive evaluation of emissions inventory data and of how that information is then applied in ozone models including consideration of the temporal and temperature dependences of emissions sources and the use of VOC speciation profiles.**

11 Acknowledgements

12 References

Abdalmogith, S.S., Harrison, R.M., Derwent, R.G. (2006). Particulate sulphate and nitrate in southern England and Northern Ireland during 2002/3 and its formation in a photochemical trajectory model. Science of the Total Environment 368, 769–780.

Amann, M., et al., 2011. Cost-effective Emission Reductions to Improve Air Quality in Europe in 2020.Scenarios for the Negotiations on the Revision of the Gothenburg Protocol under the Convention on Long-range Transboundary Air Pollution. IIASA. International Institute for Applied Systems Analysis, Schlossplatz 1, Laxenburg, A-2361, Austria.

AQEG (2009). Ozone in the United Kingdom. Report of the UK Air Quality Expert Group, AQEG. Prepared for the Department for Environment Food and Rural Affairs, the Scottish Executive, the Welsh Assembly and the Department of the Environment in Northern Ireland. Defra publications, London, 2009. ISBN 978-0-85521-184-4.

Beven, K., Freer, J., 2001. Equifinality, data assimilation, and uncertainty estimation in mechanistic modelling of complex environmental systems using the GLUE methodology. Journal of Hydrology **249**, 11-29

Bloss, C., Wagner, V., Jenkin, M.E., Volkamer, R., Bloss, W.J., Lee, J.D., Heard, D.E., Wirtz, K., Martin-Reviejo, M., Rea, G., Wenger, J.C., Pilling, M.J., 2005. Development of a detailed chemical mechanism (MCMv3.1) for the atmospheric oxidation of aromatic hydrocarbons. Atmospheric Chemistry and Physics, 5, 641-644.

Bush T, I Tsagatakis, N Passant, A Griffin and B Pearson (2010). UK Emission Mapping Methodology 2007. Report for The Department for Environment, Food and Rural Affairs, Welsh Assembly Government, the Scottish Executive and the Department of the Environment for Northern Ireland. AEA Report AEAT/ENV/R/2863 (September 2010). http://www.airquality.co.uk/reports/cat07/1010011332_UKMappingMethodReport2007.pdf

Derwent, R.G., Jenkin, M.E., Saunders, S.M. (1996). Photochemical ozone creation potentials for a large number of reactive hydrocarbons under European conditions. Atmospheric Environment 30, 181–199.

Derwent, R.G., Jenkin, M.E., Saunders, S.M., Pilling, M.J. (1998). Photochemical ozone creation potentials for organic compounds in northwest Europe calculated with a Master Chemical Mechanism. Atmospheric Environment 32, 2429–2441.

Derwent, R., Witham, C., Redington, A., Jenkin, M., Stedman, J.,Yardley, R., Hayman, G., (2009). Particulate matter at a rural location in southern England during 2006: model sensitivities to precursor emissions. Atmospheric Environment 43, 689–696

Derwent, RG, M E. Jenkin, S R. Utembe, D E. Shallcross, T P. Murrells, N R. Passant (2010a). Secondary organic aerosol formation from a large number of reactive man-made organic compounds. Science of the Total Environment 408 (2010) 3374–3381

Derwent, RG, C.S. Witham, S. R. Utembe, M. E. Jenkin and N. R. Passant (2010b). Ozone in Central England: the impact of 20 years of precursor emission controls in Europe. Environmental Science & Policy 13 (2010) 195-204.

Derwent RG, A Fraser, J Abbott, M Jenkin, P Willis and T Murrells (2010c). *Evaluating the Performance of Air Quality Models.* Report published by for The Department for Environment, Food and Rural Affairs, Welsh Assembly Government, the Scottish Executive and the Department of the Environment for Northern Ireland, June 2010. http://www.airquality.co.uk/reports/cat05/1006241607_100608_MIP_Final_Version.pdf

Hayman, G.D., J. Abbott, C. Thomson, T. Bush, A. Kent, RG Derwent, ME Jenkin, MJ Pilling, A. Rickard and L. Whitehead, (2006a) "*Modelling of Tropospheric Ozone*". Final Report (AEAT/ENV/R/2100 Issue 1) produced for the Department for Environment, Food and Rural Affairs and the Devolved Administrations on Contract EPG 1/3/200

Hayman, G.D., Y Xu, J. Abbott, T. Bush, (2006b) "*Modelling of Tropospheric Ozone*". Report on the Contract Extension produced for the Department for Environment, Food and Rural Affairs and the Devolved Administrations on Contract EPG 1/3/200, AEA Report AEAT/ENV/R/2321 Issue 1, October 2006.

Hayman, G.D., J. Abbott, T.J. Davies, C.L. Thomson, M.E. Jenkin, R. Thetford and P. Fitzgerald (2010). The ozone source–receptor model – A tool for UK ozone policy. Atmospheric Environment, 44(34), 4283-4297.

Jenkin, M. E., Murrells, T. P. and Passant, N. R (2000). The temporal dependence of ozone precursor emissions: estimation and application, AEAT/R/ENV/0355, AEA Technology, Harwell, 2000.

Jenkin, M.E., Saunders, S.M., Wagner, V., Pilling, M.J., 2003. Protocol for the development of the Master Chemical Mechanism, MCM v3 (Part B): tropospheric degradation of aromatic volatile organic compounds. Atmospheric Chemistry and Physics 3, 181-193

Jenkin M.E., Watson L.A., Utembe S.R. and Shallcross D.E. (2008). A Common Representative Intermediates (CRI) mechanism for VOC degradation. Part 1: Gas phase mechanism development. Atmospheric Environment, **42**, 7185-7195

Johnson, D., Utembe, S.R., Jenkin, M.E., Derwent, R.G., Hayman, G.D, Alfarra, M.R., Coe, H., McFiggans, G., 2006. Simulating regional scale secondary organic aerosol formation during the TORCH 2003 campaign in the southern UK. Atmospheric Chemistry and Physics 6, 403-418.

Kent, A. J. and Stedman, J. R. (2008) UK air quality modelling for annual reporting 2006 on ambient air quality assessment under Council Directives 96/62/EC and 2002/3/EC relating to ozone in ambient air. AEA Report AEAT/ENV/R/2499

Murrells, T.P., Cooke, S., Kent, A., Grice, S., Derwent, R.G., Jenkin, M., Pilling, M.J., Rickard, A. and Redington, A (2008). "*Modelling of Tropospheric Ozone. First Annual Report*" produced for The Department for Environment, Food and Rural Affairs, Welsh Assembly Government, the Scottish Executive and the Department of the Environment for Northern Ireland under Contract AQ03508, AEA Report AEAT/ENV/R/2567, January 2008.

Murrells, TP, S Cooke, A Kent, S Grice, A Fraser, C Allen, RG Derwent, M Jenkin, A Rickard, MJ Pilling, M Holland, S Utembe (2009a). Modelling of Tropospheric Ozone - Project Summary Report: 2007-2009. Report for The Department for Environment, Food and Rural Affairs, Welsh Assembly Government, the Scottish Executive and the Department of the Environment for Northern Ireland. AEA Report AEAT/ENV/R/2899 (October 2009)

Murrells, TP, S Cooke, A Kent, S Grice, A Fraser, C Allen, RG Derwent, M Jenkin, A Rickard, M Pilling, M Holland (2009b). *Modelling of Tropospheric Ozone: Annual Report 2008*. Report for The Department for Environment, Food and Rural Affairs, Welsh Assembly Government, the Scottish Executive and the Department of the Environment for Northern Ireland. AEA Report AEAT/ENV/R/2748, February 2009.

Murrells, TP, S Cooke, J Abbott, A Fraser, RG Derwent, M Jenkin, A Rickard and J Young (2011). *Modelling of Tropospheric Ozone: Annual Report 2010*. Report for The Department for Environment, Food and Rural Affairs, Welsh Assembly Government, the Scottish Executive and the Department of the Environment for Northern Ireland. AEA Report AEAT/ENV/R/3134, February 2011

Pankow J.F. (1994). An absorption model of gas/particle partitioning involved in the formation of secondary organic aerosol. Atmospheric Environment, **28**, 189–193.

Passant, N.R. (2002) Speciation of UK emissions of non-methane volatile organic compounds. AEA Technology Report ENV-0545. Culham, Abingdon, United Kingdom, 2002

Saunders, S.M., Jenkin, M.E., Derwent, R.G., Pilling, M.J., 2003. Protocol for the development of the Master Chemical Mechanism, MCM v3 (Part A): Tropospheric degradation of non-aromatic volatile organic compounds. Atmospheric Chemistry and Physics 3, 161-180.

Steinbrecher, R., Smiatek, G., Köble, R., Seufert, G., Theloke, J., Hauff, K., Ciccioli, P., Vautard, R., Curci, G (2009). Intra- and inter-annual variability of VOC emissions from natural and semi-natural vegetation in Europe and neighbouring countries, Atmospheric Environment, 43, 1380-1391, 2009

Utembe, S. R., Jenkin, M. E., Derwent, R. G., Lewis, A. C., Hopkins, J. R., and Hamilton, J. F. (2005) Modelling the ambient distribution of organic compounds during the August 2003 ozone episode in the southern UK, Faraday Discuss., 130, 311–326, 2005

Utembe, S.R., Watson, L.A., Shallcross, D.E. and Jenkin, M.E. (2009). A Common Representative Intermediates (CRI) mechanism for VOC degradation. Part 3: Development of a secondary organic aerosol module. Atmospheric Environment, 43, 1982–1990.

Vieno, M., Dore, A.J., Stevenson, D.S., Doherty, R., Heal, M.R., Reis, S., Hallsworth, S., Tarrason, L., Wind, P., Fowler, D., Simpson, D. and Sutton, M.A (2010). Modelling surface ozone during the 2003 heat-wave in the UK. Atmos. Chem. Phys., 10, 7963–7978, 2010.

Watson, L.A., Shallcross, D.E., Utembe, S.R., Jenkin, M.E. (2008). A Common Representative Intermediates (CRI) mechanism for VOC degradation. Part 2: gas phase mechanism reduction. Atmospheric Environment 42, 7196–7204. doi:10.1016/j.atmosenv.2008.07.034